Studies on solid state electrolytic dehumidifier – Modeling of its water transfer characteristics and electrode reactions

Shuichi Sakuma

Studies on solid state electrolytic dehumidifier – Modeling of its water transfer characteristics and electrode reactions

Shuichi Sakuma

Studies on solid state electrolytic dehumidifier –Modeling of its water transfer characteristics and electrode reaction

Chapter 1

Introduction

1.1. Statement of purpose

This thesis presents the characteristics of a solid polymer electrolytic (SPE) dehumidifier which uses a solid state proton-conductive membrane. Such solid state ionic devices as the dehumidifier have been used,

to solve environmental problems such as water improvement,

for energy conversion apparatus such as fuel cells,

to control environmental conditions such as humidity, oxygen concentration.

An SPE dehumidifier using SPE membrane has been developed. The SPE dehumidifier has been used for a measure to protect electric and electronics devices from the problems caused by high humidity. This type of dehumidifying devices has several advantages of no-drain, space saving and small input-power compared to conventional dehumidifying techniques such as those using a Peltier element or space heater. However, there have been few reports about the dehumidifying characteristics of such type of dehumidifying devices as the SPE dehumidifier.[Yamauchi et al.1].

Purposes of this thesis are

(1) To obtain a physical model applicable to the SPE dehumidifier that can explain water transfer occurred in the dehumidifier,

(2) To quantify the dehumidifying performance for specific application conditions

(3) To clarify the relation between the current and the electrode potential across the boundary between electrode and solid state proton-conductive membrane of SPE dehumidifier.

These results will be useful for further development and improvement of the SPE dehumidifier and also for the understanding on the techniques to apply the proton-conductive SPE membrane in industrial means.

1.2. Scope of the studies

1.2.1. Review of investigations on proton-conductive electrolytic

membrane

The SPE dehumidifier is a device using the technology of proton-conductive solid polymer electrolytic membrane. Several studies have been reported on the physical properties of proton-conductive electrolytic membranes [2,3,4,5,6].

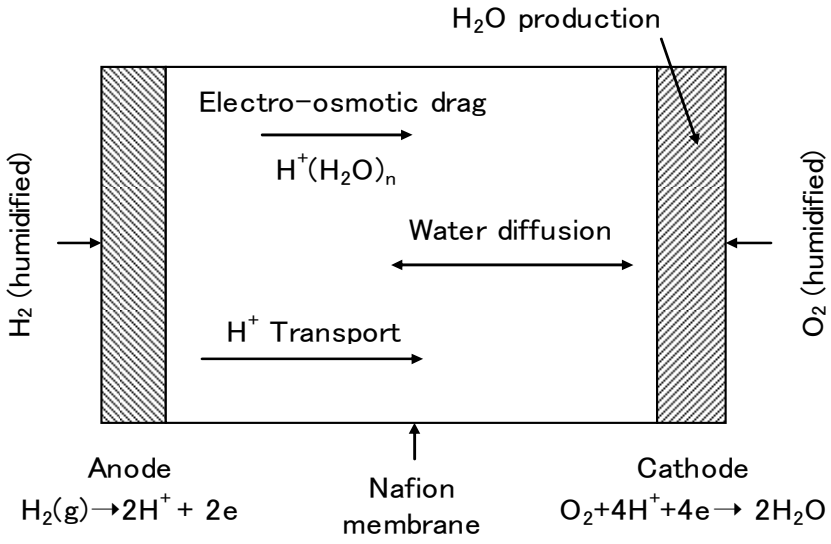

Fig. 1.1 Schematics of fuel cell illustrating modes of water transfer[3]

Zawodzinski et al. reported transport properties of Nafion 117, such as diffusion coefficient of water in the membrane and the protonic conductivity of the membrane as the function of membrane water content [3]. One of the purposes of their studies was to apply them to polymer electrolyte fuel cells (PEFC). Polymer electrolyte fuel cells (PEFC) employ proton conductive ionomers such as Nafion, as their electrolytes. Fig. 1.1 shows schematic illustration of the membrane-electrode assembly of a proton-conductive type PEFC given by Zawodzinski et al.[3]. Water is carried into fuel cell with humidified gas through the surfaces of gas diffusion electrodes and passes through each electrode to the electrode/membrane interface. Protons produced at anode by decomposition of hydrogen are drifted to the cathode. Water molecules move in the membrane to the cathode accompanied by proton. This movement is called as electro-osmotic drag of water. Water is produced at the cathode by combination of proton and oxygen. As a result of electro-osmotic drag of water and water production at the cathode, gradient distribution of water is formed in the membrane and so water is diffused from the cathode to the

anode. These are thought to be the phenomena relating to proton-conductive PEFCs. The SPE dehumidifier has the similar construction to the PEFC, although the SPE dehumidifier is a kind of an electrolytic cell.

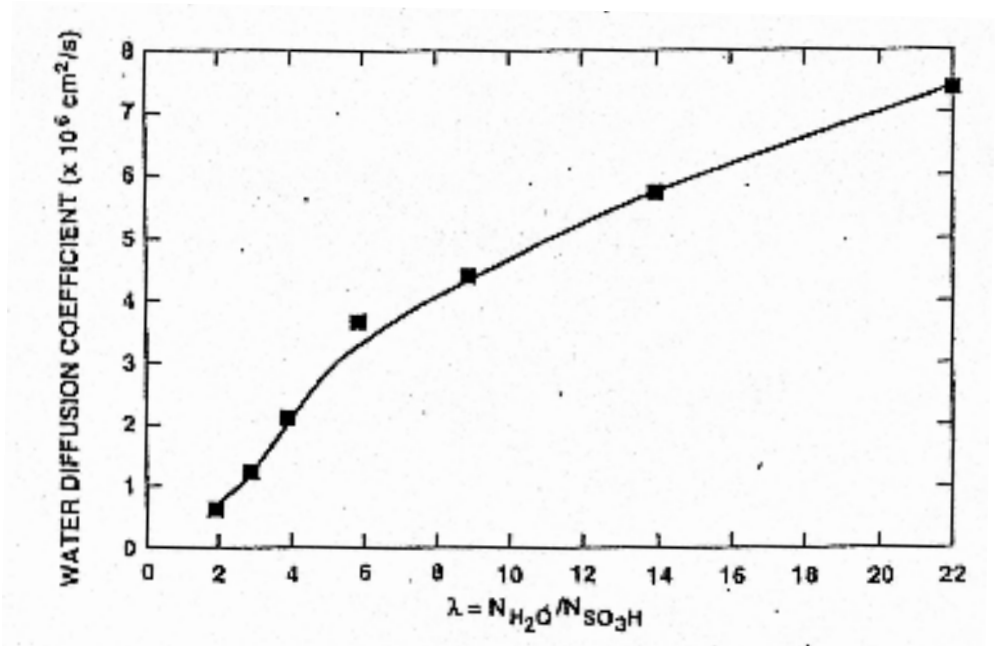

Fig. 1.2 Self-diffusion coefficient of water in Nafion as a function of extent of membrane hydrogen [3]

Yeo et al. measured the diffusion coefficient of water in Nafion 115 (Dupont) and they gave an Arrhenius type formula that the diffusion coefficient depends on temperature [2]. Zawodzinski et al. also showed water diffusion coefficient in Nafion 117 and the water diffusion coefficient was given as a function of water content (the number of water molecules per sulfonic group (H_2O/SO_3H)) as shown in Fig.1.2 [3]. Nguyen et al. also investigated water diffusion coefficient in Nafion of different thickness under different temperature[4], and showed that the diffusion coefficient of water in Nafion 117 was more strongly influenced by the water content than that obtained by Zawodzinski et al. According to these reports, the diffusion coefficient of water in Nafion depends on temperature and water content. However, those results were different in some degree with each other because of different heat treatments of the membrane and some other processes.

Electrical conductivity is also the important parameter to decide the

operating property of the device using the proton-conductive electrolytic membrane. Fig.1.3 shows electrical conductivity versus water content (λ =H_2O mol/SO_3H mol) of Nafion 117 by Zawodzinski et al. They reported that the electrical conductivity of Nafion 117 was roughly proportional to water content expressed by the ratio of water molecules per sulfonic group (H_2Omol/SO_3Hmol) in the membrane[3]. Fig.1.4 shows another measurement of electrical conductivity of Nafion 117 measured by Anantaraman et al [5]. In contrast with the results of Zawodzinski et al., electrical conductivity depends more strongly on the water content of the membrane. However, both results show that the electrical conductivity should depend strongly on the water content of the membrane.

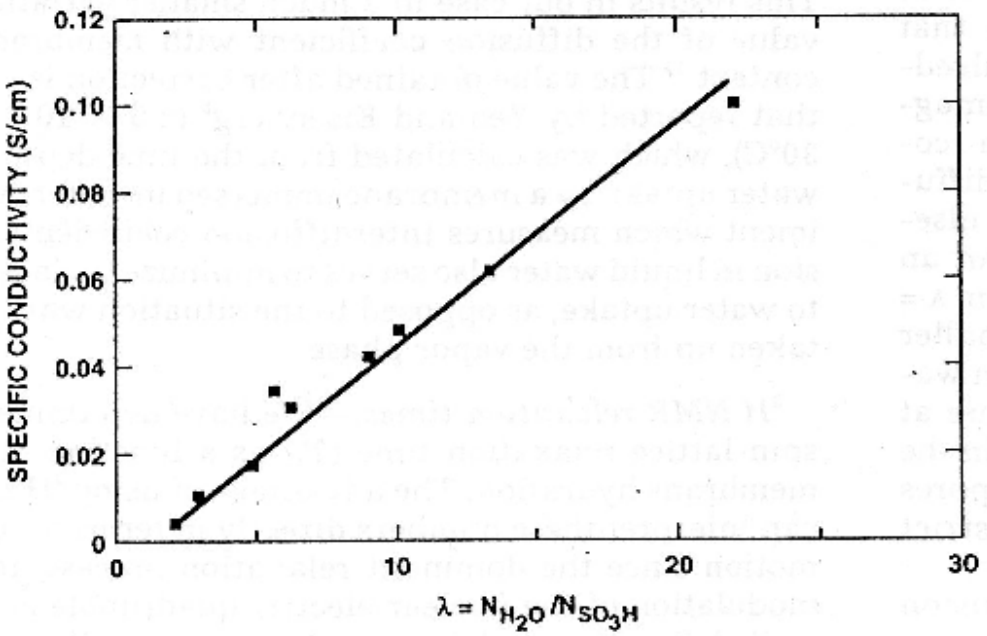

Fig. 1.3 Electrical conductivity of Nafion 117 as a function of water content [3]

Figure 1.5 shows water content (H_2O mol/SO_3 mol) of Nafion 117 versus relative humidity surrounding the membrane, measured by Hinatsu et al [7]. As seen in this figure, water content in the membrane depends considerably on relative humidity of the space surrounding the membrane.

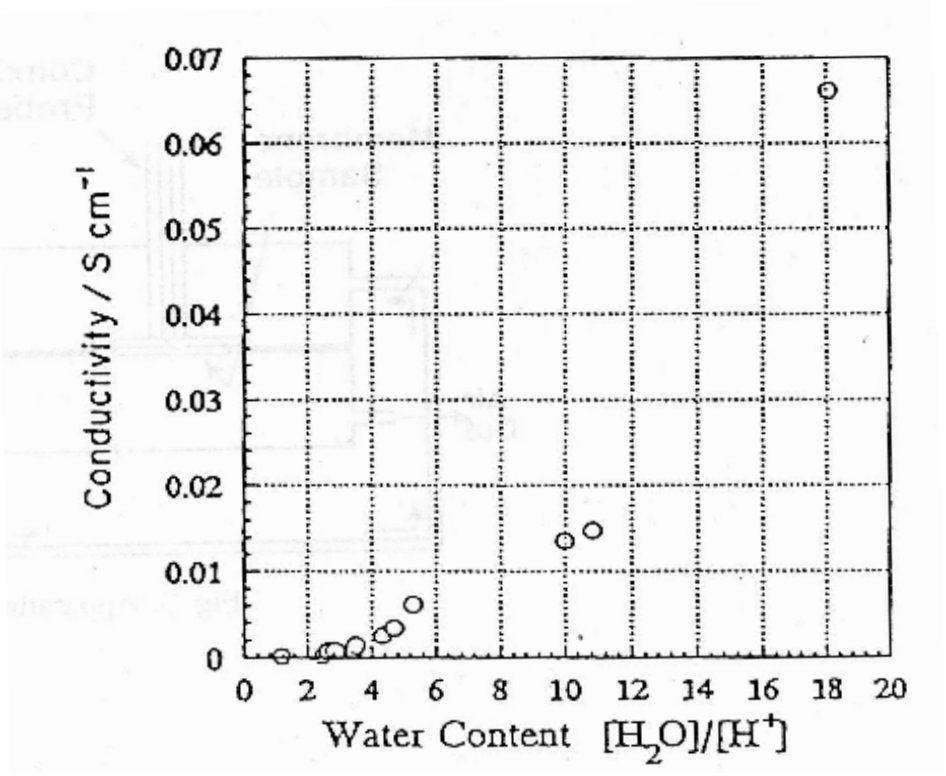

Fig. 1.4 Electrical conductivity of Nafion 117 as a function of water content [5]

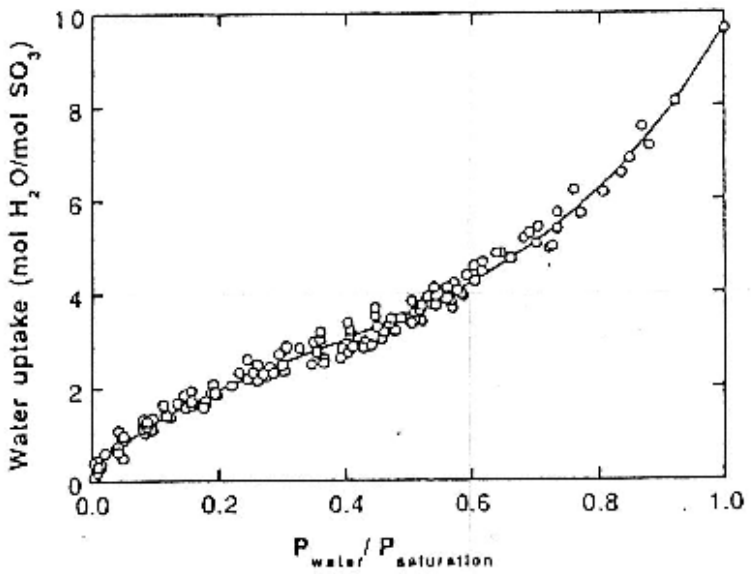

Fig. 1.5 Water content of Nafion 117 against relative humidity [7]

Performance of PEFCs or devices using electrolytic cells depends on the electrical conductivity. The electrical conductivity depends on water content of the membrane. The water content of the membrane depends on relative humidity of the space surrounding the membrane. The understanding on the relation between properties of electrolytic membrane and environmental conditions surrounding the membrane will be very important to improve the performance of PEFCs or devices using electrolytic cells.

A physical model to predict the performance of the dehumidifier will be build using parameters such as conductivity, electro-osmotic drag effect, diffusion of water in the membrane in relation to its environmental conditions.

1.2.2. Review of studies on measuring methods of electrical conductivity of electrolytic membrane

Measurement of the conductivity of an electrolytic membrane is usually carried out with 2-probe AC method or 4-probe AC method. Although four-probe AC method are effective to avoid the measuring errors resulted from the interface between electrode and membrane, the method is difficult to apply the electrical conductivity measurement in the direction of membrane thickness. Two-probe AC method can be easily applied to such measurement. However, it is necessary to pay attention to the interface contact between electrode and membrane, because the measurement is considerably influenced by the contact conditions.

Some papers reported that the conductivity of electrolytic membrane may be anisotropic because of pretreatment such as hot-pressing [8]. Therefore, it is better to measure the conductivity in the direction of the membrane in actual use.

The devices using electrolytic cells are composed of not only an electrolytic membrane but also diffusion electrode on its each surface. Therefore, not only the conductivity of membrane itself but also the voltage across the electrode/membrane interface under the actual operating conditions may be necessary. Measurement of the voltage across the interface may be carried out using a specimen with reference electrodes in addition to the main electrodes to carry the current. However, it is necessary to pay attention for the interpretation of the results because this

method can be influenced by the electrical polarization on the reference electrodes.

1.2.3. Model for SPE dehumidifier previously proposed by Yamauchi et al.[1]

Yamauchi et al. proposed a physical model [1] for SPE dehumidifier using proton-conductive electrolytic membrane (Nafion 117). Fig. 1.6 shows the model. The model is composed of a homogeneous membrane filled with water and electrodes on its both surfaces which can pass through water molecules. Assumptions using for the model are

(1) water content in the membrane depends on water density in the space surrounding the membrane in equilibrium conditions.

(2) The rate of water transferred across the membrane surfaces depends on the difference from the water content in equilibrium conditions. Water is transferred to decrease the difference from the equilibrium conditions.

(3) Current in the dehumidifying device is in proportion to water content in the membrane.

(4) Water in the homogeneous membrane moves from the anode to the cathode only by electro-osmotic drag.

This model could explain the dehumidifying performance of the SPE dehumidifier well. However, calculated current changes such as its initial steep change just after switch-on of source power and the change following the initial steep change do not agree with the measured current changes sufficiently. The model can not explain the emission of water from the cathode to the space facing the cathode because of the assumption of the homogeneous membrane.

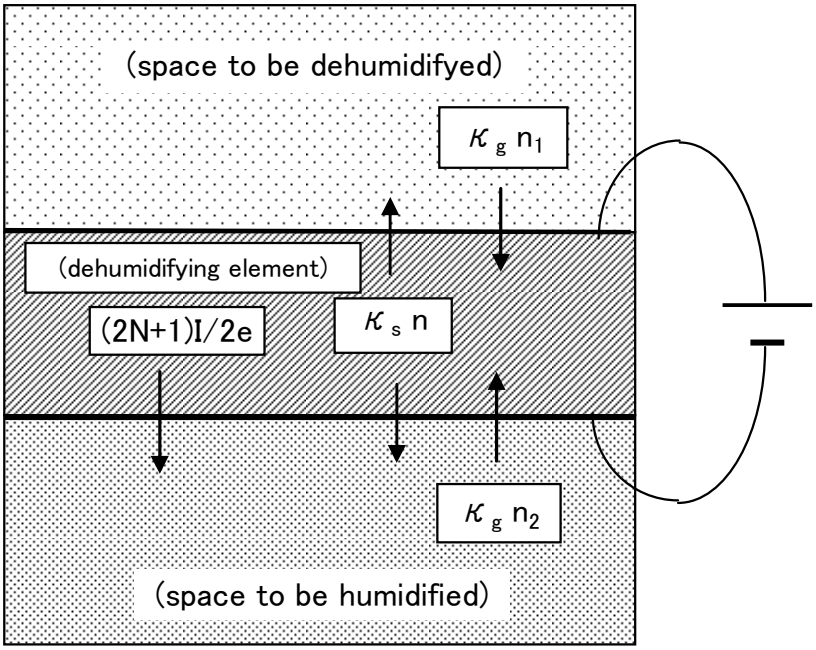

Fig. 1.6 Single phase model for SPE dehumidifier proposed by Yamauchi ea al. [1]

1.3. Pretreatment of the dehumidifying element of this studies

The dehumidifying element is made of electrolytic membrane (Nafion 117) and two electrodes, one is a meshed metal with platinum black catalysis and the other is carbon paper with a catalysis of mainly platinum black. Some properties of Nafion 117 are shown in Table 1. The membrane samples are pretreated in the following way: (1) boiling in dilute hydrogen peroxide, (2) then several-time washing in distilled water, (3) boiling in 1M HCℓ and (4) cleaning procedure in distilled water several times.

The electrodes are fixed on the surface of the membrane processed as mentioned above, by hot-pressing.

Table 1.1 Properties of Nafion 117

Nafion 117(Dupont data)

	property	mark	value	unit	remarks
1	Typical thickness	d	183	μm	at 23 ^{0}C, RH=50%
2	Basic weight/g ·m^{-2}	m	360	g･m^{-2}	at 23 ^{0}C, RH=50%
3	Specific Gravity	ρ_g	1.98		at 23 ^{0}C, RH=50%
4	Conductivity	σ	0.1	Scm^{-1}	high frequency impedance measurement
5	Available Acid Capacity	q_a	0.9	meq･g^{-1}	(at 23^{0}C, RH=50% membrane weight)
6	Total Acid Capacity/meq ·g^{-1}	q_t	0.95-1.01	meq･g^{-1}	(at 23^{0}C, RH=50% membrane weight)
7	water content	m_w	5	weight%	at 23^{0}C, RH=50% compared to dry weight
8	water uptake	m_{w100}	38	weight%	soaked at 100^{0}C water for 1hour, compared to dry weight

Other data

	property	mark	value	unit	remarks
9	equivalent weight	m_{eq}	1100	g･eq^{-1}	
10	ion exchange capability	q_{ex}	0.91	meq･g^{-1}	
11	electric conductivity/S·cm^{-1}	σ	0.1	S･cm^{-1}	high frequency impedance measurement 5kHz, condition temperature 30 centigrade, water content21(H_2O/SO_3Hmol)
12	H_2O gas diffusion coef./cm^2･s^{-1}	D	7.30E-06	cm^{2}s^{-1}	diffusion imaging method(self difusion coef.), condition 30 centigrade, water content 21(H_2O/SO_3Hmol)

1.4. Expected finding and things to further development and improvements

Industrial use of the technology of electrolytic membrane has been extended to many fields of application such as fuel cells, water improvement and other environmental applications. For the application to these fields, development of high conductivity membrane with a long operating life is desired to achieve higher power/efficiency performance. However, there have been few reports on the operating life of electrolytic membrane or devices using the membranes maybe because of the lack of approaching means. Attentions are also directed to humidity supplied to devices using the electrolytic membrane because the humidity is found to affect significantly the performance of these devices.

This thesis describes the relation between the electrical

characteristics and the dehumidifying performance of the SPE dehumidifier. The membrane of the SPE dehumidifier is filled with water. The dehumidifier decomposes water into protons and oxygen. Perhaps, water molecules in the membrane are decomposed and the current flows. Therefore, the dehumidifying performance should be directly affected by the water content in the membrane. On the other hand, humidity of the space surrounding the device would determine the water content of the membrane under equilibrium conditions. Therefore, the dehumidifying performance will be indirectly affected by the humidity. Resultantly the dehumidifying performance would be higher when the humidity is higher.

In chapter 2, two-layer model of the SPE dehumidifier using proton-conductive electrolytic membrane (Nafion 117) is presented. The SPE dehumidifier is represented into two parts, one is anode-side layer and the other is cathode-side layer. The dehumidifier represented by two layers is put over a hole on the wall of a chamber. Inside of the chamber is dehumidified and the outside is humidified, while the dehumidifier is being operated.

The water contents of both layers and the humidities of its surrounding spaces can be calculated under the given conditions of ambient temperature and initial states of the water contents and the water densities. The validity of the model is verified by comparing the results calculated using the model and the measuring results. It is also found that current flowing in the element strongly depends on the water content in the vicinity of the anode in the element.

In chapter 3, the two-layer model of the dehumidifier is applied to the system in which the vessel to be dehumidified has some leakage area. Such condition is likely in actual use. It is practically important to know how long it takes to attain the steady-state humidity and what the attainable humidity is in the chamber for the specific application condition. They would depend on the dehumidifying capability of the dehumidifier and the leakage of humidity. The amount of the leakage would depend on not only the leakage area but also its shape, position and the ambient condition of atmosphere. Hence, equivalent leakage area is introduced to treat the system in which the chamber has some leakage.

It is shown that the rate of the change of water content in the element is much lower than the rate of water transfer through the element for most of the actual applications. Although the two-layer model is basically

composed of four differential equations, the system can be approximately expressed by one differential equation for such case. Therefore, a time onstant of the humidity change and an attainable humidity in the chamber can be obtained. They are represented in a diagram.

Physical properties in the system under steady-state conditions are discussed and the relations of the water contents in both layers to humidities facing the anode and the cathode are also given.

The characteristics of the SPE dehumidifier under a constant applied voltage are described in chapter 2 and chapter 3. Voltage-current (V-I) characteristics of the SPE dehumidifier are presented in chapter 4. The following results were obtained as it is shown in chapter 2 and 3, by comparing the measuring results and the results calculated using two-layer model.

(1) Current produced by the decomposition of water molecules is proportional to water supply to the anode surface of the element under steady-state conditions.

(2) Current flowing in the dehumidifier is proportional to the water content in the vicinity of the anode.

Results obtained by V-I measurement are interpreted by adding above results.

The measurements of V-I characteristics were made using a specially modified dehumidifying element with four electrodes which includes two electrodes to carry the main current and two other electrodes to observe the voltages applied across the electrical double layers. Although such method as using the reference electrodes are affected by the electrical polarization formed on the reference electrodes, voltage changes across the layer can be traced if the polarization is small.

V-I characteristics were interpreted in consideration of these results obtained in chapter 2 and 3. The following formula is derived.

$$I_{st} = const. \times (water\ content\ at\ anode) \times \exp(FV_a / RT)$$

Here, F, R *and* T are Faraday constant, gas constant and temperature, respectively. V_a is the voltage applied across anode-side double layer, which is the anode-side boundary voltage between the anode and the SPE membrane.

In chapter 5, the following problems are described.

(1) measuring method of the dehumidifying performance

(2) problems of the two-layer model

In chapter 6, conclusions of this studies on the dehumidifying characteristics of SPE dehumidifier are described. The following results are summarized.

(1) relations between water content in the dehumidifying element and humidity under equilibrium conditions.

(2) Relation between water content in the membrane and humidity under steady state conditions when current flows.

(3) Relation between current and water content in the element

(4) Water transfer in and through the element

(5) Relation between current and the voltage across the electric double layers

(6) The electrical conductivity of Nafion 117 and its temperature dependence

References

[1] Yamauchi S, Sakuma S, Nakatani H, Mitsuda H, "Mass Transfer Equations of Electrolytic Water Removal Device Using Solid Polymer Electrolytic Membrane", Trans. IEE of Japan, Vol. 120-A, No. 5, pp.607-613, 2000.

[2] Yeo S.C., Eisenberg A, "Physical properties and Supermolecular Structure of Perfluorinated Ion-Containing (Nafion) Polymers", J. Applied Polymer Science, Vol. 21, pp875-898, 1977.

[3] Zawodzinski TA Jr., Derouin C, Radzinski S, Sherman RJ, Smith VT, Springer TE, Gottesfeld S, "Water Uptake by and Transport Through Nafion 117 Membranes", J. Electrochem. Soc., Vol. 140, No. 4, pp.1041-1047, 1993.

[4] Nguyen T, Guante J, Vanderborgh N, "Ion Transport through Polyperfluorosulfonic Acid Membranes", Mat. Res. Soc. Symp. Proc., Vol. 135, p.367-376, 1989.

[5] Anantaraman AV, Gardner CL, "Studies on ion-exchange membrane", J. Electroanalytical Chem., 414, pp.115-120, 1996.

[6] Zawodzinski, TA Jr. Neeman M, Sillerud LO, Gottesfeld S, "Determination of Water Diffusion Coefficients in Perfluorosulfonate

Ionomeric Membranes", J. Phys. Chem., Vol. 95, No. 15, pp.6040-6044, 1991.

[7] Hinatsu JT, Mizuhara M, Takenaka H, "Water Uptake of Perfluorosulfonic Acid Membranes from Liquid Water and Water Vapor", J. Electrochem. Soc., Vol. 141, No. 6, pp.1493-1498, 1994.

[8] Shuhua Ma, Kuse A, Siroma Z, Yasuda K, "Measuring conductivity of proton conductive membranes in the direction of thickness", Espec Technology Report No. 20,

Chapter 2

Modeling of water transfer characteristics of solid polymer electrolytic (SPE) dehumidifier

Abstract A model for a dehumidifying device using a solid polymer electrolyte membrane (Nafion 117, Dupont) is proposed. The dehumidifier in the model is represented by a physical model composed of a two-layer membrane and electrodes on the membrane surfaces. Measurement of the membrane weight shows that the ratio of the water content of the membrane to humidity in the surrounding air is a function of temperature under equilibrium conditions. The results for the water ratio are used for determining the parameters required for the modeling. The electrical resistance of the dehumidifier was measured and is given as a function of temperature and the membrane water content. Simulation of the characteristics of the dehumidifying device is presented, using the model, and the results are found to agree with the measured characteristics of the device. An attempt to determine the parameters describing the dehumidifying processes are also reported.

List of symbols

D : Diffusion coefficient of water in the dehumidifying element / $cm^2\ s^{-1}$

e : Electron charge=1.602×10^{-19} / C

I : Current of the dehumidifying element/ A

I_{st} : Current at steady state condition/ A

j : Current density of the dehumidifying element /a cm^{-2}

κ_g : Coefficients relevant to the diffusion velocity of water from the air to the membrane / cm s^{-1}

κ_s : Coefficient relevant to the diffusion velocity of water from the membrane to the air. This is defined by $k_s = k_{so}\ exp(-W_s/RT)$./cm s^{-1}

L : Thickness of the dehumidifying element = 0.017 / cm

M_o : Molecular weight of water

$m_{g,p}$: Water mass in the space facing the anode/ g

N_A : Avogadro number=6.02×10^{23} / mol^{-1}

R : Gas constant =8.31/ Pa $m^3\ k^{-1}\ mol^{-1}$

RH_{tx} : Relative humidity at time t_x,

R_m : Electrical resistance of the membrane of the device/ Ω

$p_{g,p}$, $p_{g,n}$: Water vapor pressure in the air facing the anode and the cathode, respectively

R_s : Electrical resistance of the dehumidifying element / Ω

S : Area of the dehumidifying element of the device / cm^2

t : Time/ s

T_g : Temperature of the gas space surrounding the dehumidifying element / K

U_s : Applied voltage to the dehumidifying element / V

$V_{g,p}$, $V_{g,n}$: Volumes of the spaces facing the anode and the cathode, respectively.

W_s : Difference in potential energy between water in the air and in the element/J mol^{-1}

$\langle X \rangle_{[t1,t2]}$: Average value of variable X during the period from t_1 to t_2

α : Average number of water molecules carried by a proton moving to the cathode (electro-osmotic drag coefficient)

δ :Water content in the dehumidifying element represented by $molH_2O/molSO_3H$

$\Delta m_{g,p}$: the change in water mass in the dehumidifying space/ g

Δt : Time required for the change in water mass in the dehumidifying space / s

λ : Water content in the dehumidifying element represented by $gH_2O/gSPE_{dry}$

ρ_s, ρ_g :Water content of the dehumidifying element of the device and water density in the air surrounding the element, respectively / g cm^{-3}

$\rho_{g,p}$, $\rho_{g,n}$: Water content in the air facing the anode (positive electrode) and the cathode (negative electrode), respectively/ g cm^{-3}

$\rho_{s,p}$, $\rho_{s,n}$: Water contents in the anode half and cathode half of the dehumidifying element including its inner surfaces defined by a two-layer model of the element / g cm^{-3}

$\rho_{g,sat}$: Saturated water density in the air / g cm^{-3}

$\rho_{s,o}$: Initial water content in the dehumidifying element at switching-on of the device / g cm^{-3}

Subscript g : Gas space

Subscript n : Negative electrode or cathode

Subscript on : At the switching-on

Subscript p : Positive electrode or anode

Subscript s : Polymer electrolytic dehumidifying element

Subscript sat: Saturated condition

Subscript st : Steady state condition

Subscript ti : Time t_i

2.1 Introduction

An electrolytic dehumidifying device using a solid polymer electrolyte (SPE) membrane has been developed as a protective measure against problems caused by high humidity. The dehumidifying device was found to effectively maintain a high reliability of electrical and electronic devices by controlling the humidity in the space containing them. The device consists of a proton-conductive solid polymer electrolyte and porous electrodes with a catalytic layer composed of noble metal particles. When a DC voltage is applied to the electrodes, the device can dehumidify the space facing the anode and humidify the space facing the cathode [1]. This type of electrolytic dehumidifying device has several advantages of no-drain, space-saving and small input-power compared to conventional dehumidifying techniques such as those using a Peltier element or space heater.

This chapter proposes a model of the dehumidifying device using an SPE membrane. The device in the model is expressed by a two-layer membrane and electrodes on the membrane surfaces. Measurement of the membrane weight shows that the ratio of the water content in the membrane to the humidity in the surrounding air is a function of temperature under equilibrium conditions. The results for the water ratio are used to determine the parameters required for modeling. The electrical resistance of the dehumidifier is measured and is given as a function of the temperature and membrane water content. Simulation of the characteristics of the device is presented, using the model, and the results are found to agree with the measured characteristics. We also report an attempt to determine the parameters describing the dehumidifying processes.

2.2 Modeling of dehumidifying device

2.2.1 Basic equations for the model

The following reactions occur at the anode and the cathode when a DC voltage is applied to the dehumidifying device [1].

$$2H_2O \rightarrow 4H^+ + O_2 + 4e \quad \text{at the anode} \qquad (2\text{-}1)$$

$$4H^+ + O_2 + 4e \rightarrow 4H_2O \quad \text{at the cathode} \qquad (2\text{-}2)$$

These reactions are influenced by the applied voltage, temperature and water content of the membrane. Figure 2.1 is a schematic diagram explaining the dehumidifying process. As shown in Fig.2.1(a), the device is placed on the open hole in the wall of chamber P to dehumidify the chamber. The device is operated by supplying a DC electrical source. Figure 2.1(b) shows the details of the two-layer model to represent the dehumidifying element. The dehumidifying element is represented by two parts, an anode side and a cathode side. This element can receive water from the space and also emit water to the surrounding space through its surfaces. On applying a DC electrical source to the device, water in the vicinity of the anode is decomposed and protons are

produced. The protons are driven toward the cathode together with some water molecules and combined with oxygen at the cathode to produce water. As a result, the water content at the cathode side becomes higher than that at the anode, and then water diffuses from the cathode to the anode. Excess water at the cathode also diffuses to the space through the cathode surface. As a result, the humidity in chamber P is decreased.

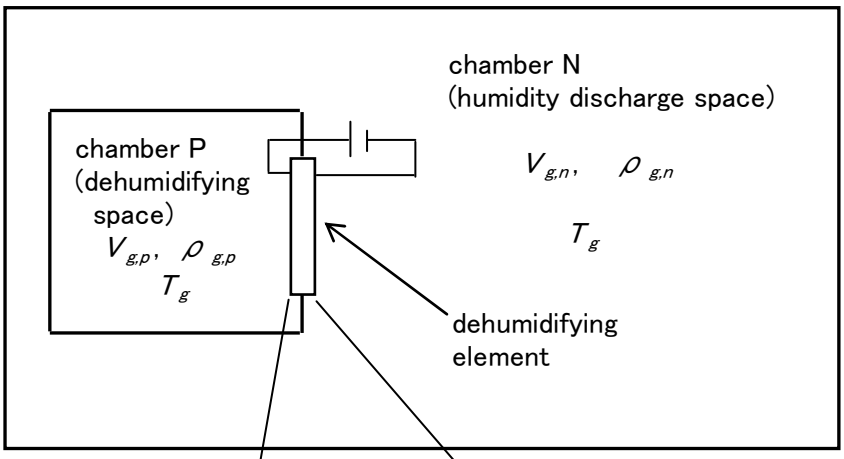

(a) System with two spaces separated by the dehumidifying device

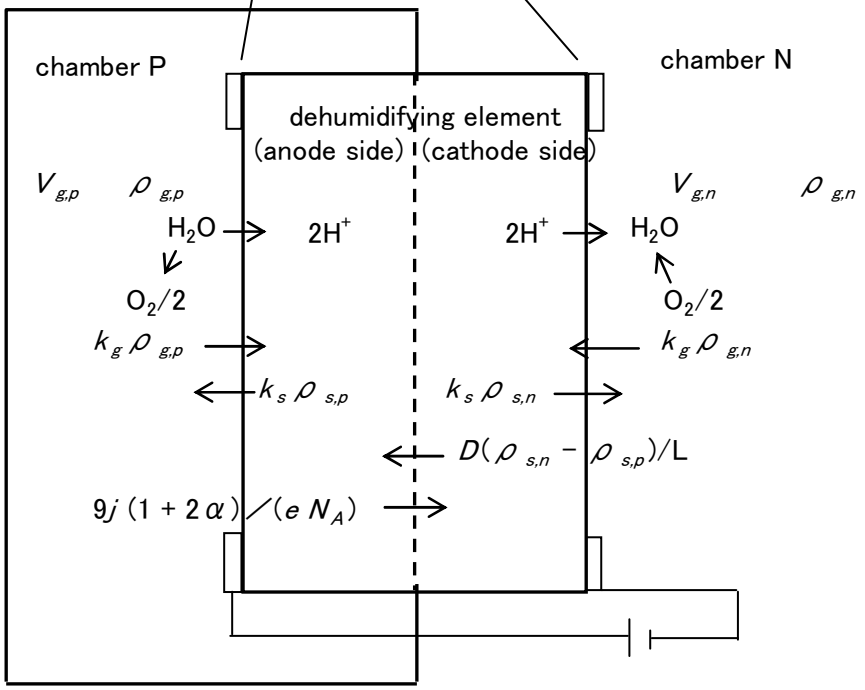

(b) Two-layer model for dehumidifying element made from a solid polymerelectrolyte (SPE) membrane

Fig.2.1 System for the study of the characteristics of the dehumidifying device and a two-layer model for the device, (a) System with two spaces separated by the dehumidifying device, (b) Two-layer model for dehumidifying element made from solid polymer electrolytic (SPE) membrane.

The following equations are assumed for the system shown in Fig.2.1.

$$\frac{d\rho_{g,p}}{dt} = \frac{S}{V_{g,p}}(\kappa_s \rho_{s,p} - \kappa_g \rho_{g,p}) \tag{2-3}$$

$$\frac{d\rho_{g,n}}{dt} = \frac{S}{V_{g,n}}(\kappa_s \rho_{s,n} - \kappa_g \rho_{g,n}) \tag{2-4}$$

$$\frac{d\rho_{s,p}}{dt} = \frac{2}{L}\left\{(\kappa_g \rho_{g,p} - \kappa_s \rho_{s,p}) + \frac{D}{L}(\rho_{s,n} - \rho_{s,p}) - (\frac{1}{2} + \alpha)\frac{18j}{eN_A}\right\} \tag{2-5}$$

$$\frac{d\rho_{s,n}}{dt} = \frac{2}{L}\left\{(\kappa_g \rho_{g,n} - \kappa_s \rho_{s,n}) - \frac{D}{L}(\rho_{s,n} - \rho_{s,p}) + (\frac{1}{2} + \alpha)\frac{18j}{eN_A}\right\} \tag{2-6}$$

$$j = \frac{I}{S} \tag{2-7}$$

$$I = \frac{U_s}{R_s} \tag{2-8}$$

$$R_s = R_s(\rho_s, T_g) \tag{2-9}$$

2.2.2 Parameter determination

Figure 2.2 shows a schematic diagram giving typical conditions for this system.

In the equilibrium condition at off-switching of the DC voltage source, eqs. (2-3), (2-4), (2-5) and (2-6) are then reduced as follows.

$$\rho_{g,p} = \rho_{g,n} \equiv \rho_g \tag{2-10}$$

$$\rho_{s,p} = \rho_{s,n} \equiv \rho_s \tag{2-11}$$

$$\kappa_s \rho_s = \kappa_g \rho_g \tag{2-12}$$

The coefficient κ_s in the left part of eq. (2-12) is a coefficient relating to the vaporization rate of water from the element to the air and can be expressed by the following equation.

$$\kappa_s = \kappa_{so} \exp\{-W_s / RT_g\} \tag{2-13}$$

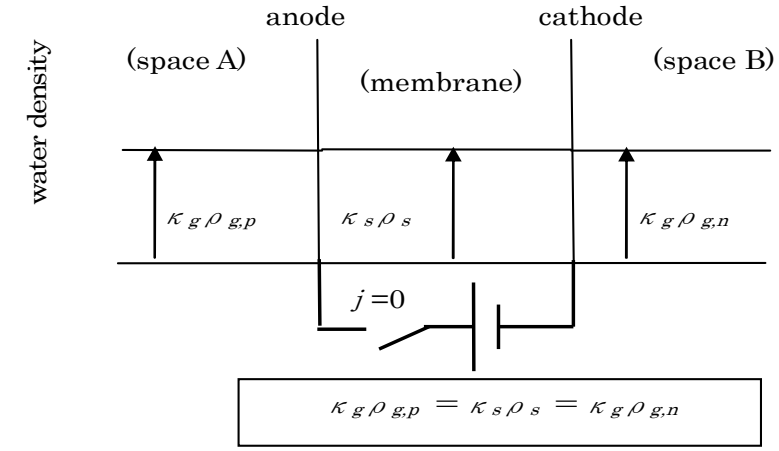

(a) equilibrium condition at switch-off

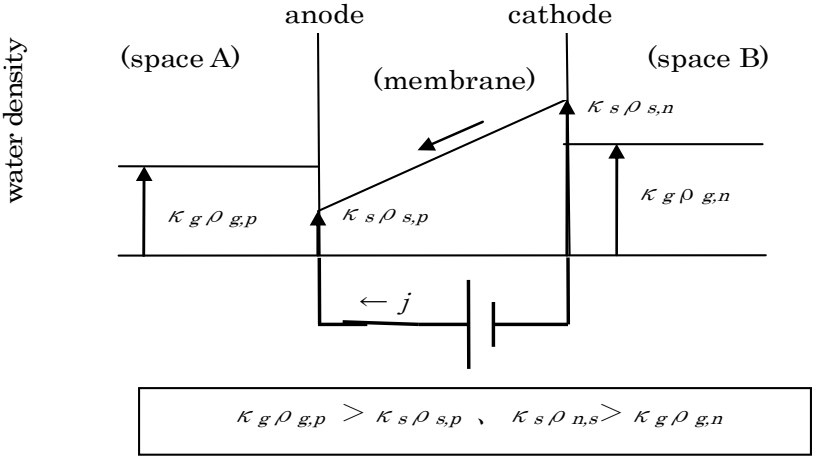

(b) dehumidifying period at switch-on

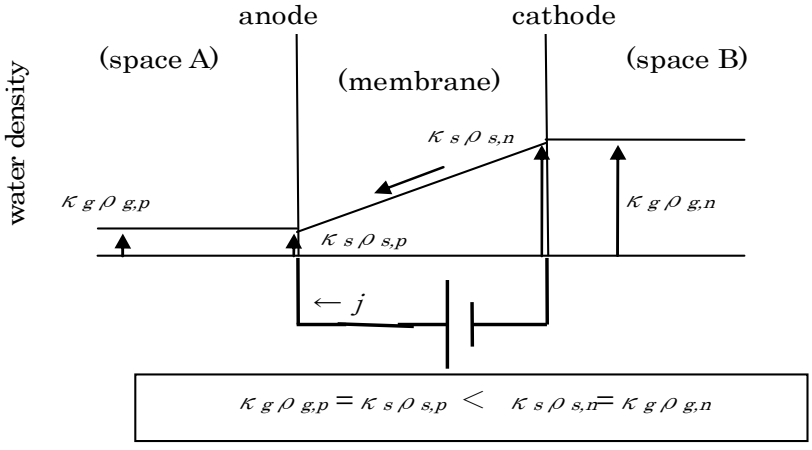

(c) steady state condition at switch-on

Fig. 2.2 Water density of dehumidifying element and its surrounding space, (a) Equilibrium condition at switch-off, (b) Dehumidifying period at switch-on, (c) Steady-state condition at switch-on

W_s in eq.(2-13) is the energy difference between water in the air and that in the element. Substituting (2-13) into (2-12), eq.(2-12) is expressed as

$$\rho_s / \rho_g = \kappa_g / \kappa_{so} \exp\{W_s / RT_g\} \tag{2-12a}$$

The values of κ_g / κ_{so} and W_s can be obtained by weight measurement of the membrane at various temperatures and humidities.

After long-time operation of the device, the system attains steady-state as shown in Fig.2.2(c). The equations of (2-3) to (2-6) are then reduced as follows.

$$\kappa_s \rho_{s,p} = \kappa_g \rho_{g,p} \tag{2-14}$$

$$\kappa_s \rho_{s,n} = \kappa_g \rho_{g,n} \tag{2-15}$$

$$\frac{D}{L}(\rho_{s,n} - \rho_{s,p}) = \left(\frac{1}{2} + \alpha\right)\frac{18j}{eN_A} \tag{2-16}$$

Because equations (2-14) to (2-16) are valid under the steady-state condition, the net transportation of water through the surfaces of the element is zero and dehumidification by the current flow is cancelled by the back diffusion of water in the dehumidifying element.

Substituting eqs.(2-14) and (2-15) into (2-16), eq.(2-16) is transformed as follows.

$$\frac{DS}{L}\frac{k_g}{k_s}\left(\rho_{g,n} - \rho_{g,p}\right) = \left(\frac{1}{2} + \alpha\right)\frac{18I_{st}}{eN_A} \tag{2-16a}$$

The device can dehumidify space A under the transient condition shown in Fig.2.2(b). The dehumidifying capability of the device is defined as the rate of water mass removed from Chamber P in Fig.2.1. Thus, the capability can be obtained by the measurement of time Δt in which the humidity in the chamber changes from RH_{t1} to RH_{t2}. The capability can be expressed as follows.

$$\Delta m_{g,p} / \Delta t = V_{g,p} \rho_{g,sat} (RH_{t2} - RH_{t1}) / 100 / \Delta t \tag{2-17}$$

The dehumidifying capability expressed by (2-17) can be transformed by making use of eq.(2-3) as follows.

$$\frac{\Delta m_{g,p}}{\Delta t} = -\frac{V_{g,p}}{(t_2 - t_1)} \int_{t1}^{t2} \frac{d\rho_{g,p}}{dt} dt = \frac{S}{(t_2 - t_1)} \int_{t1}^{t2} (\kappa_g \rho_{g,p} - \kappa_s \rho_{s,p}) dt \qquad (2\text{-}18a)$$

If RH_{t1} and RH_{t2} are selected within the range $\kappa_g \rho_{g,p} \gg \kappa_s \rho_{s,p}$, eq.(2-18a) can be approximated as follows.

$$\frac{\Delta m_{g,p}}{\Delta t} = \frac{S}{(t_2 - t_1)} k_g \int_{t1}^{t2} \rho_{g,p} dt = S k_g < \rho_{g,p} >_{[t1,t2]} \qquad (2\text{-}18b)$$

The k_g values can be obtained by substituting the dehumidifying capability obtained from the measurement. The value of k_{so} can also be derived by substituting k_g into eq.(2-12a).

On the other hand, the dehumidifying capability can also be expressed by making use of eq.(2-5) as follows.

$$\begin{aligned} \frac{\Delta m_{g,p}}{\Delta t} &= \frac{1}{(t_2 - t_1)} \left[-\frac{LS\rho_{s,0}}{2} + \frac{9(1+2\alpha)}{eN_A} \int_{t1}^{t2} I dt - \frac{DS}{L} \int_{t1}^{t2} (\rho_{s,n} - \rho_{s,p}) dt \right] \\ &\cong \frac{9(1+2\alpha)}{eN_A} < I >_{[t1,t2]} - \frac{DS}{L} < \rho_{s,n} - \rho_{s,p} >_{[t1,t2]} \end{aligned} \qquad (2\text{-}19)$$

As seen in eq.(2-19), the dehumidifying capability is the difference between dehumidification by current flow produced by the decomposition of water molecules and back diffusion occurring due to the gradient of the water content in the element. Equation (2-19) can be simplified to eq.(2-20) when the dehumidifying capability is calculated using data measured during a period far from the steady-state condition.

$$\frac{\Delta m_{g,p}}{\Delta t} \cong \frac{9(1+2\alpha)}{eN_A} < I >_{[t1,t2]} - 2\frac{DS}{L} \rho_{s,0} \qquad (2\text{-}20)$$

Unknown factors of D and α can be derived from simultaneous eqs. (2-16) and (2-20) if we have measured the dehumidifying capability and current and can estimate the water content in the membrane by using the method shown in this section.

The dehumidifying element is composed of a proton-conductive solid polymer electrolytic membrane (Nafion 117) with porous electrodes on its surfaces. The electrodes have a catalytic layer composed of noble metal particles surrounded by Nafion to promote electrolysis.

The electrical circuit of this electrolyte with electrodes can be approximated as three parallel R-C circuits [7] as shown in Fig. 2.3. Elements of these parallel- circuits are referred to as the resistances of the bulk, R_{bul}, grain/boundary, R_{gr}, and

electrode/membrane boundary, R_{elec}, and the capacitances C_{bul}, C_{gr} and C_{elec} in parallel with these resistances. R_{bul} and R_{gr} are the resistance of the membrane itself. Usually, an impedance measurement of an electrolytic device is carried out by changing the frequency of the AC voltage.

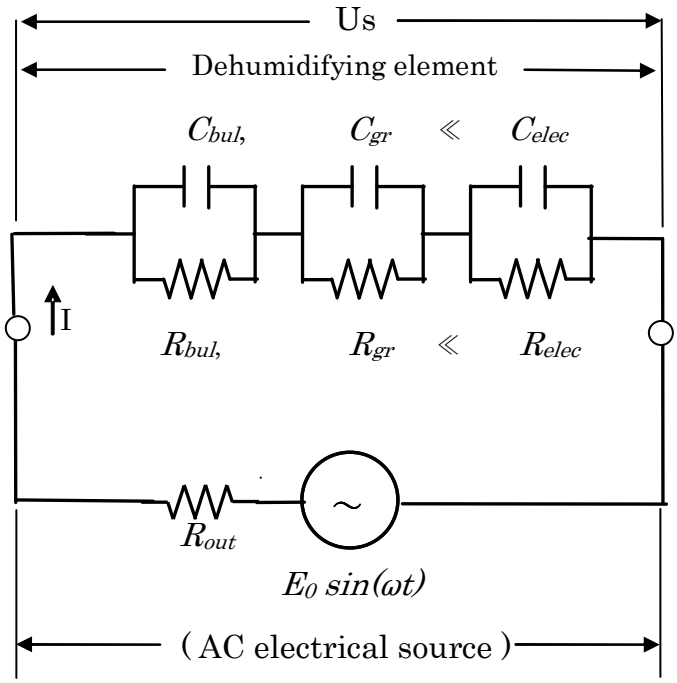

Fig.2.3 Impedance measurement of dehumidifying element

The resistance and capacitance of the electrode/membrane boundary (R_{elec}, C_{elec}) are much larger than those of the membrane itself. Therefore, a much higher frequency of the applied AC voltage than the natural frequency of the electrode/membrane boundary circuit should be selected to evaluate the resistance of the membrane itself.

2.3 Experiment

2.3.1 Measurement of water content in SPE membrane

The measurement of the water content in the membrane (Nafion 117) was carried out using the following procedures. A membrane sheet with dimensions 12 cm × 13 cm was put in a constant-humidity and constant-temperature vessel for more than 2 hours. The sheet was then removed from the vessel and its weight was measured. The measurements were carried out quickly because the weight gradually decreases by water

vaporization. The measurements were carried out for a temperature range 283K~313K and a humidity of 40%~80% in the vessel. The dry weight of the membrane was estimated by linear extrapolation of the weight measurements. The dry weight of the membrane with area 12 cm × 13 cm was estimated to be 4.92 g by linear extrapolation. The specific gravity of the dry membrane is calculated to be 1.855 assuming that the membrane thickness is constant (L = 0.017 cm). The water contents of the membrane were then estimated for each condition.

Figure 2.4 shows a typical example of time variation of the weight change of the membrane after the membrane is removed from the vessel of 303 K and 80% humidity to an environment of 303 K and 45% humidity. The time constant of the weight change of the membrane is obtained from the slope of the data. From the slope in the initial stage and around 800 s, the time constants are found to be about 600 ~ 700 s. Hence, the measurement of membrane weight in equilibrium with the environment in the temperature/humidity controlled vessel should be conducted quickly depending on the required accuracy. We adopted the value measured within 20 s after removing the membrane from the vessel as the weight in equilibrium with the environment in the vessel.

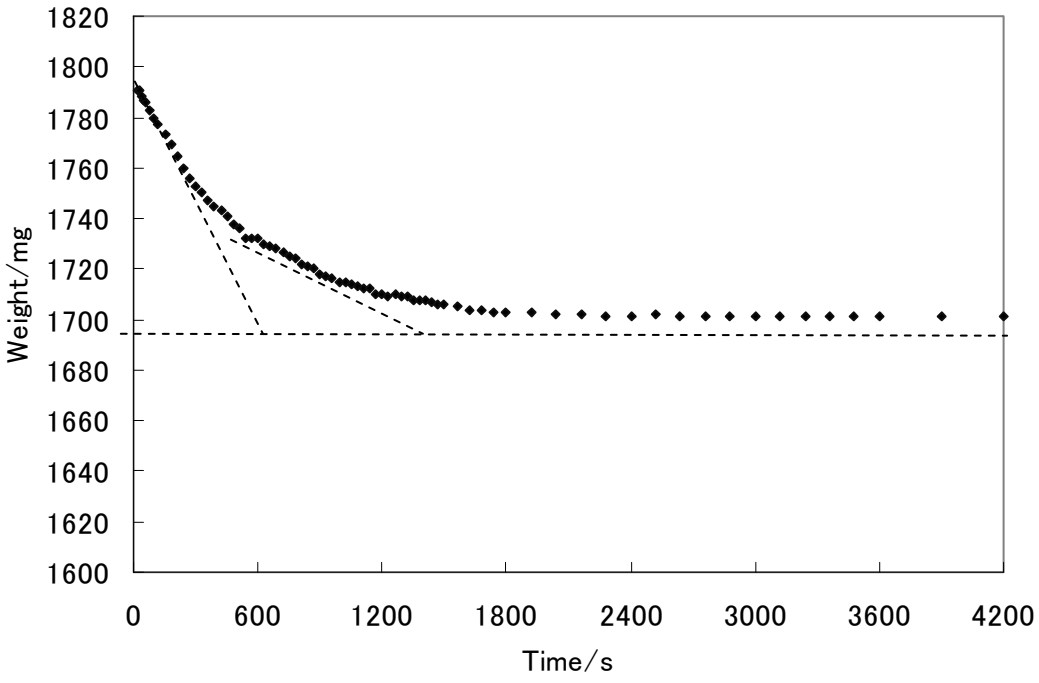

Fig. 2.4 Weight change of membrane (Nafion 117) after changing the condition from 303K、80% to 303K、45% at t=0

Figure 2.5 shows the ratio of water content in the membrane to humidity in the vessel, obtained by the weight measurement. The water content ρ_s is calculated assuming that the membrane thickness is 0.017 cm. As shown in Fig. 2.5, the ratio ρ_s/ρ_g mainly depends on the temperature under the equilibrium condition.

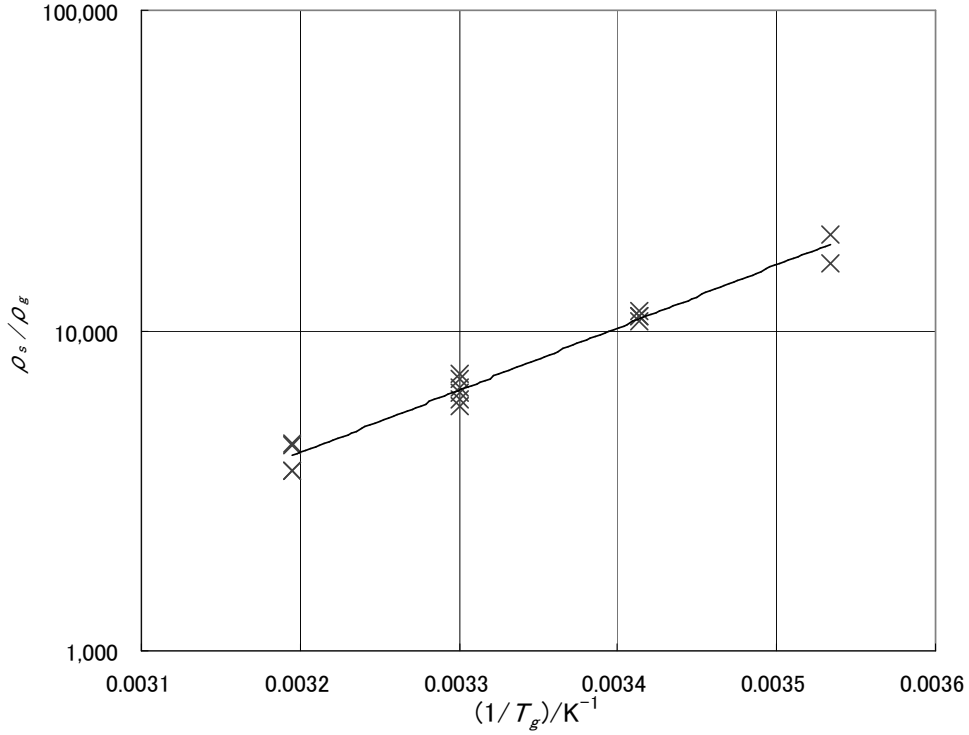

Fig. 2.5 Ratio of water content in SPE membrane to humidity in the surrounding air under equilibrium conditions

The following equation can be derived from the result in Fig. 2.5.

$$\rho_s / \rho_g = \kappa_g / \kappa_{so} \exp(4500 / T_g) \tag{2-21}$$

$$\kappa_g / \kappa_{so} = 2.3 \times 10^{-3} \tag{2-22}$$

2.3.2 Determination of the coefficients κ_g and κ_{so} relating to water transfer across the surface of the element

To determine the coefficients of κ_g and κ_{so}, an experiment to determine the dehumidifying capability of the device was carried out using the experimental set-up

shown in Fig. 2.1. A dehumidifying element with area 100 cm^2 and a chamber of volume 51 dm^3 were used. The time required for the reduction of the humidity in the chamber from RH_{t1} to RH_{t2} was measured, and the dehumidifying capability was then calculated. The value of κ_g was then estimated using eq.(2-18b).

Table 2.1 Dehumidifying capability of dehumidifying device (the time required for humidity change in the space of Vg,p from RH_{t1} to RH_{t2})

Test case	T_g/K	RH_{t1} /%	RH_{t2} /%	<I>$_{[t1,t2]}$ /A	Required time/s	Dehumidifying capability/g s^{-1}	Estimated value of k_g /cm s^{-1}
Case A	303	60	50	3.86	364	4.14×10^{-4}	0.257
Case B	303	60	50	3.63	402	3.75×10^{-4}	0.233
Case C	293	80	62	3.6	600	2.59×10^{-4}	0.223
Case D	293	41	31	–	600	1.44×10^{-4}	0.244

Volume of dehumidifying space V_{gp} = 51 dm^3
Area of dehumidifying element S = 100 cm^2

Table 2.1 shows the results for the dehumidifying capability of the device. Coefficient κ_g relevant to the diffusion velocity of water from the air to the membrane can be estimated by substituting the dehumidifying capability into Eq. (2-18b). These results are also shown in Table 2.1. Estimated values of κ_g are around 0.24 cm s^{-1} for 293 K ~ 303 K and do not depend so much on temperature and humidity in the measured ranges. Substituting κ_g = 0.24 cm s^{-1} into Eq. (2-22), the coefficient κ_{so} can be obtained as follows.

$$\kappa_g = 0.24 \qquad cm\ \ s^{-1} \qquad (2\text{-}23)$$

$$\kappa_{so} = 1.1\times10^{2} \qquad cm\,s^{-1} \qquad (2\text{-}24)$$

2.3.3 Determinations of the diffusion coefficient of water in the membrane and the number of water molecules carried by a proton moving to the cathode.

The system in Fig. 2.1 reaches a steady-state condition described by eqs.(2-14)-(2-16) within several hours of the operation of the device. Physical quantities under the

Table 2

steady-state condition were measured using the experimental set-up shown in Fig. 2.1. Table 2.2 shows the physical quantities measured under the steady-state conditions.

Table 2.2 Physical quantities under steady state conditions (humidifying space $V_{g,n}$ was kept at humidity RH_{t1} during the experiment)

Test case	Tg/K	RH_{t1} /%	RH_{st} /%	I_{t0} /A	I_{st} /A	$D/(1+2\alpha)/cm^2\ s^{-1}$ (calculated by eq.(2-16a))
Case C	293	80	3.3	10	1.6	1.79×10^{-7}
Case D	293	41	<0.5	8	0.8	1.70×10^{-7}
Case E	303	65	0.5	10	1.5	1.91×10^{-7}
Case F	303	61	0.8	9.5	1.2	1.64×10^{-7}

Tg : ambient temperature

RH_{t1} : initial humidity in the spaces Vg,p and Vg,n

RH_{st} : humidity in the space Vg,p under steady state condition

I_{t0} :initial current at switch-on

I_{st} : current under the steady state condition

By substituting measured quantities shown in Table 2.2 into eq.(2-16a), the values of $D/(1+2\alpha)$ for each case were estimated, and are also shown in Table 2.2. The estimated values are about 1.8×10^{-7} cm^2 s^{-1} for 293 K~303 K. The values do not depend so much on temperature and humidity in the range.

$$D/(1+2\alpha)= 1.8\times10^{-7} \quad \text{cm}^2\ \text{s}^{-1} \tag{2-25}$$

The values of α and D can be separately obtained by substituting eq.(2-25) into eq.(2-20) as follows:

$$\alpha = 1.3 \tag{2-26}$$

$$D = 6.2\times10^{-7} \quad (\text{cm}^2\ \text{s}^{-1}) \tag{2-27}$$

The obtained α and D are assumed to be valid at least within the range 293 K to 303 K.

2.3.4 Determination of electrical resistance of the dehumidifying element

The resistance of the dehumidifying element with area 100 cm^2 was measured under different temperatures and humidities. An HP 4192A LF impedance analyzer (YHP) was used. The impedance was measured using the AC internal voltage of the analyzer. The AC voltage was supplied to the element via 50 Ω of internal resistance of the analyzer. Figure 2.6 shows the impedances measured by varying the frequency of the AC voltage. The resistance of the element was found to be about 0.28 Ω. An AC voltage of 1 V was selected for the measurement. Therefore, the actual voltage applied to the element itself

was about 0.28/50 V. The electrolysis of water cannot occur under such conditions as the resistance measurement, because the voltage is much less than the electrolysis voltage (1.23 V) of the element .

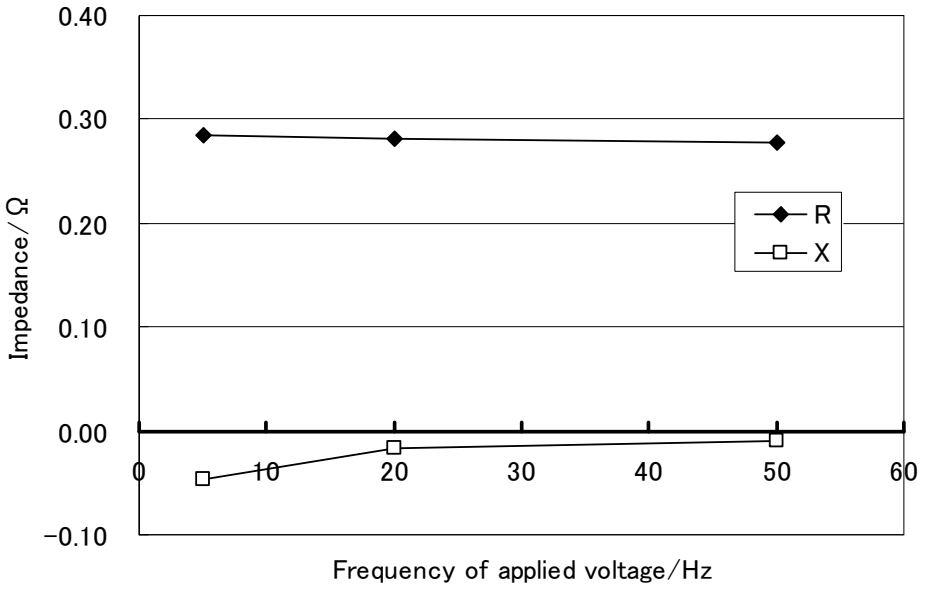

Fig. 2.6 Impedance measurement of dehumidifying element with area 100 cm²

The resistance values measured are around 0.28 Ω and do not depend so much on the voltage frequency from 5 Hz to 50 Hz. The measured reactance values are from −0.01 Ω to −0.05 Ω. The reactance is much smaller than the resistance in the frequency range. As a result, the element can be expressed as a series Rs-Cs circuit composed of a resistance of around 0.28 Ω and a capacitance of around 0.3 F to 0.7 F. The capacitance estimated to be 0.3 F to 0.7 F should be the electrode/membrane boundary capacitance C_{elec}, and the resistance of around 0.28 Ω should be the resistance of the membrane(R_m), that is, the sum of R_{bul} and R_{gr}. Thus, the resistance of the membrane itself can be obtained by applying an AC voltage.

An AC voltage at a frequency of 5 Hz was selected to measure the resistance of the element to avoid the effect of the parallel capacitance of the element itself. The measurements were conducted in the temperature range 303 K-333 K and the humidity range 50% - 90%. The measured resistances are shown in Table 2.3 and Fig. 2.7. The best fit equations for the element of area 100 cm² are also expressed in Fig.2.7 and are unified in the following form.

$$R_m = \frac{0.67 \times 10^{-3} \exp(670/T_g)}{\rho_s} + 0.173 \qquad /\Omega \tag{2-28}$$

Here, ρ_s is in g cm^{-3}.

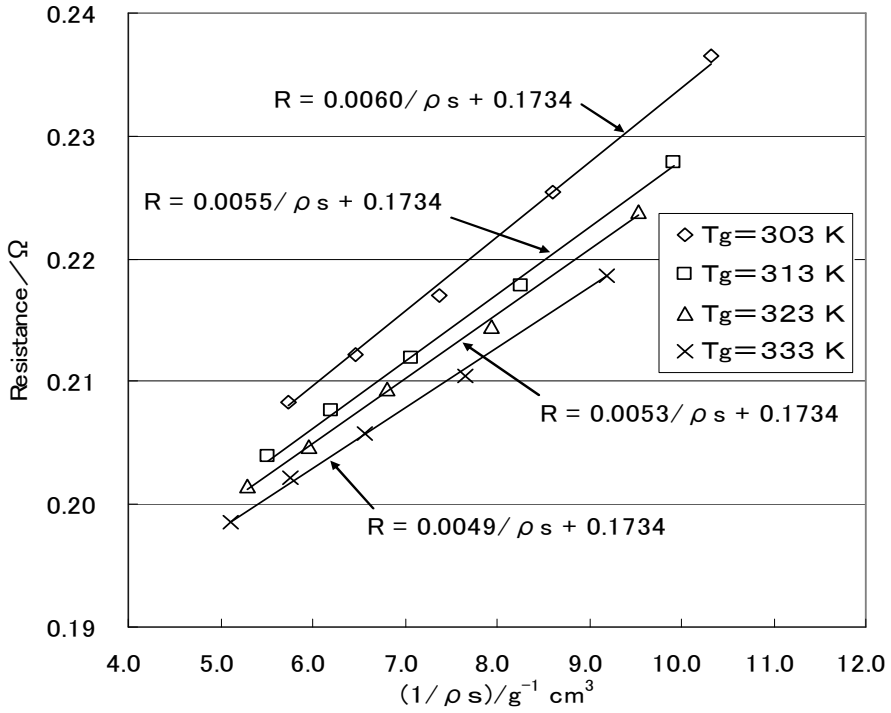

Fig.2.7 Electrical resistance of the dehumidifying element with the area of 100 cm^2 vs. water content in the membrane

It can be seen that the resistance linearly changes with the inverse of the water content in the element and also depends on its ambient temperature.

In the case where the DC voltage applied to the element is high enough to produce electrolysis, the whole resistance of the element is the sum of the resistance of the membrane expressed by eq. (2-28) and the electrode/membrane boundary resistance, R_{elec}. The resistance R_{elec} is assumed to also be affected by the water content in the boundary, especially the water content in the vicinity of the anode because the water content near the anode directly affects the amount of electrolysis. Therefore, the resistance R_{elec} can be assumed to be proportional to the inverse of the water content at the anode. The entire resistance of the element can then be expressed as follows.

$$R_s = R_{elec} + R_m = \frac{A(T_g)}{\rho_{s,p}} + eq.(2-28) \tag{2-29}$$

Table 2.3 Measured electrical resistance of the dehumidifying element of area 100 cm^2

Tg/K	ambient humidity /%	ρ_g /g cm^{-3}	ρ_s /g cm^{-3}	λ (H_2O/SO_3H)	δ (gH_2O/gSPE)	resistance /Ω (meas.)
303	50	1.48×10^{-5}	0.095	3.2	0.052	0.237
303	60	1.78×10^{-5}	0.114	3.8	0.062	0.225
303	70	2.08×10^{-5}	0.133	4.5	0.073	0.217
303	80	2.38×10^{-5}	0.152	5.1	0.083	0.212
303	90	2.67×10^{-5}	0.171	5.8	0.093	0.208
313	50	2.49×10^{-5}	0.099	3.3	0.054	0.228
313	60	2.99×10^{-5}	0.119	4.0	0.065	0.218
313	70	3.48×10^{-5}	0.139	4.7	0.076	0.212
313	80	3.98×10^{-5}	0.158	5.3	0.087	0.208
313	90	4.48×10^{-5}	0.178	6.0	0.097	0.204
323	50	4.04×10^{-5}	0.103	3.5	0.056	0.224
323	60	4.84×10^{-5}	0.124	4.2	0.068	0.215
323	70	5.65×10^{-5}	0.144	4.9	0.079	0.209
323	80	6.46×10^{-5}	0.165	5.6	0.090	0.205
323	90	7.27×10^{-5}	0.185	6.3	0.101	0.201
333	50	6.36×10^{-5}	0.107	3.6	0.058	0.219
333	60	7.64×10^{-5}	0.128	4.3	0.070	0.211
333	70	8.91×10^{-5}	0.150	5.0	0.082	0.206
333	80	1.02×10^{-4}	0.171	5.8	0.093	0.202
333	90	1.15×10^{-4}	0.192	6.5	0.105	0.199

ρ_s : calculated by eq.(21)

Though we do not have additional data on $A(T_g)$, the same expression as eq.(2-28) was applied to $A(T_g)$ to simulate the characteristics of the dehumidifying device.

2.4 Simulation of the characteristics of the dehumidifying device

Experiments to determine the characteristics of the dehumidifying device were carried out using the experimental set-up in Fig. 2.1. A chamber of volume 51 dm^3 shown in Fig.2.1 was located in a temperature-humidity controlled vessel. The time dependence of the humidity and temperatures for both the inner volume and the outer volume of the vessel and the current were then measured. The experimental results were compared to the simulation based on the idea shown in section 2.2.

Figure 2.8 shows a comparison of the experimental and calculated results for the change in humidity and current after switching-on of the dehumidifying device when the ambient temperature and humidity were 293 K and 80 %, respectively. The dehumidification of the chamber started at t=0, and the current rapidly decreased at the early stages. Thereafter, the current and humidity of the chamber decreased more slowly to the steady state. The changes in the humidity and the current in the calculation are

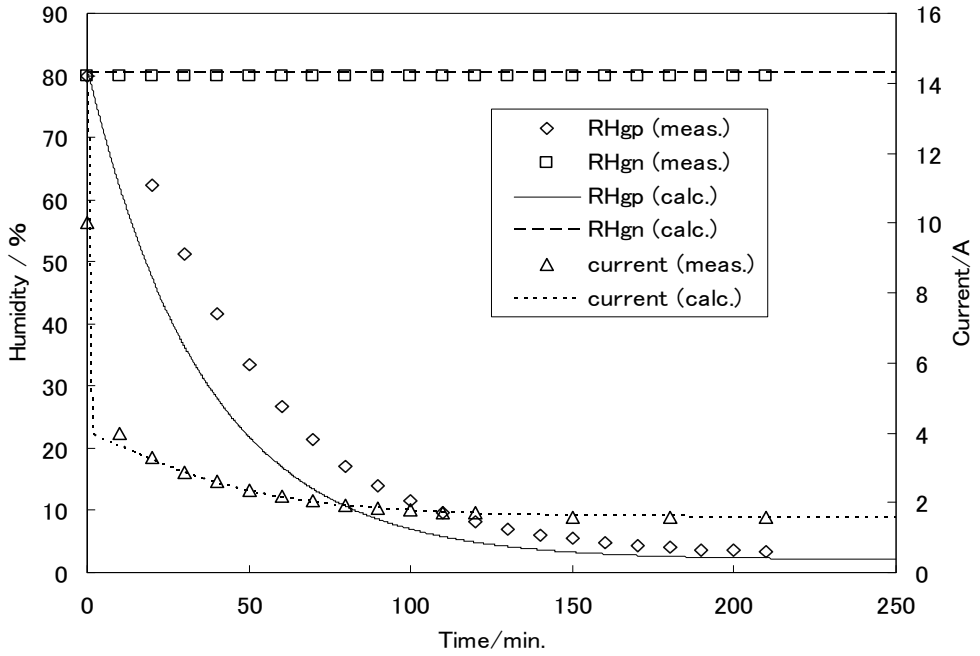

Fig. 2.8 Comparison of experiment and simulation on the humidity change of 51 dm^3 space under the outer condition of 293 K, 80% humidity.

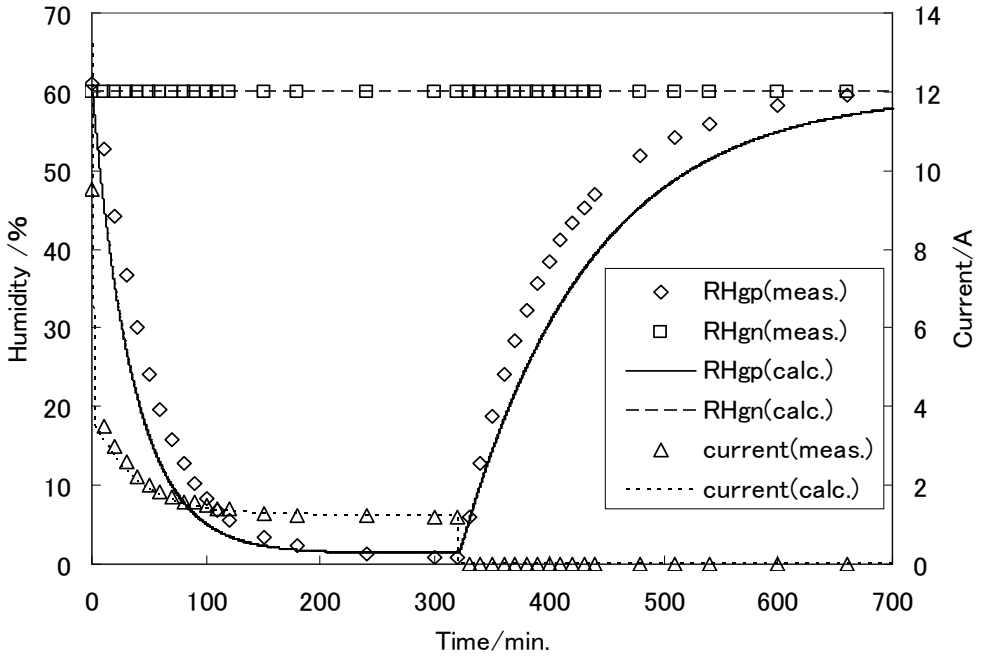

Fig. 2.9 Comparison of experiment and simulation on the humidity change of 51 dm^3 space under the outer condition of 303 K, 60% humidity

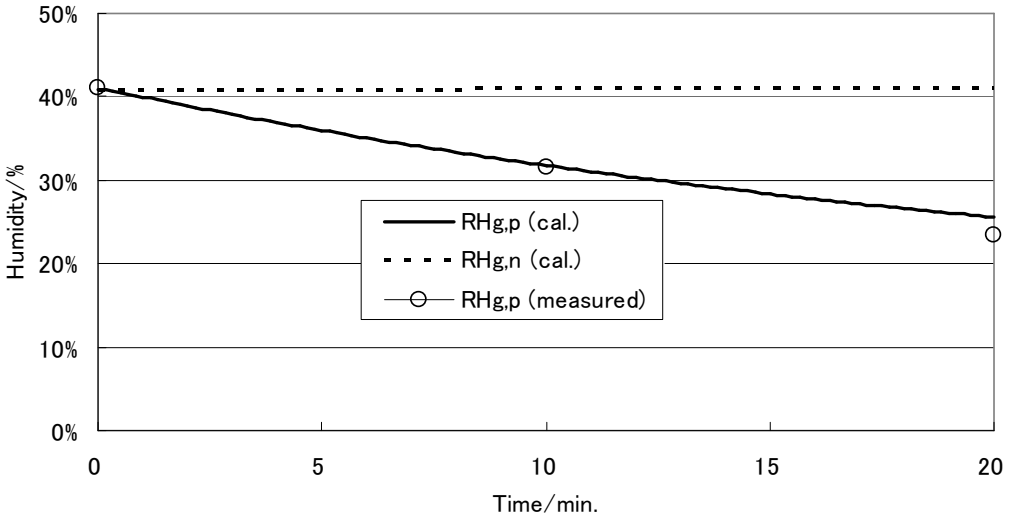

(a) Humidity change in the chamber

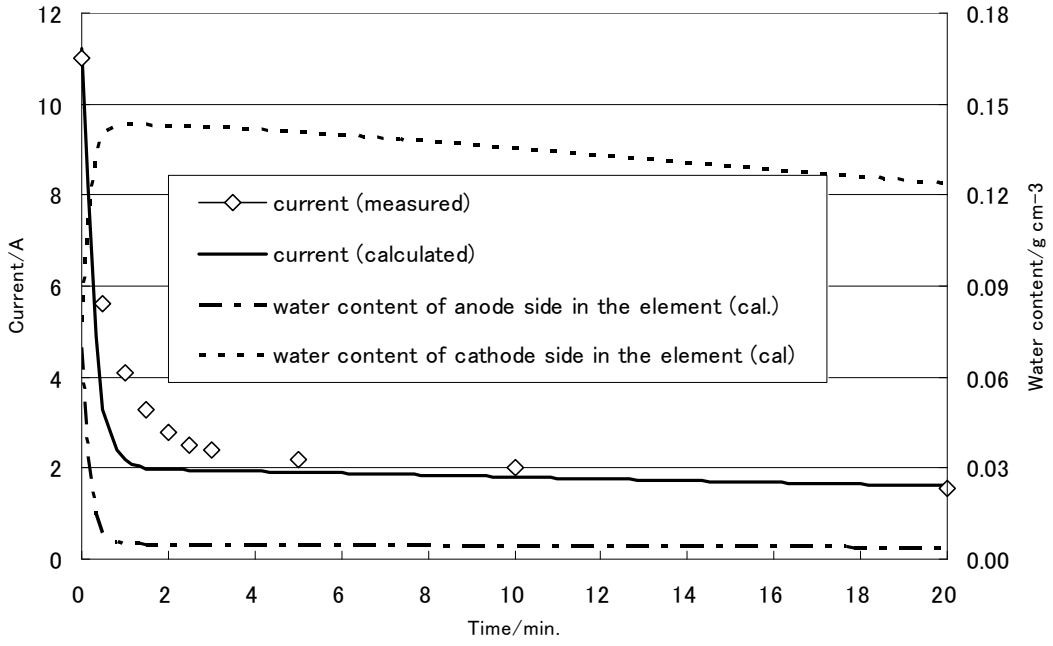

(b) Changes in current and water content

Fig. 2.10 Initial change in current and water contents of the dehumidifying element with the area of 100 cm^2 during dehumidification of a chamber with the volume 50 ℓ (temperature and humidity outside the chamber were kept at 293K and 40%)

similar to the measured ones. Figure 2.9 shows another example of the changes in the humidity and current after switch-on at t=0 and switch-off at around 320 min. After switch off, the humidity in the chamber recovered to the ambient humidity. The time variations in the humidity of the dehumidifying chamber and the current for simulation are similar to those of the experiment. Figure 2.10 shows detailed comparison of the initial change in current and water content between the experiment and calculation under the condition of 293 K and 40%. The initial change by calculation agrees well with that by experiment.

From the simulation, the rapid decrease of current at the early stages just after switching-on of the device is found to be caused by the decrease of water content in the element near the anode that causes the increase in resistance of the element. This is caused by electrolysis of the water in the element. As a result, the water content becomes lower at the anode side and higher at the cathode side. Thus a gradient of water content is formed in the element. The rapid decrease of current occurs during this period. After forming the gradient in the water distribution, dehumidification of the space begins and a current change begins to follow the humidity change in the space.

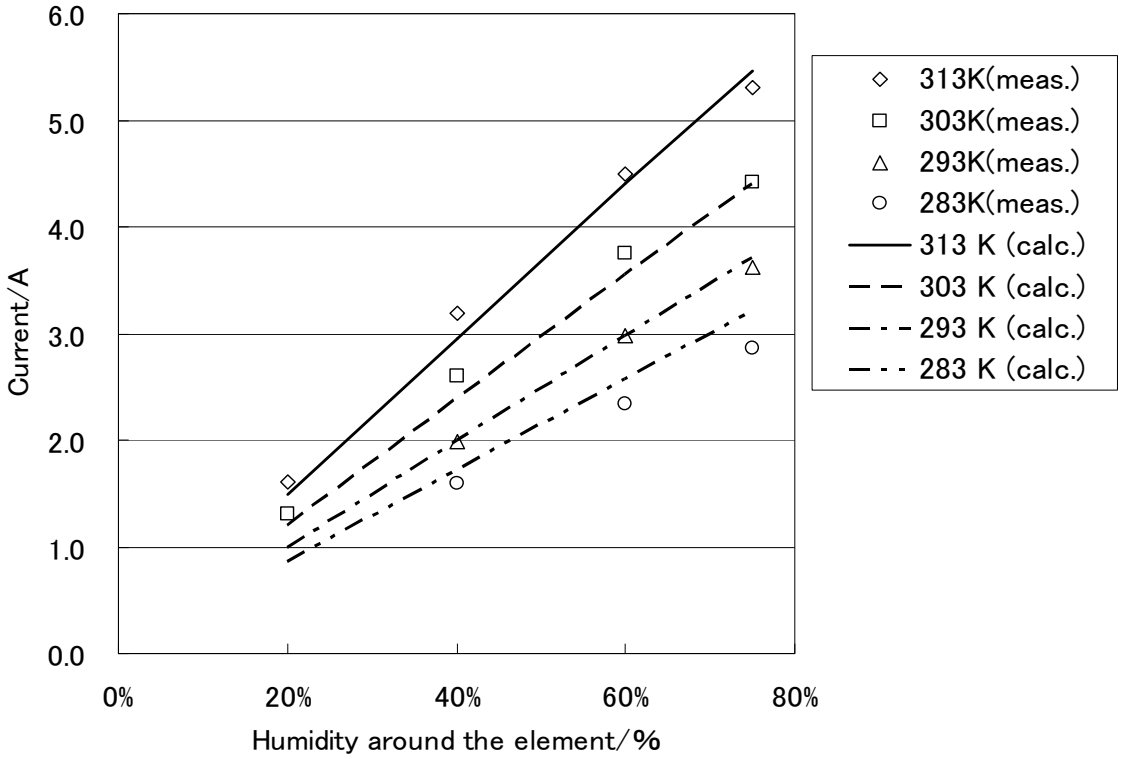

Fig. 2.11 Steady state current flowing in the dehumidifying element exposed in open air (S=100 cm^2, under the condition $\rho_{g,p} = \rho_{g,n}$)

Figure 2.11 shows a comparison of the steady-state current calculated by the model with the measurement. The steady-state current flowing in the dehumidifying element of area 100 cm^2 was measured under the condition in which the dehumidifying element was exposed in open air (that means $\rho_{g,p}=\rho_{g,n}$). The calculated results are similar to those of the measurement. Thus, this model seems to be valid at least in the range shown in Fig.2.11.

2.5 Discussion

The two-layer model expresses both the transient characteristics and the steady-state characteristics of the dehumidification of the device using an SPE membrane very well. Thus, the model can be assumed to reflect the real characteristics of the SPE dehumidifying device.

The ratio of the water content in the membrane to that in the ambient air mainly depends on the temperature under the equilibrium condition. The difference in potential energy W_s (= $4500R$) of water between that in the air and that in the membrane (Nafion 117) is estimated to be 37.3 kJ mol^{-1} from the curve in Fig. 2.5. This is slightly lower than the vaporization energy of liquid water (= 40.7 kJ mol^{-1}). The energy W_s is around the vaporization energy of liquid water, therefore, the water content in the membrane also depends on the relative humidity. Hinatsu et.al. reported previously that the water content of Nafion 117 depends on the relative humidity of the space surrounding the membrane[4]. Water contents in this experiment are compared with those by Hinatsu et al. in Table 2.4. The water content in the present work agrees with the results of Hinatsu et al.

Table 2.4 Comparison of water content vs. relative humidity

	Our experiment		Results of Hinatsu et al.[4]	
RH/%	$gH_2O/gSPE$	$molH_2O/molSO_3H$	$gH_2O/gSPE$	$molH_2O/molSO_3H$
40	0.04	2.4	0.05	3
60	0.06–0.07	3.8–4.3	0.06	4
80	0.08–0.09	5.1–5.9	0.09	6

The water vapor transmission rate (q) is defined as the amount of water vapor (Q) passing through a membrane per unit time and unit area and is given by eq.(2-30) . From the two-layer model, the water vapor permeability coefficient (P) of the dehumidifying element is given by eq.(2-31) as a function of parameters used in the model.

$$q \equiv \frac{Q}{St} = \frac{D}{L}\frac{\kappa_g}{\kappa_s + 2D/L}(\rho_{g,n} - \rho_{g,p}) = \frac{D}{L}\frac{\kappa_g m_o}{\kappa_s + 2D/L}\frac{(p_{g,n} - p_{g,p})}{RT_g} = P\frac{(p_{g,n} - p_{g,p})}{L} \quad (2\text{-}30)$$

$$P = D\frac{\kappa_g}{\kappa_s + 2D/L}\frac{m_o}{RT_g} \quad (2\text{-}31)$$

Where m_0 is the mass of one-mol water.

The diffusion coefficient obtained by the present study is 6.2×10^{-7} ($cm^2\ s^{-1}$) for Nafion 117 with the water molecules per sulfonate (λ = 2~6 (H_2O/SO_3H)) under temperatures of 293 K to 303 K. Yeo et al. measured the diffusion coefficient of water in Nafion 115 with λ=22 and gave the following equation [2].

$$D = 6.0\times10^{-3}\times\exp\left(-20.2\times10^{3}/(RT_g)\right) \qquad cm^2 \quad s^{-1} \qquad (2-32)$$

This equation gives 1.9×10^{-6} $cm^2\ s^{-1}$ at T_g= 303 K. Zawodzinski et al. also show water diffusion coefficients in Nafion 117 as a function of λ and give coefficients of 0.6×10^{-6} to 3.7×10^{-6} $cm^2\ s^{-1}$ for λ from 2 to 6 at 303 K [6]. Nguyen et al. investigated the diffusion coefficients of water in Nafion of different thicknesses under different temperatures [3]. Nguyen showed that the diffusion coefficient for Nafion 117 with a water content of 2% - 6% of dry membrane weight is 1.5×10^{-7} - 6.0×10^{-7} $cm^2\ s^{-1}$ at 333 K [3]. According to these reports, the diffusion coefficient depends on temperature and water content. It was not shown here that a temperature dependence of the diffusion coefficient because they did not have sufficient data for the determination of this dependence. However, the my opinion is that the diffusion coefficient in the membrane depends on temperature as reported by those papers. Our simulation by the two-layer model can be improved by introducing a dependence on temperature and water content.

The number of water molecules α carried by a proton moving toward the cathode is referred to as the electro-osmotic drag coefficient [6]. It was obtained as 1.3 from the experiment under temperatures of 293 K to 303 K and relative humidities of 40% to 80%. Zawodzinski et al. reported that the electro-osmotic drag coefficient for Nafion 117 exposed to liquid water at 303 K is 2.5 to 2.9 with λ=22 and they suggest a substantial decrease in the electro-osmotic drag coefficient as the water content is lowered[6]. The difference in our result from theirs may result from the difference in the water contents in our element from that of Zawodzinski et al.

Typical values of our results under steady-state and transient conditions in the environment of 303 K, 60% are shown in Table 2.5. Under the steady-state condition, water transported by both current and electro-osmotic drag is cancelled by back diffusion.

As a result, dehumidifying capability at the steady-state condition is zero. The dehumidifying capability under the transient condition shown in Table 2.5 is calculated to be 4.1×10^{-4} g s^{-1}. From the simulation, the amount of water transported by electro-osmotic drag is nearly cancelled by that from back diffusion.

The electrolytic membrane of the element is covered by porous electrodes on both of its surfaces. Therefore, the actual area to transport water across the surfaces may be less than the area S of the membrane itself. We assume in our work that the water transportation area across the surfaces is S for simplification. The D and a estimated by the present work may be influenced by this assumption.

Table 2.5 Typical values by simulation

	steady state condition shown in (2−c) of Fig.2	transient condition shown in (2−b) of Fig.2
Tg / K	303 K	303 K
RHg,p / %	0.5	55
RHg,n / %	60	60
I / A	1.3	3.7
Water by current	1.2×10^{-4} g s^{-1}	3.5×10^{-4} g s^{-1}
water by electro−osmotic drag	3.1×10^{-4} g s^{-1}	9.0×10^{-4} g s^{-1}
water by back diffusion	4.3×10^{-4} g s^{-1}	8.4×10^{-4} g s^{-1}
net water transported	0. g s^{-1}	4.1×10^{-4} g s^{-1}

The electrical resistance of the dehumidifying element was measured using an impedance analyzer with a frequency controllable AC source. Anantaraman et al. reported the effect of humidity on the conductivity of Nafion 117 [5]. They measured the conductance by a high frequency impedance method. Electrical resistivity at 303 K measured by Anantaraman et al depends much more on the relative humidity in the surrounding air than that obtained in the present paper. However, the values are nearly the same around a relative humidity of 50%.

2.6 Conclusions

A two-layer model for a dehumidifying device making use of a solid polymer electrolyte (SPE) membrane is presented. By comparing the model simulation with experimental measurements, the model is found to express the characteristics of the device well. This model is effective in understanding the behavior of such a device using an SPE membrane. The ratio of the water content in the SPE membrane to that in ambient air under equilibrium conditions is presented as a function of temperature. The electrical resistance of the dehumidifying element using the SPE membrane was

measured by making use of an AC voltage at 5 Hz. The resistance was expressed as a function of temperature and the water content in the membrane. The resistance is used for estimation of the current flowing through the dehumidifying element and it can be approximated by eq. (2-29) during operation. The temperature dependency of the diffusion of water and the electro-osmotic drag in the membrane were not reflected in this chapter. The simulation could be improved by introducing this dependency.

References

[1] Yamauchi S, Sakuma S, Nakatani H, Mitsuda K., "Mass Transfer Equations of Electrolytic Water Removal Device Using Solid Polymer Electrolytic Membrane", Trans. IEE of Japan, Vol. 120-A, No. 5, pp. 607-613, 2000.

[2] Yeo S.C, Eisenberg A, "Physical Properties and Supermolecular Structure of Perfluorinated Ion-Containing (Nafion) Polymers", J. of Applied Polymer Science, Vol. 21,pp. 875-898, 1977.

[3] Ngyen T, Guante J, and Vanderborgh N, "Ion Transport through Polyperfluorosulfonic Acid Membranes", Mat. Res. Soc. Symp. Proc. ,Vol. 135, pp. 367-376, 1989.

[4] Hinatsu JT, Mizuhara M, Takenaka H, "Water Uptake of Perfluorosulfonic Acid Membranes from Liquid Water and Water Vapor", J Electrochem. Soc., Vol. 141, No. 6, pp.1493-1498, 1994.

[5] Anantaraman AV, Gardner CL, "Studies on ion-exchange membrane", J Electroanalytical Chem., Vol. 414, pp. 115-120, 1996.

[6] Zawodzinski TA Jr., Derouin C, Radzinsli S, Sherman RJ, Smith VT, Springer TE, Gottesfeld S, "Water Uptake by and Transport Through Nafion 117 Membranes", J Electrochem. Soc., Vol. 140, No. 4, pp. 1041-1047, 1993.

[7] Ikuta H, "AC impedance method for solid electrolyte", Electrochemistry, Vol. 68, No.5, pp. 356-360, 2000.

Chapter 3

Analysis of dehumidifying characteristics of solid polymer electrolytic (SPE) dehumidifier

Abstract A two-layer model for an SPE dehumidifier is applied to a system in which the chamber to be dehumidified has some leakage area. By introducing this area, the attainable humidity in the chamber, which is the steady-state humidity to be attained after a long-time dehumidification, can be defined. Experimental results of dehumidification by an SPE dehumidifier are compared to the calculations based on the two-layer model for the SPE dehumidifier, which was presented in chapter 2. Equations for the two-layer model are simplified by making use of assumptions for the current characteristics and a constant environmental condition, and it is reduced to equations including a differential equation on the time variation of the humidity in the chamber. The differential equation to describe the attainable humidity in the chamber and time constant for the dehumidification is obtained. The current flowing in the dehumidifier under steady-state conditions is also given as a function of the humidities in the spaces facing the anode and the cathode. A diagram to estimate the attainable humidity and the time required for dehumidification from the dehumidifying area and leakage area is also presented.

List of symbols

Variables

D : Diffusion coefficient of water in the dehumidifying element / $cm^2\ s^{-1}$

e : Electron charge = 1.602×10^{-19} / C

I : Current of the dehumidifying element /A

κ_g : Coefficient relevant to the diffusion velocity of water from the air to the SPE membrane /cm s^{-1}

κ_s : Coefficient relevant to the diffusion velocity of water from the membrane to the air /cm s^{-1}

L : Thickness of the dehumidifying element = 0.017 /cm

N_A : Avogadro's number = 6.02×10^{23} /mol^{-1}

RH : Relative humidity / %

Rs : Electrical resistance of the dehumidifying element / Ω

S : Area of the dehumidifying element /cm^2

$S\ell$: Equivalent leakage area with the rate constant kg of water transfer /cm^2

t : Time /s

Tg : Temperature of the gas space surrounding the dehumidifying element /K

Us : Voltage applied to the dehumidifying element = 3 /V

$V_{g,p}$, $V_{g,n}$: Volumes of the spaces facing the anode and the cathode /cm^3, respectively

α : The average number of water molecules carried by a proton moving to the cathode

ρ_g, ρ_s : Water density in the air surrounding the dehumidifying element and water content of the element /g cm^{-3}, respectively

$\rho_{g,p}$, $\rho_{g,n}$: Water density in the air facing the anode (positive electrode) and cathode (negative electrode) /g cm^{-3} , respectively

$\rho_{s,p}$, $\rho_{s,n}$: Water contents in the anode half and the cathode half of the dehumidifying element defined by two-layer model of the dehumidifier /g cm^{-3}

Subscripts

G : Gas space

N : Negative electrode or cathode

P : Positive electrode or anode

S : Solid polymer electrolytic dehumidifying element

3.1 Introduction

Ionic membranes have been used increasingly in many industrial areas such as fuel cell technology, chemical engineering for water improvement. Several studies on the transport properties of water and ions through the membranes and a fuel cell model have been reported [1,2,3]. These studies are quite important for understanding the transport mechanism to predict the optimum operating conditions for industrial use. Zawodzinski et al. investigated the transport properties through a Nafion 117 membrane and described the membrane conductivity as a function of the water content as well as the temperature dependence of the membrane conductivity[1]. Anantaraman et al. also reported the effect of humidity on the conductivity of Nafion [2]. However, these studies evaluated the conductivity of the

electrolytic membrane itself. Although such conductivity is necessary for constructing a complete model, a combined element made from the electrolytic membrane and the electrodes on the membrane surfaces are used in practical applications. Therefore, the impedance or current characteristics of the entire element is necessary for practical applications.

A dehumidifying device using a SPE membrane has been developed as a protective measure against problems caused by high humidity. This device consists of a proton-conductive solid polymer electrolyte and porous electrodes with a catalytic layer composed of noble metal particles. This device can dehumidify the space facing the anode and humidify the space facing the cathode when a DC voltage is applied to the electrodes [4]. The dynamic characteristics of the SPE dehumidifier were numerically analyzed and found to be well explained by a two-layer model for the SPE dehumidifier [5]. The input parameters used in our model were obtained from our experiments. The relation of the water content and humidity obtained in our experiments were similar to that reported by Hinatsu et al. [6]. The dependence of the electrical conductance of the SPE dehumidifiers on the water content in our experiment is not as high as the dependence of the electrical conductance of the membrane itself (Nafion 117) reported by Anantaraman et al. [2], though a direct comparison could be difficult because of the difference in the components.

SPE dehumidifiers are used in containers for scientific instruments, outdoor-type vessels containing electrical and electronic devices, etc. For these practical applications, it is very important to estimate how long it takes to reach the required humidity or what the attainable humidity is. The time to reach the required humidity and finally attainable humidity after a long dehumidification depends on the leakage area of the vessel.

The humidity change in a chamber and current change flowing in the dehumidifying element were measured and compared to those calculated by a simulation based on a two-layer model. The formula for the current under steady-state conditions is given as a function of the humidity of the spaces facing the anode and cathode. A differential equation, which gives the time constant and the humidity to be finally attained under steady-state conditions, are derived from the two-layer model for the SPE dehumidifier. A diagram to give the relation of the dehumidifying capability of a SPE dehumidifier and attainable humidity in the chamber is derived. This diagram is very useful for practical use of the SPE dehumidifier.

3.2 Application of two-layer model of SPE dehumidifier to a system in which the chamber to be dehumidified has a leakage area

The basic equations for the two-layer model were proposed in chapter 2 and analysis by the two-layer model was made for a chamber with no leakage area[5]. It was concluded that the model was valid for estimations of the current change and dehumidifying performance. In this chapter, the model is applied to a system in which the chamber has some leakage area. Figure 3.1a and 3.1b show the water flow of an SPE dehumidifier expressed by the two-layer model and the system of dehumidification by the dehumidifier in which a chamber has a leakage area (Sℓ), respectively. The basic equations of the two-layer model can be modified as eqs.(3-1) to (3-4). Eqs.(3-1) and (3-2) include the terms which express the leakage area (Sℓ) between the inside and outside of the chamber. It is very difficult to determine the leakage area because the quantity of the actually leaked water may change depending on the shape and position of the area, etc. Hence, we define in this chapter that the leakage area Sℓ is the equivalent area based on the assumption that the rate constant for water transfer is κ_g, which is the coefficient relevant to the diffusion velocity of water from the air to the SPE membrane defined in chapter 2[5]. Therefore, the leakage area must be determined from the humidity under steady-state conditions which is realized after a long dehumidification time of the chamber.

Eqations (3-5) to (3-7) define the current characteristics of the SPE dehumidifier, which were also obtained from our study shown in chapter 2 [5]. It was found that the electrical resistance of the dehumidifier strongly depends on the water content $\rho_{s,p}$ of the anode side in the dehumidifying element [5].

$$V_{g,p}\frac{d\rho_{g,p}}{dt} = S(\kappa_s\rho_{s,p} - \kappa_g\rho_{g,p}) + S\ell\kappa_g(\rho_{g,n} - \rho_{g,p}) \tag{3-1}$$

$$V_{g,n}\frac{d\rho_{g,n}}{dt} = S(\kappa_s\rho_{s,n} - \kappa_g\rho_{g,n}) - S\ell\kappa_g(\rho_{g,n} - \rho_{g,p}) \tag{3-2}$$

$$\frac{LS}{2}\frac{d\rho_{s,p}}{dt} = -S(\kappa_s\rho_{s,p} - \kappa_g\rho_{g,p}) + \frac{DS(\rho_{s,n} - \rho_{s,p})}{L} - \frac{18I(1+2\alpha)}{2eN_A} \tag{3-3}$$

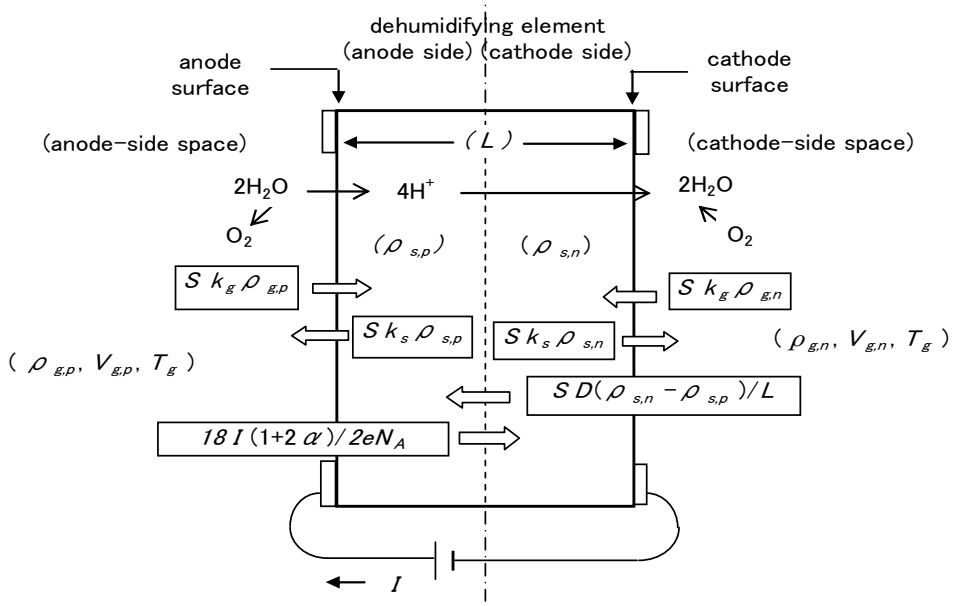

(a) Water flow expressed by two-layer model for SPE dehumidifier

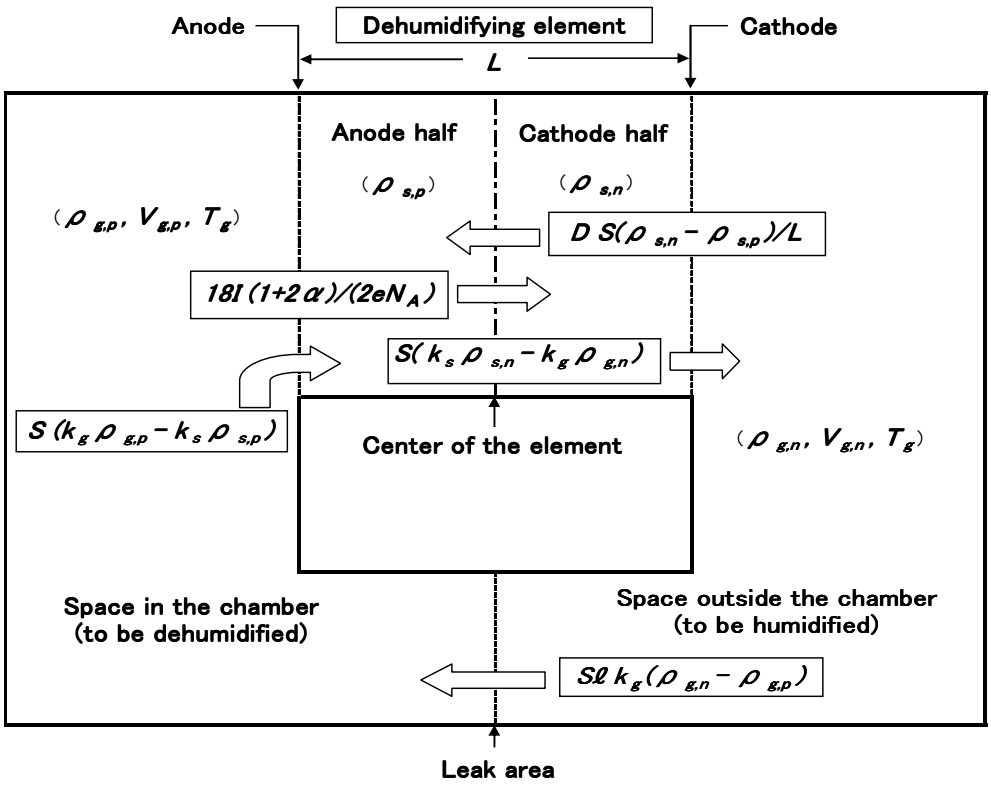

(b) Water transfer by SPE dehumidifier when the chamber has a leakage area

Fig.3.1 Two-layer model for SPE dehumidifier and water transfer by SPE dehumidifier when the chamber has a leakage area Sℓ.

$$\frac{LS}{2}\frac{d\rho_{s,n}}{dt} = -S(\kappa_s\rho_{s,n} - \kappa_g\rho_{g,n}) - \frac{DS(\rho_{s,n} - \rho_{s,p})}{L} + \frac{18I(1+2\alpha)}{2eN_A} \qquad (3\text{-}4)$$

$$I = \frac{U_s}{R_s} = \frac{U_s S}{\frac{B(T_g)}{\rho_{s,p}} + r_{s0}} \cong \frac{U_s S\rho_{s,p}}{B(T_g)} \qquad (3\text{-}5)$$

$$B(T) = 6.7\times10^{-2}\times\exp(670/T_g) \qquad /\Omega cm^2 g\, cm^{-3} \qquad (3\text{-}6)$$

$$r_{s0} = 17.3 \qquad /\Omega cm^2 \qquad (3\text{-}7)$$

If the time variation of the water content in the dehumidifying element is much lower than the other terms, eqs. (3-3) and (3-4) can be reduced to the following equations.

$$\frac{d\rho_{s,p}}{dt} = 0, \quad \frac{d\rho_{s,n}}{dt} = 0, \quad then$$

$$\rho_{s,p} = \frac{\kappa_g(\frac{D}{L} + \kappa_s)\rho_{g,p} + \kappa_g\frac{D}{L}\rho_{g,n} - \kappa_s\frac{18I(1+2\alpha)}{2eN_AS}}{\kappa_s(\frac{2D}{L} + \kappa_s)} \qquad (3\text{-}8)$$

$$\rho_{s,n} = \frac{\kappa_g\frac{D}{L}\rho_{g,p} + \kappa_g(\frac{D}{L} + \kappa_s)\rho_{g,n} + \kappa_s\frac{18I(1+2\alpha)}{2eN_AS}}{\kappa_s(\frac{2D}{L} + \kappa_s)} \qquad (3\text{-}9)$$

Substituting equation (3-8) into equation (3-1), equation (3-1) can also be reduced to the following form.

$$\frac{d\rho_{g,p}}{dt} + \frac{k_g}{V_{g,p}}\left\{\frac{S\frac{D}{L} + S\ell\left(\frac{2D}{L} + k_s\right)}{\frac{2D}{L} + k_s}\right\}\rho_{g,p} = \frac{k_g}{V_{g,p}}\left\{\frac{S\frac{D}{L} + S\ell\left(\frac{2D}{L} + k_s\right)}{\frac{2D}{L} + k_s}\right\}\rho_{g,n}$$
$$-\frac{k_s}{V_{g,p}}\left\{\frac{9(1+2\alpha)I}{(\frac{2D}{L} + k_s)eN_A}\right\} \qquad (3\text{-}10)$$

Equation (3-10) can be valid when the time variation in the water content in the element can be neglected. An equation similar to eq. (3-10) could be derived by substituting eq. (3-9) into eq. (3-2).

Substituting eq.(3-5) into eq.(3-8), the following equations for the water content of the anode side of the dehumidifier and the current are obtained.

$$\rho_{s,p} = \frac{\kappa_g(\frac{D}{L}+\kappa_s)\rho_{g,p} + \kappa_g \frac{D}{L}\rho_{g,n}}{\kappa_s\left\{\frac{2D}{L}+\kappa_s+\frac{18(1+2\alpha)U_s}{2eN_A B(T_g)}\right\}} \tag{3-11}$$

$$I = \frac{U_s S}{B(T)} \frac{k_g(\frac{D}{L}+k_s)\rho_{g,p} + k_g \frac{D}{L}\rho_{g,n}}{k_s\left\{\frac{2D}{L}+k_s+\frac{18(1+2\alpha)U_s}{2eN_A B(T_g)}\right\}} \tag{3-12}$$

Substituting eq.(3-11) into eq.(3-1), then the set of basic equations is reduced as follows.

$$\frac{d\rho_{g,p}}{dt} + \frac{\kappa_g S}{V_{g,p}}\left\{\frac{\frac{D}{L}+\frac{18(1+2\alpha)U_s}{2eN_A B(T)}}{\kappa_s+\frac{2D}{L}+\frac{18(1+2\alpha)U_s}{2eN_A B(T_g)}}+\frac{S\ell}{S}\right\}\rho_{g,p} = \frac{\kappa_g S}{V_{g,p}}\left\{\frac{\frac{D}{L}}{\kappa_s+\frac{2D}{L}+\frac{18(1+2\alpha)U_s}{2eN_A B(T_g)}}+\frac{S\ell}{S}\right\}\rho_{g,n} \tag{3-13}$$

$$\frac{d\rho_{g,n}}{dt} + \frac{\kappa_g S}{V_{g,n}}\left\{\frac{\frac{D}{L}}{\kappa_s+\frac{2D}{L}+\frac{18(1+2\alpha)U_s}{2eN_A B(T_g)}}+\frac{S\ell}{S}\right\}\rho_{g,n} = \frac{\kappa_g S}{V_{g,n}}\left\{\frac{\frac{D}{L}+\frac{18(1+2\alpha)U_s}{2eN_A B(T)}}{\kappa_s+\frac{2D}{L}+\frac{18(1+2\alpha)U_s}{2eN_A B(T_g)}}+\frac{S\ell}{S}\right\}\rho_{g,p} \tag{3-14}$$

Eq.(3-13) can be also written in the following form.

$$\frac{dRH_{g,p}}{dt} + \frac{\kappa_g S}{V_{g,p}}\left\{\frac{\frac{D}{L}+\frac{18(1+2\alpha)U_s}{2eN_A B(T)}}{\kappa_s+\frac{2D}{L}+\frac{18(1+2\alpha)U_s}{2eN_A B(T_g)}}+\frac{S\ell}{S}\right\}RH_{g,p} = \frac{\kappa_g S}{V_{g,p}}\left\{\frac{\frac{D}{L}}{\kappa_s+\frac{2D}{L}+\frac{18(1+2\alpha)U_s}{2eN_A B(T_g)}}+\frac{S\ell}{S}\right\}RH_{g,n} \tag{3-13a}$$

Equations (3-13) and (3-13a) can be used for the estimation of the time variation of the humidity in the chamber under the conditions that the rate of water transmitted from the anode space to the cathode space through the dehumidifier is much higher than that of the water content change in the dehumidifier.

From eqs.(3-13) and (3-13a), useful parameters of the time constant that is the time required for dehumidification and the steady-state humidity to be attained after a long-time dehumidification of the chamber can be

obtained as follows.

$$\left.\frac{RH_{g,p}}{RH_{g,n}}\right|_{t=\infty} = \frac{\dfrac{D/L}{\kappa_s + 2D/L + 18(1+2\alpha)U_s/2eN_A B(T_g)} + \dfrac{S\ell}{S}}{\dfrac{D/L + 18(1+2\alpha)U_s/2eN_A B(T_g)}{\kappa_s + 2D/L + 18(1+2\alpha)U_s/2eN_A B(T_g)} + \dfrac{S\ell}{S}} \tag{3-15}$$

$$\tau = \frac{V_{g,p}}{\kappa_g S} \frac{1}{\dfrac{D/L + 18(1+2\alpha)U_s/2eN_A B(T_g)}{\kappa_s + 2D/L + 18(1+2\alpha)U_s/2eN_A B(T_g)} + \dfrac{S\ell}{S}} \tag{3-16}$$

By substituting the values for the SPE dehumidifying element estimated in chapter 2 into eq.(3-13) or (3-13a), the following equations are derived.

$$\frac{d\rho_{g,p}}{dt} + \frac{0.245}{V_{g,p}}(0.96\,S + S\ell)\rho_{g,p} = \frac{0.245}{V_{g,p}}(0.021\,S + S\ell)\rho_{g,n} \tag{3-17}$$

$$\frac{dRH_{g,p}}{dt} + \frac{0.245}{V_{g,p}}(0.96\,S + S\ell)RH_{g,p} = \frac{0.245}{V_{g,p}}(0.021\,S + S\ell)RH_{g,n} \tag{3-18}$$

$$\left.\frac{RH_{g,p}}{RH_{g,n}}\right|_{t=\infty} = \frac{0.021\,S + S\ell}{0.96\,S + S\ell} \tag{3-19}$$

$$\tau = \frac{V_{g,p}}{0.245(0.96\,S + S\ell)} \tag{3-20}$$

The coefficients included in these equations were calculated for the ambient temperature of 303K. These coefficients of 0.96 and 0.021 are changed from 0.95 to 0.97 and 0.019 to 0.023, respectively, for the temperature range of 293K to 313K. The dependence of these coefficients on the temperature is very small. Therefore, the estimation by eqs. (3-19) and (3-20) would be approximately valid within this temperature range.

3.3 Experiments

(1) Case 1: Sℓ ≅ 0. The humidity change in a chamber with a volume of 51 dm^3 and with a leakage area as small as possible was measured under the conditions that the temperature and humidity surrounding the chamber remain constant. The time variation of the current was also measured.

The measured humidity and current are compared to the calculations based on a two-layer model.

(2) Case 2: $S\ell \cong \infty$. The current of the dehumidifier located in the open air under the steady-state conditions is measured and compared to the calculations based on a two-layer model.

The quantity of the actual water leakage is the rate coefficient of the water transferred through the leakage multiplied by the leakage area. The rate coefficient depends on the shape and position of the area as well as the area itself. Therefore, we define that the leakage area $S\ell$ is the equivalent area based on the assumption that the rate coefficient for water transfer is κ_g. It can be estimated by making use of eq. (3-15) from the experiment of the attainable humidity. By introducing such equivalent leakage areas, the attainable humidity determined by eq. (3-15) and/or (3-19) can be defined.

3.3.1 Experiment case(1) and calculation using two-layer model

A chamber with a volume of 51 dm^3 and a dehumidifying element with an area of 100 cm^2 were used in this experiment case (1).

Figure 3.2 shows a comparison of the measured dehumidification characteristics (293K) with the one calculated using the basic formulas (3.1) to (3.6) of a two-layer model. The calculation of the current change and humidity change in the chamber well agree with the measured one over the entire processes. The dehumidification started at t=0 by switching-on the DC supply in this experiment. A rapid decrease in the current is seen just after switching-on in Fig. 3.2 and it was explained in chapter 2 that this is caused by the rapid decrease in the water content on the anode side in the element to form a gradient distribution of the water content in the element as shown in Fig.3.2(b). After the formation of a gradient-shaped distribution, the current change mainly depends on the humidity change in both spaces facing the anode and the cathode. If the change of the humidity in the chamber is slow, the water content in the dehumidifying element would slowly change and be nearly the same as that under steady-state conditions, depending on both the humidity inside and outside the chamber.

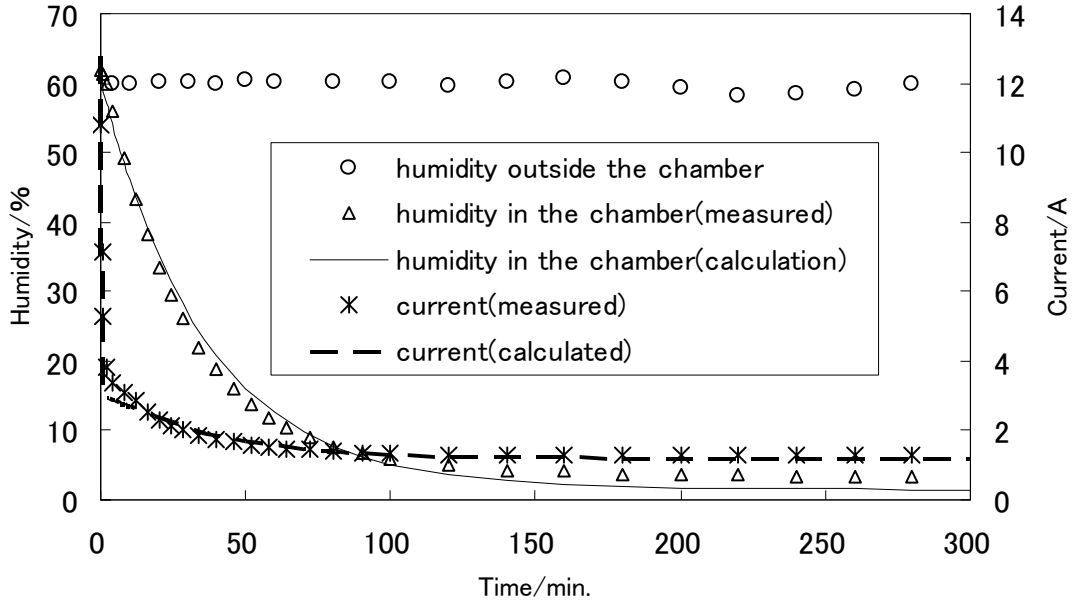

(a) Long-time dehumidifying characteristics of the SPE dehumidifier

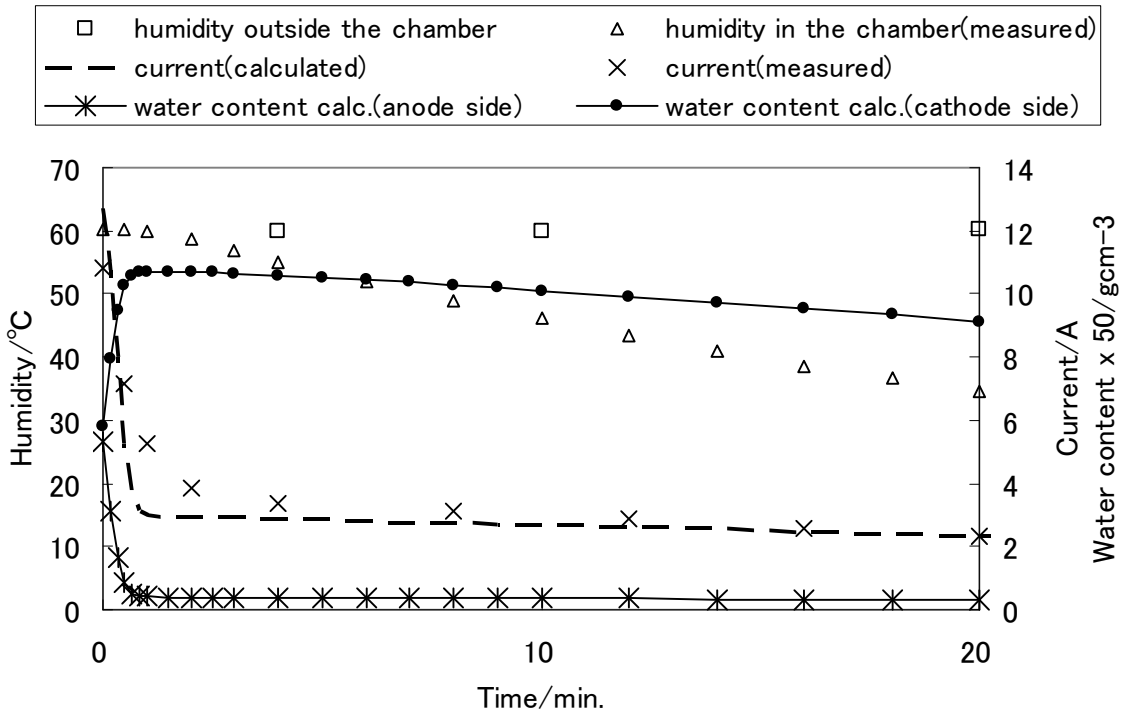

(b) Comparison of initial change in the current

Fig.3.2 Dehumidifying characteristics of the SPE dehumidifier (293K, 60%) (Vg,p = 5 1ℓ, S = 100 cm^2).

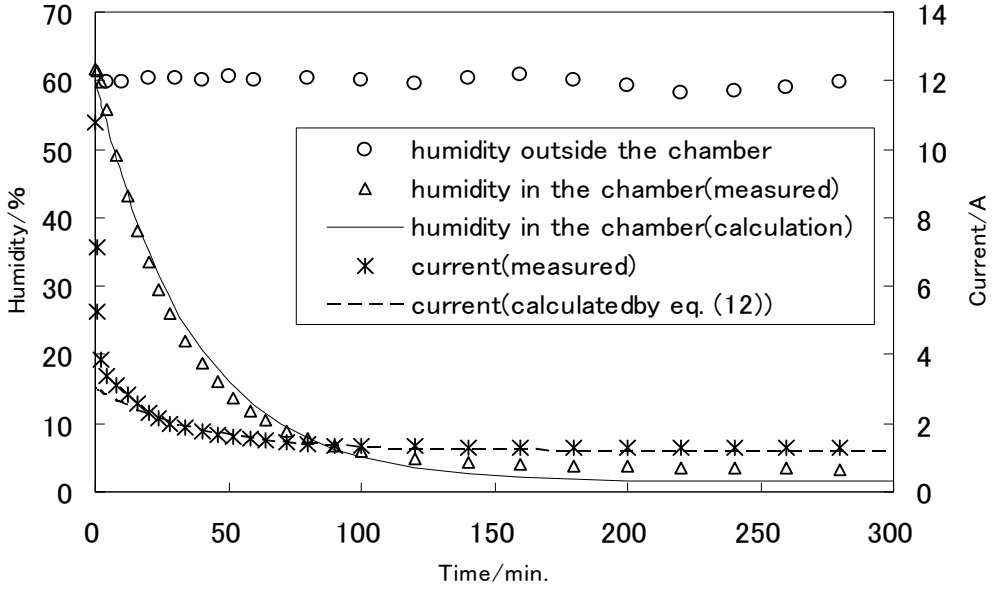

(a) Comparison of measured dehumidifying process and the calculated values

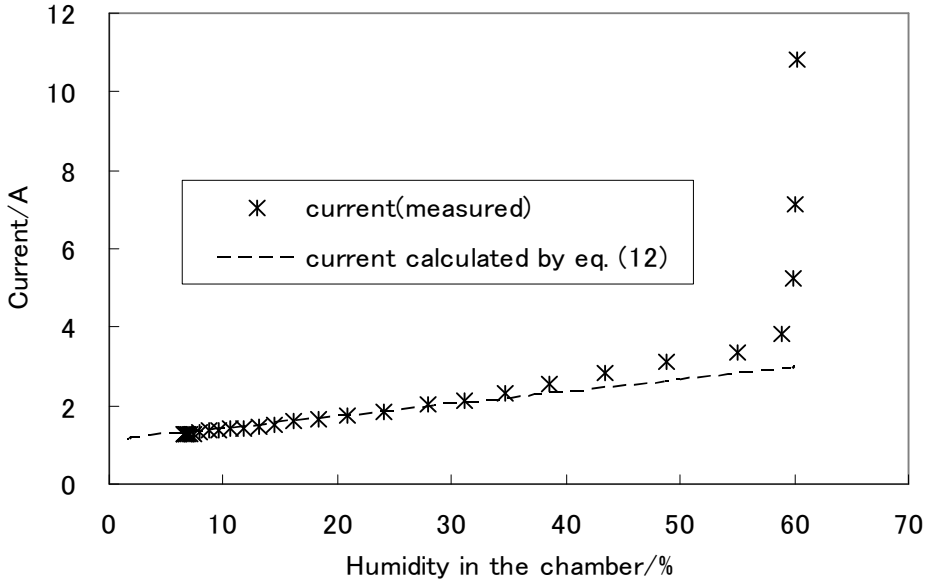

(b) Comparison of measured current and the calculated values using eq. (12)

Fig.3.3 Dehumidifying characteristics of SPE dehumidifier under the conditions that the temperature and humidity outside the chamber are maintained at 293K and 60%, respectively

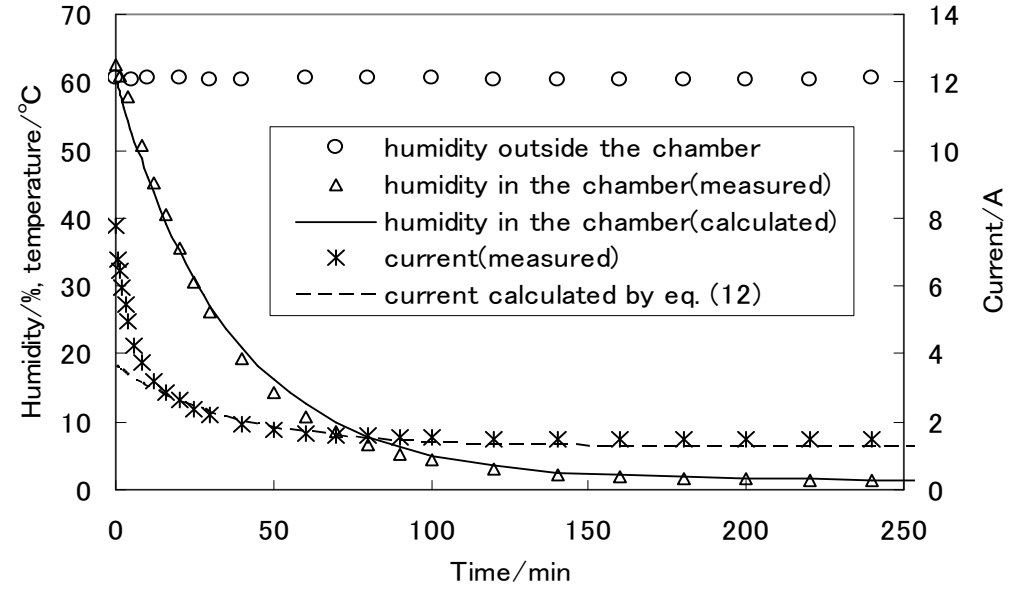

(a) Comparison of measured dehumidifying process and the calculated values

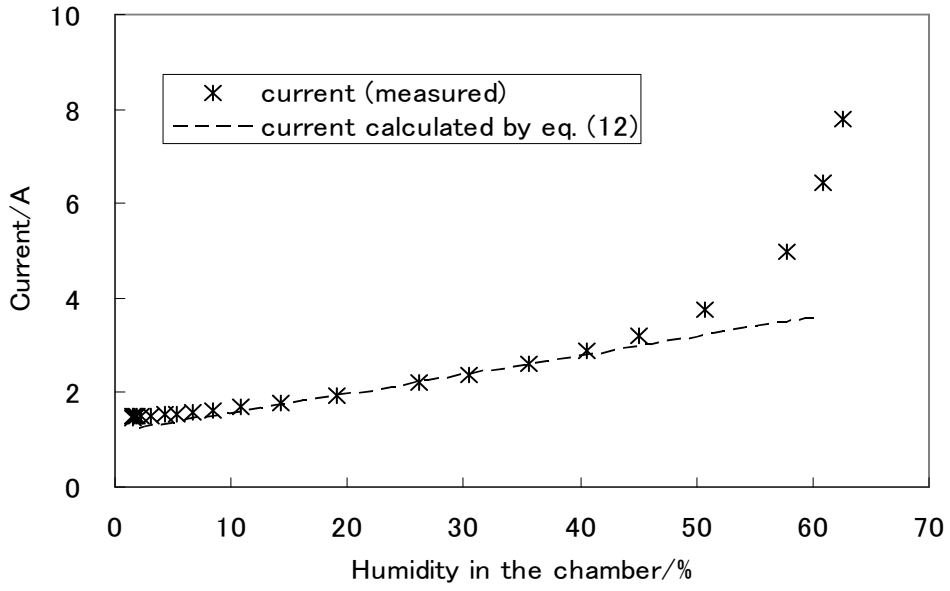

(c) Comparison of measured current and the calculated values using eq. (12)

Fig.3.4 Dehumidifying characteristics of SPE dehumidifier under the conditions that the temperature and humidity outside the chamber are maintained at 303K and 60%, respectively.

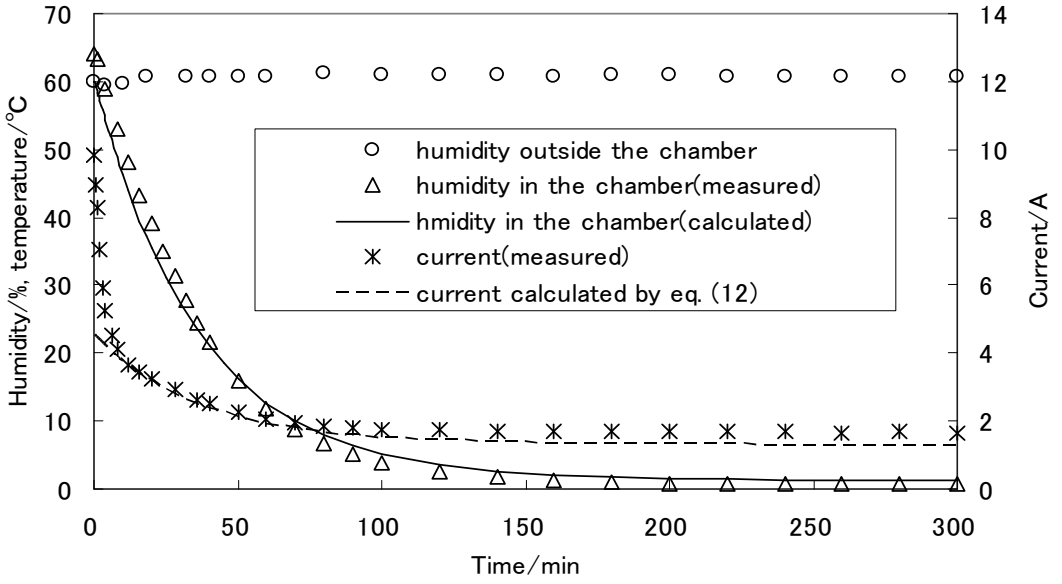

(a) Comparison of measured dehumidifying process and the calculated values

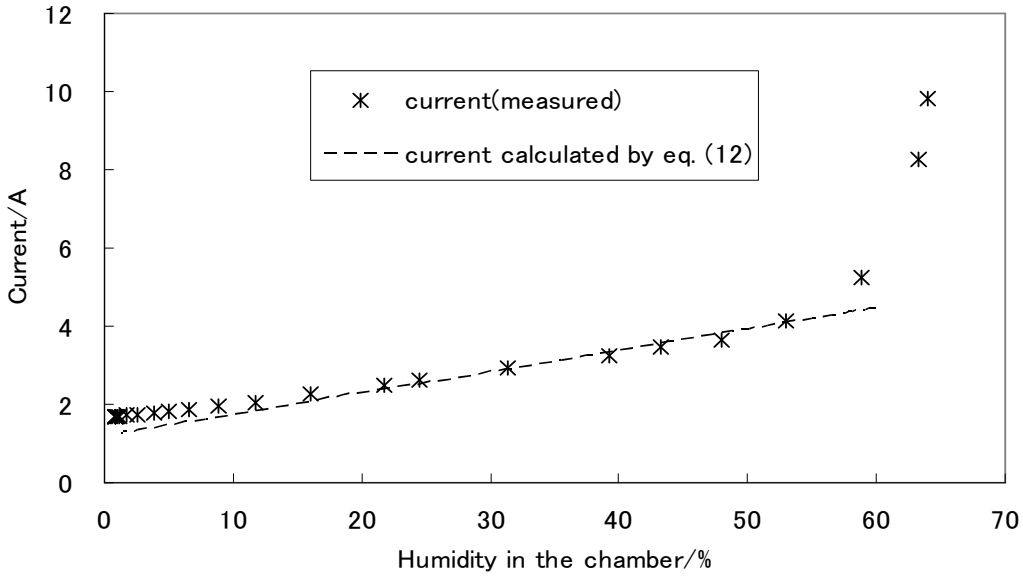

(b) Comparison of measured current and the calculated values using eq. (12)

Fig.3.5 Dehumidifying characteristics of SPE dehumidifier under the conditions that the temperature and humidity outside the chamber are maintained at 313K and 60%, respectively.

Figure 3.3(a) shows a comparison of the measured dehumidification process (293K) of the same data as shown in Fig.3.2 and the one calculated by eq. (3-13), that is derived by using assumptions (3-8) and (3-9). As seen in Fig.3.3(a), the calculations well agree with the measured ones except for the period just after switching-on. From this observation, eqs. (3-8) and (3-9) are assumed to be valid for almost the entire process except for a few minutes just after switching-on. Figure 3.3(b) traces the relation between the current and humidity in the chamber for the same data as shown in Fig.3.3(a). The current calculated by eq. (3-12) is also shown in Fig.3.3(b). The measured current linearly changes with the humidity in the chamber and well agrees with the calculation except for the higher humidity range, which corresponds with the period just after switching-on.

Figures 3.4 and 3.5 are other examples obtained for different temperatures (300K and 313K). As the measured current in these figures agreed with the calculations assuming eq. (3-12), the current for almost the entire period, except for the period just after switching-on, must be nearly the same under steady-state conditions.

3.3.2 Experiment case(2) and calculation by the two-layer model

Figure 3.6 shows a comparison of the calculation and measurement for the relation of the current and humidity surrounding the element. The measurement was made under the condition that the tested dehumidifying element was located in open air. The calculation of the current was made using eq. (3-12). It was found in Fig.3.6 that the calculation well agrees with the measurement. Therefore, eq.(3-12) can determine the steady-state current even for an open air condition.

From the results shown in Fig.3.3 to Fig.3.6, the current under a steady-state condition can be expressed by eq.(3-12) and then the water content in the anode side of the element can also be expressed by eq.(3-11).

When eq.(3-12) is valid, eq.(3-1) can be reduced to the simplified form as expressed by eqs.(3-13) or (3-13a), and then the attainable humidity and the time constant to change the humidity in the chamber can be given by eqs.(3-15) and (3-16), respectively. Eqs. (3-15) and (3-16) indicate the relation of the attainable humidity vs. (S, Sl) and the time constant vs. (S, Sl). Therefore, these equations can be expressed in a diagram as shown by Fig. 3.7. This diagram gives a set of variables (RHg,p/RHg,n, τ) corresponding to another set of variables(S, Sl). This diagram would be useful to estimate the performance of a dehumidifier required for a specific application.

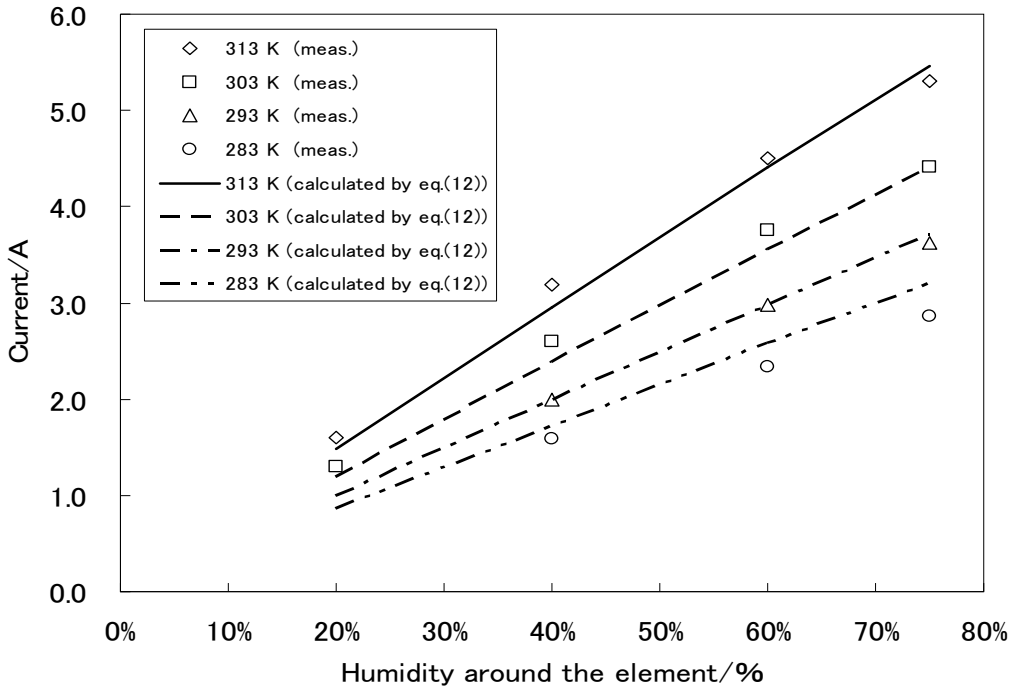

Fig.3.6 Steady state current flowing in the dehumidifying element exposed to the open air (S=100 cm^2, under the condition $\rho_{g,p} = \rho_{g,n}$)

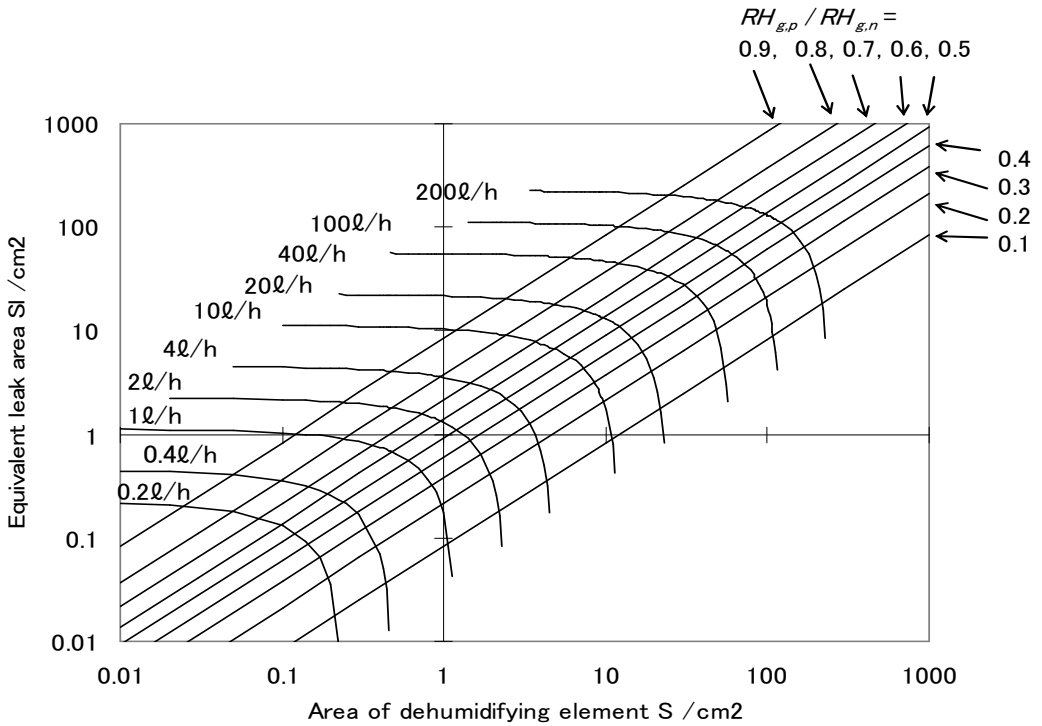

Fig.3.7 Diagram to estimate attainable humidity and time constant for dehumidification from S and Sℓ

3.4 Results and discussion

The current was expressed as a function of the water content on the anode side in the element as shown in eq. (3-5). The water content of the anode side, assuming steady-state conditions, was expressed by eq. (3-11) as a function of the humidities of the spaces facing both the anode and the cathode. The water content of the anode side can be interpreted as the one in the vicinity of the anode because the water contents in the element defined by the two-layer model are the water contents represented at the electrode surfaces in the element. Therefore, eq.(3-5) can be assumed to be the current represented as a function of the water content in the vicinity of the anode. Equation (3-11) can also be assumed to be the water content in the vicinity of the anode under a steady-state condition when the humidity of both spaces facing the anode and the cathode is given. When a steady-state condition is attained under the surrounding condition of 303K and 60%, the water content $\rho_{s,p}$ calculated by eq. (3-11) is about 8 mg cm^{-3}. The value of λ (N_{H2O}/N_{SO3H}) corresponding to the $\rho_{s,p}$ is about λ=0.3. This is very low and there was no information about the impedance for such a low λ, but the current calculated by the method mentioned in section 3.3 well agrees with the measured current within the measured ranges.

Anantaraman et al. reported the effect of humidity on the conductivity of Nafion 117[2]. They measured the conductance by a high frequency impedance method. The electrical conductivity of Nafion 117 for λ=1.18 to 18 measured by them depends much more on the relative humidity in the surrounding air than that of our results presented in chapter 2. They also measured the conductivity of Nafion 117 with a humidity gradient and the results showed the strong dependence of the conductivity on the humidity. Zawodzinski et al. reported the conductance of Nafion 117 as a function of the water content in the membrane [1]. They showed that the conductance decreases roughly linear with decreases in the water content of the membrane. Although these reports deal with the conductance of the membrane itself and direct comparison with our results with them is not possible, the conductance of the dehumidifying element here strongly depends on the water content of the element. There are no other references found about the electrical conductance for such a low water content of λ=0.3. As a major part of the voltage drop would mainly be concentrated in the vicinity of the anode, it seems to be valid that the current characteristics are strongly influenced by the water content near the anode.

Assuming that the values of $S\ell$ and I in eq.(3-10) are zero, the equation

can determine some useful parameters like the water vapor transmission rate (WVTR) as follows.

$$WVTR \equiv \frac{V_{g,p}}{S}\frac{d\rho_{g,p}}{dt} = \frac{D}{L}\left(\frac{\kappa_g}{2D/L+\kappa_s}\right)(\rho_{g,n}-\rho_{g,p}) \tag{3-21}$$

The WVTR rate is defined using the parameters of the permeability P as follows[7].

$$WVTR = \frac{P}{L}(p_{g,n}-p_{g,p}) \tag{3-22}$$

By comparing eqs.(21) and (22), the permeability P can be expressed by the parameters used in the two-layer model.

$$P = \frac{D\kappa_g}{2D/L+\kappa_s}\frac{18\times10^{-6}}{RT_g} = 9.8\times10^{-12} \quad [g\ cm^{-1}s^{-1}Pa^{-1}] \tag{3-23}$$
$$(at\ Tg = 303K)$$

The typical value of WVTR at the temperature of 303K and humidity difference of 100% is calculated to be 2.4×10^{-6} [g cm^{-2} s^{-1}] using eq. (3-22) and (3-23). This value is on the same order as the water transmitted just by the current during the operation of the dehumidifier.

The time variations in the current and chamber humidity calculated using the two-layer model well agree with those of the measured characteristics. The current rapidly decreased for a few minutes just after switching-on the SPE dehumidifier. Thereafter, the current and humidity of the chamber more slowly decreased toward the steady-state. These characteristics can be explained by the two-layer model. The time to form the gradient distribution would take at least a few minutes and the time constant for the dehumidification would be from several tens minutes to several hours for most practical applications. Therefore, eqs.(3-12) and (3-13) are valid for most practical applications.

Equation (3-12) gives the steady-state current as a function of the humidity surrounding the element. The measured current well agrees with the one calculated using eq. (3-12). Therefore, the measured current for almost the entire period except for the period just after switching-on must be nearly the same as that under the steady state conditions. Eq.(3-11) must also be valid under the steady-state conditions.

As eq.(3-12) is valid, the two-layer model expressed by the set of equations from (3-1) to (3-4) can be reduced to the simplified form as eq.

(3-13) or (3-13a).

3.5 Conclusions

The current characteristics of a solid polymer electrolytic (SPE) dehumidifier was analyzed using the two-layer model of the SPE dehumidifier. Calculations of the current and humidity changes of the dehumidification process by the two-layer model well agree with the measured ones.

Current flowing in the element was approximated to be proportional to the water content in the vicinity of the anode as expressed by eq. (3-5).

The current flowing in the element under steady-state conditions can be expressed by eq.(3-12) as a function of its surrounding humidity. The water content in the vicinity of the anode can also be expressed by eq. (3-11) as a function of the humidity.

The dehumidification performance by the SPE dehumidifier for practical applications can be approximately estimated by eq. (3-13) or (3-13a). These equations produce a diagram which describes the relation between a set of parameters (the attainable humidity, time constant for dehumidification) and a set of parameters (the dehumidifying area, equivalent leakage area of the chamber). The diagram seems to be practically useful for selecting the dehumidifier performance required for specific application conditions.

References

[1] Zawodzinski TA Jr, Derouin C, Radzinski S, Sherman RJ, Smith VT, Springer TE, Gottesfeld S., “Water Uptake by and Transport Through Nafion 117 Membranes”, J Electrochem Soc., Vol. 140, No. 4, pp. 1041-1047, 1993.

[2] Anantaraman AV, Gardner CL, “Studies on ion-exchange membranes. Part 1. Effect of humidity on the conductivity of Nafion”, J Electroanalytical Chem., Vol. 414, pp.115-120, 1996.

[3] Springer TE, Zawodzinski TA, Gottesfeld S. “Polymer Electrolyte Fuel Cell Model”, J Electrochem. Soc., Vol. 138, No. 8, pp. 2334-2342, 1991.

[4] Yamauchi S, Sakuma S, Nakatani H, Mitsuda K, “Mass Transfer Equations of Electrolytic Water Removal Device Using Solid Polymer Electrolyte Membrane”, Trans. IEE of Japan, Vol. 120-A, No. 5, pp. 607-613, 2000.

[5] Sakuma S, Yamauchi S, Takai O, “Water transfer simulation of an electrolytic dehumidifier”, J Appl. Electrochem., Vol. 39, pp. 815-825, 2009.

[6] Hinatsu JT, Mizuhara M, Takenaka H, “Water Uptake of Perfluorosulfonic

Acid Membranes from Liquid Water and Water Vapor", J Electrochem. Soc., Vol. 141, No. 6, pp.1493-1498, 1994.

[7] Society of Polymer Science Japan, "Polymer and humidity", Saiwai Shobo, p.242, 1972.

Chapter 4

Voltage-current characteristics of solid polymer electrolytic (SPE) dehumidifier

Abstract Measurements of the V-I characteristics of a solid polymer electrolytic (SPE) dehumidifier were done using a modified SPE dehumidifier with four electrodes which include two electrodes to carry the main current and two other electrodes to observe the voltages applied to the electrical double layer, which are the boundary voltages between the electrodes and the SPE membrane. The measured results were analyzed using the Butler-Volmer equation to examine the validity of the measurements.

The current flowing in the dehumidifier is produced by the decomposition of water near the anode. Therefore, under a steady-state condition, the current should be proportional to the supply rate of water to the anode. On the other hand, a two-layer model for the SPE dehumidifier presented in chapter 2 and 3 showed that the current flowing in the dehumidifier was roughly proportional to the water content in the vicinity of the anode. These results were introduced for interpretation of the V-I measurements of the SPE dehumidifier.

It was concluded that the current of the dehumidifier was expressed in the form of a Butler-Volmer equation as a function of the electrode boundary voltages which were the voltages across the boundary between the electrodes and the SPE membrane. An experimental formula for the current under a steady-state condition was given as a function of the water content near the anode and the boundary voltages.

List of symbols

Variables

A : Area of the dehumidifying element /cm^2

B : Coefficient of rate constant /cm s^{-1}

$C_a(T)$: Coefficient to give steady-state current /A cm g^{-1}

$C_I(T)$: Coefficient to give steady-state current /A cm g^{-1}

c_R : Molar concentration of reductant /mol cm^{-3}

c_O : Molar concentration of oxidant /mol cm^{-3}

D : Diffusion coefficient of water in the dehumidifying element /cm^2 s^{-1}

$E_{0,a}$: Voltage across the anode-side boundary when the current is zero /V

E_a : Electrical potential of anode /V

E_c : Electrical potential of cathode /V

E_m : Electrical potential of electrode /V

E_s : Electrical potential of solid polymer electrolytic membrane /V

E_{sa} : Electrical potential of the anode-side end of SPE membrane /V

E_{sc} : Electrical potential of the cathode-side end of SPE membrane /V

F : Faraday constant =96,440 /C

I : Current of the dehumidifying element /A

I_a, I_c : Anode current and cathode current, respectively /A

I_{st} : Steady-state current /A

I_{sat} : Saturated current /A

k : Rate constant of oxidation or reduction /cm s^{-1}

$k_{a,+}$, $k_{a,-}$: Rate constants of oxidation and reduction at the anode-side double layer /cm s^{-1}

$k_{c,+}$, $k_{c,-}$: Rate constants of oxidation and reduction at the cathode-side double layer /cm s^{-1}

L : Thickness of the dehumidifying element /cm

RH : Relative humidity /%

R : Gas constant =8.31 /J mol^{-1} K^{-1}

Rs : Electrical resistance of the dehumidifying element /Ω

T : Temperature of the air space surrounding the dehumidifying element /K

β_a, β_c : Transfer coefficients defined for anode-side boundary and cathode-side boundary, respectively

$\Delta^* G$: Gibbs activation energy /J mol^{-1}

$\Delta\phi_m^o$: Standard electrode potential when all chemical materials have activity values of 1 /V

κ_g : Coefficient relevant to the diffusion velocity of water from the air to the SPE membrane /cm s^{-1}

κ_s : Coefficient relevant to the diffusion velocity of water from the membrane to the air /cm s^{-1}

ρ_g : Water density in the air surrounding the dehumidifying element /g cm^{-3}

$\rho_{s,a}$, $\rho_{s,c}$: Water contents in the vicinity of the anode and in the vicinity of the cathode of the dehumidifying element /g cm^{-3}

$\rho_{s,o}$: Water content of the dehumidifying element equilibrium with

environmental humidity /g cm^{-3}

Subscripts

a : Positive electrode or anode

c : Negative electrode or cathode

g : Gas space

s : Solid polymer electrolytic dehumidifying element

\+ : Oxidation

– : Reduction

4.1 Introduction

The dehumidifying processes of the dehumidifying device can be simulated well by a two-layer model for the dehumidifying device that was proposed in chapters 3, and it was also shown that the current flowing in the device was proportional to water content in the vicinity of the anode when the applied voltage was constant[1,2].

In this chapter, an experiment involving the V-I characteristics of the dehumidifying device is presented. The experiment was done using a modified dehumidifying device, which had two reference-electrodes in order to measure the electrode-membrane voltages, in addition to the normal electrodes carrying the main current. The V-I characteristics were analyzed using the water content at the anode introduced in chapter 3 and estimated by comparison with the Butler-Volmer equation. The dependences of the current on the anode voltage and cathode voltage were obtained experimentally. The voltage supported by the SPE membrane itself was also estimated from the voltage difference between the reference electrodes.

These results will be useful in understanding what kind of reaction should determine the rate of the reaction.

4.2 Operating principle of SPE dehumidifying device

4.2.1 Relation of overvoltage and current

The principle of the dehumidification by the SPE dehumidifier is shown in Fig.4.1. Electrode reactions at the anode and the cathode are given by the following formulas.

At the anode,

$$2H_2O(\ell) \rightarrow 4H^+(aq) + O_2(g) + 4e^- \quad (4\text{-}1)$$

At the cathode,

$$4H^+(aq) + O_2(g) + 4e^- \rightarrow 2H_2O(\ell) \quad (4\text{-}2)$$

Water molecules near the anode in the dehumidifying element are decomposed into protons and oxygen. Protons drift to the cathode and combine with oxygen to form water near the cathode. The electrolysis of water and the recombination of protons and oxygen occur at the boundary between the electrodes and the membrane. At the anode, water is supplied from the space facing the anode and from the cathode by diffusion. The anode-side boundary and cathode-side boundary are denoted as the anode-side double layer and cathode-side double layer, respectively. The electrolysis and the recombination of water are performed with the aid of the voltage differences across each double layer. The current produced by the decomposition of water molecules at the anode must be proportional to the supply rate of water molecules to the anode under a steady-state condition.

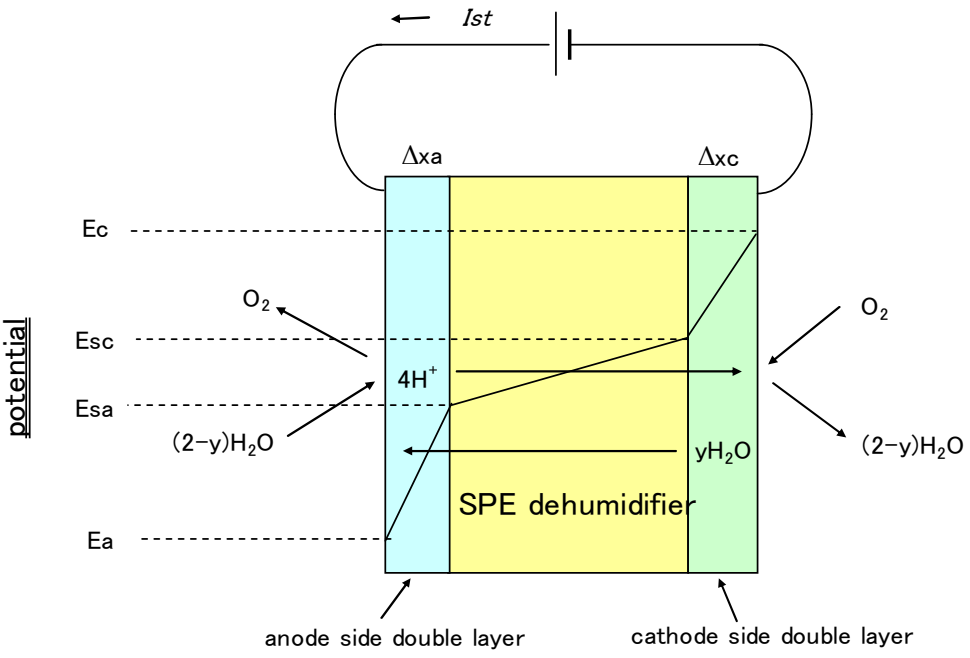

Fig.4.1 Principle and water flow of SPE dehumidifying element and electrical potentials at the anode-side boundary, cathode-side boundary and membrane bulk

When no current flows in the element, the anode and cathode are equilibrium with the SPE membrane to form electrical double layers near the

electrodes. These electrical double layers produce electrical potential differences between the electrodes and the membrane. The potential difference between the electrodes and SPE membrane are given by the Nernst equation as follows:

$$E_m - E_s = \Delta\phi_m^\circ - \frac{RT}{4F}\ell n\frac{a_{H_2O}^2}{a_{H^+}^4 a_{O_2}} \quad (4\text{-}3)$$

Here, E_m and E_s are the electrical potentials of electrode and membrane, respectively. $\Delta\phi_m^\circ$ is the standard electrode potential, and it means the electrical potential of the electrode to the SPE membrane when all chemical materials have activity values of 1. This electrode potential relative to the SPE membrane can not be measured in principle. The electrode potential is usually given and measured by a potential difference relative to a standard electrode such as a standard hydrogen electrode. However, the changes in the potential across the double layer can be measured if the polarization or its change formed at the reference electrode is small.

On the other hand, when current flows in the dehumidifying element, the current can be expressed as follows.

At the anode,

$$I_a = FA(k_{a,+}c_R - k_{a,-}c_O) \quad (4\text{-}4)$$

At the cathode,

$$I_c = FA(k_{c,-}c_O - k_{c,+}c_R) \quad (4\text{-}5)$$

Here, F and A are the Faraday constant and the dehumidifying area of the element, respectively. The values of $k_{a,+}$, $k_{a,-}$, $k_{c,+}$ and $k_{c,-}$ are the rate constants of oxidation and reduction at the anode-side double layer and those at the cathode-side double layer, respectively. The values of c_O and c_R are the molar concentrations of oxidant and reductant in the reaction, respectively.

The rate constants can be expressed as follows [3].

$$k = B\exp(-\Delta^* G / RT) \quad (4\text{-}6)$$

Here, $\Delta^* G$ and B are the Gibbs activation energy and a coefficient with

the same dimension as the rate constant, respectively. Substituting eq.(4-6) into eq.(4-4), the following equation is obtained.

$$I_a = FA\left\{B_{a,+}c_R \exp(-\Delta^* G_a / RT) - B_{a,-}c_O \exp(-\Delta^* G_c / RT)\right\} \tag{4-7}$$

The Gibbs activation energy in eq.(4-7) is given for the voltage difference $\Delta\phi_m$ across the electrical double layer as follows [3]:

$$\begin{aligned} \Delta^* G_c &= \Delta^* G_c(0) + \beta F \Delta\phi_m \\ \Delta^* G_a &= \Delta^* G_a(0) - (1-\beta) F \Delta\phi_m \end{aligned} \tag{4-8}$$

Substituting eq.(4-8) into eq.(4-7), the following equation is obtained.

$$\begin{aligned} I_a = {} & FAB_{a,+}c_R \exp(-\Delta^* G_a(0)/RT)\exp\left\{(1-\beta_a)F\Delta\phi_m / RT\right\} \\ & - FAB_{a,-}c_O \exp(-\Delta^* G_c(0)/RT)\exp\left\{-\beta_a F\Delta\phi_m / RT\right\} \end{aligned} \tag{4-9}$$

β_a is transfer coefficient at the anode.

The following Butler-Volmer equation is obtained, assuming that $\Delta\phi_m = E_{0,a}$, when $I_a = 0$,

$$\begin{aligned} I_a = {} & i_{0,a}\exp\left\{(1-\beta_a)F(E_a - E_{sa} - E_{0,a})/RT\right\} \\ & - i_{0,a}\exp\left\{-\beta_a F(E_a - E_{sa} - E_{0,a})/RT\right\} \end{aligned} \tag{4-10}$$

Here,

$$\begin{aligned} i_{0,a} &= FAB_{a,+}c_R \exp(-\Delta^* G_a(0)/RT)\exp\left\{(1-\beta_a)FE_{0,a}/RT\right\} \\ &= FAB_{a,-}c_O \exp(-\Delta^* G_c(0)/RT)\exp(-\beta_a FE_{0,a}/RT) \end{aligned} \tag{4-11}$$

On the other hand, the current at the cathode can be described as follows by applying a procedure similar to that above.

$$\begin{aligned} I_c = {} & i_{0,c}\exp\left\{\beta_c F(E_{sc} - E_c - E_{0,c})/RT\right\} \\ & - i_{0,c}\exp\left\{-(1-\beta_c)F(E_{sc} - E_c - E_{0,c})/RT\right\} \end{aligned} \tag{4-12}$$

Here, β_c is the transfer coefficient at the cathode.

Under a steady state condition,

$$I_a = I_c \equiv I_{st} \tag{4-13}$$

As shown in eqs.(4-10) and (4-12), these currents flowing in devices such as the SPE dehumidifier are expected to depend on the exponent of the potential difference across the double layers.

4.2.2 Consideration of the steady-state current and the effect of water concentration on the current

The current flowing in the dehumidifying element is produced in the anode-side double layer by the decomposition of water molecules. Therefore, the current under a steady-state condition should be proportional to the supply rate of water to the anode area. The authors showed the relation between the steady-state current of the dehumidifying element and the water content in the vicinity of the electrodes in chapter 3, as follows:

$$I_{st} = C'(T)\left\{ A(\kappa_g \rho_g - \kappa_s \rho_{s,a}) + \frac{DA(\rho_{s,c} - \rho_{s,a})}{L} \right\} \tag{4-14}$$

$$I_{st} = C'(T)\left\{ A(\kappa_s \rho_{s,c} - \kappa_g \rho_g) + \frac{DA(\rho_{s,c} - \rho_{s,a})}{L} \right\} \tag{4-15}$$

Here, $\rho_{s,a}$ and $\rho_{s,c}$ are the water contents in the vicinity of the anode and cathode of the element, respectively. ρ_g is the water density of the space surrounding the element. The first and second terms on the right side of eq.(4-14) are the water supply rates to the anode area from the space facing the anode and from the cathode by diffusion, respectively. In eq. (4-15), the first term and the second term on the right side are the water rate emitted from the cathode area to the space facing the cathode and to the anode through the element by diffusion, respectively. The water content of the element under the equilibrium condition ($I_{st} = 0$) is written as ρ_{so} and the following quantity of $\Delta\rho_s$ is introduced.

$$\kappa_s \rho_{so} = \kappa_g \rho_g \tag{4-16}$$

$$\begin{aligned} \rho_{s,a} &= \rho_{so} - \Delta\rho_s \\ \rho_{s,c} &= \rho_{so} + \Delta\rho_s \end{aligned} \tag{4-17}$$

Eqs. (4-14) and (4-15) can be transformed using eqs. (4.16) and (4.17) as follows:

$$I_{st} = C'(T)A\left(\kappa_s + \frac{2D}{L} \right)\Delta\rho_s \equiv C_I(T)A\Delta\rho_s \tag{4-18}$$

The coefficient of $C_I(T)$ can be estimated by the following equation, because the current should have a saturated value of I_{sat}, when the supply rate of water to the anode has a maximum value, that is, $\Delta\rho_s$ is nearly equal to ρ_{so}. Assuming that the maximum rate of water supply is realized when $\Delta\rho_s = \rho_{so}$.

$$C_I(T) = I_{sat} / (A \rho_{so}) \tag{4-19}$$

From eqs.(4-17), (4-18) and (4-19), the following equation is obtained.

$$\begin{aligned} \rho_{s,a} &= \rho_{s,o}(1 - I_{st} / I_{sat}) \\ \rho_{s,c} &= \rho_{s,o}(1 + I_{st} / I_{sat}) \end{aligned} \tag{4-20}$$

On the other hand, the current of the SPE dehumidifying element was found to be proportional to the water content in the vicinity of the anode, and the following formula was given in the previous chapter, when the applied voltage is constant.

$$I_{st} = C_a(T) A \rho_{s,a} \tag{4-21}$$

This equation can be expanded as the following formula to apply to the case where the applied voltage is changed.

$$I_{st} = C_a'(T) A \rho_{s,a} f(E_a - E_{s,a}) \tag{4-22}$$

By substituting eq.(4-20) into (4-22), the following formula is obtained.

$$f(E_a - E_{s,a}) = \frac{1}{C_a'(T) A \rho_{s,o}} \quad \frac{I_{st}}{(1 - I_{st} / I_{sat})} \tag{4-23}$$

Because the cathode current flows by the reduction of protons at the cathode to form water, the relation of the cathode current and the density of protons at the cathode may be expressed as follows.

$$I_{st} = C_c(T) A_c \left[H^+\right] g(E_{sc} - E_c) \tag{4-24}$$

Here, $\left[H^+\right]$ is the concentration of protons at the cathode. However, the information on the concentration of protons at the cathode is unknown so far. Therefore, the relation of the cathode current and the cathode-side boundary voltage will be shown as the current vs. the boundary voltage by a Tafel plot.

The feature of $f(E_a - E_{s,a})$ and $g(E_{sc} - E_c)$ can be obtained from the data for the V-I measurements by graphical representation of $I_{st} / (1 - I_{st} / I_{sat})$ vs. $V_{a,sa}$. Also, I_{st} vs. $V_{sc,c}$.

4.3 Experiments

The experimental set-up for the V-I measurements of the SPE

dehumidifying element is shown in Fig.4.2. The tested element has four electrodes, two normal electrodes carrying the main current and two reference electrodes to measure the potential difference between the anode and membrane or the cathode and membrane. The main electrodes carrying the main current have a larger area of about 70mm×70mm square, each with a hole of 15mm×15mm in their centers. The two reference electrodes with a smaller area of 10mm ×10mm square are positioned on the holes in the center

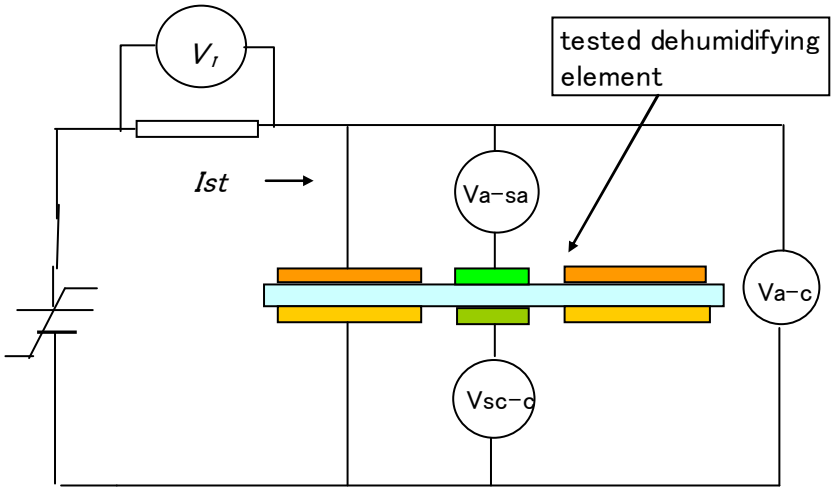

(a) test circuit for V-I measurement

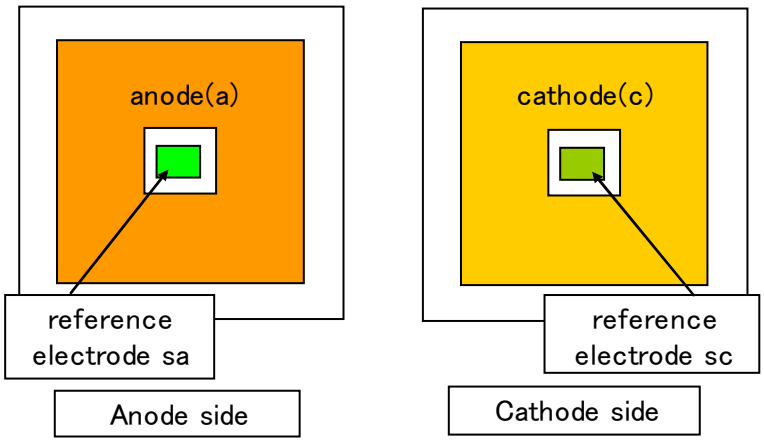

(b) SPE dehumidifying element with four electrodes

Fig.4.2 Test circuit and dehumidifying element for V-I experiments with SPE dehumidifier

of the larger electrodes. The main current flows across the larger electrodes, and the reference electrodes with smaller areas are used to measure the

voltage change between the main current electrodes and the membrane. The measured voltages are denoted as $V_{a,c}$, the applied voltage between the anode and cathode, $V_{a,sa}$, the anode-side boundary voltage between the anode and anode-side reference electrode, and $V_{sc,c}$, the cathode-side boundary voltage between the cathode-side reference electrode and the cathode. The V-I measurements were carried out by varying the applied voltage step by step. The test element equipped with a reference electrode to measure a voltage difference to main electrodes was shown by Yamauchi et al. [4].

The tested element is composed of a Nafion 117 membrane and four electrodes on both its surfaces. The four electrodes are made of porous electrodes and a catalyst mainly composed of platinum black.

The element was placed in an open box in order to avoid an effect by forced convection from its surrounding environment. The element with the open box was placed in a vessel controlling the temperature and humidity therein.

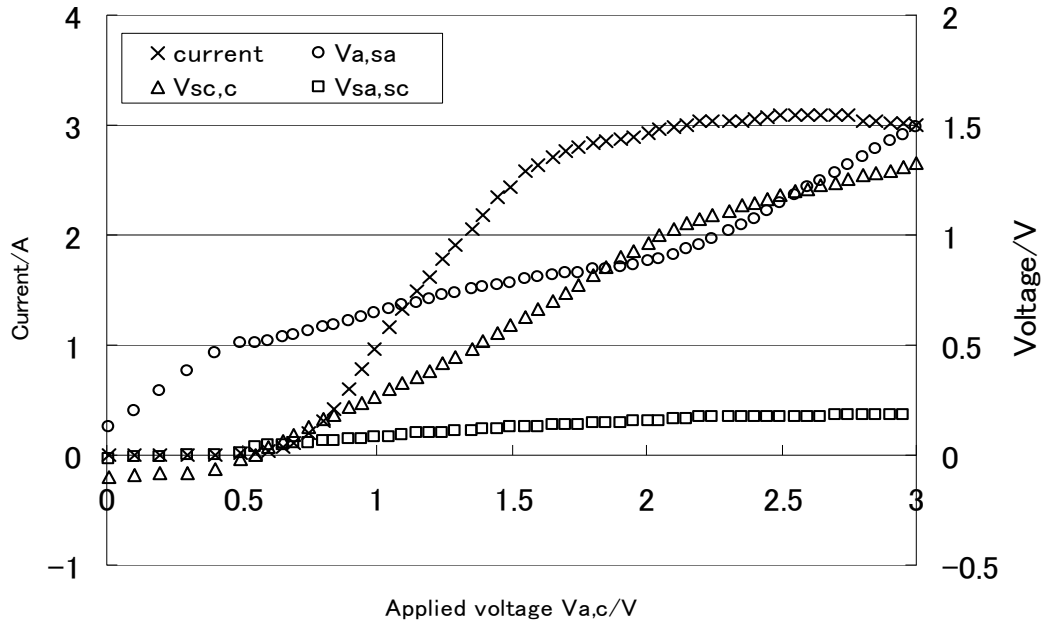

Fig.4.3 V-I measurements for the temperature and relative humidity (RH) of 313K and 60%

Figure 4.3 shows typical data obtained by V-I measurements under the conditions of 313K and 60%. The current does not increase with an increase

in applied voltage in its smaller region, but the current is increased linearly in the middle region of the applied voltage. In the higher voltage, the current becomes saturated. The saturated value seems to reflect a rate-determining step.

The anode-side boundary voltage of $V_{a,sa}$ increases at a rate similar to the increase in applied voltage in the smaller voltage region. The increasing rate of the voltage then decreases in the middle voltage region, and in the higher region, the increasing rate of the voltage increases again. The increasing rate of the anode-side boundary voltage is the smallest in the region where the increasing rate of current is the highest. Thus, the anode-side boundary voltage quite effectively causes a current increase.

The voltage of $V_{sc,c}$ does not increase with the increase in the applied voltage in its smaller region. The voltage then increases, linearly with the current increase in the middle voltage region, and in the higher region, the rate of voltage increase is suppressed. The increasing rate of the cathode-side boundary voltage is the highest in the region where the increasing rate of current is the highest. The cathode-side boundary voltage seems to be mainly proportional to the current or the supply rate of protons to the cathode.

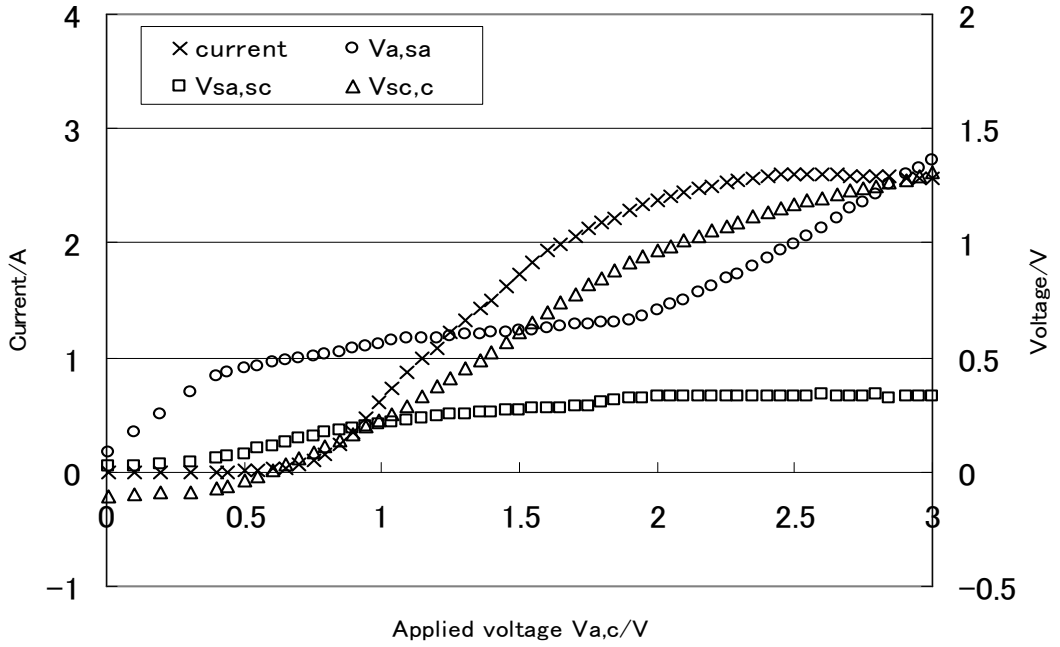

Fig.4.4 V-I measurements for the temperature and relative humidity (RH) of 303K and 60%

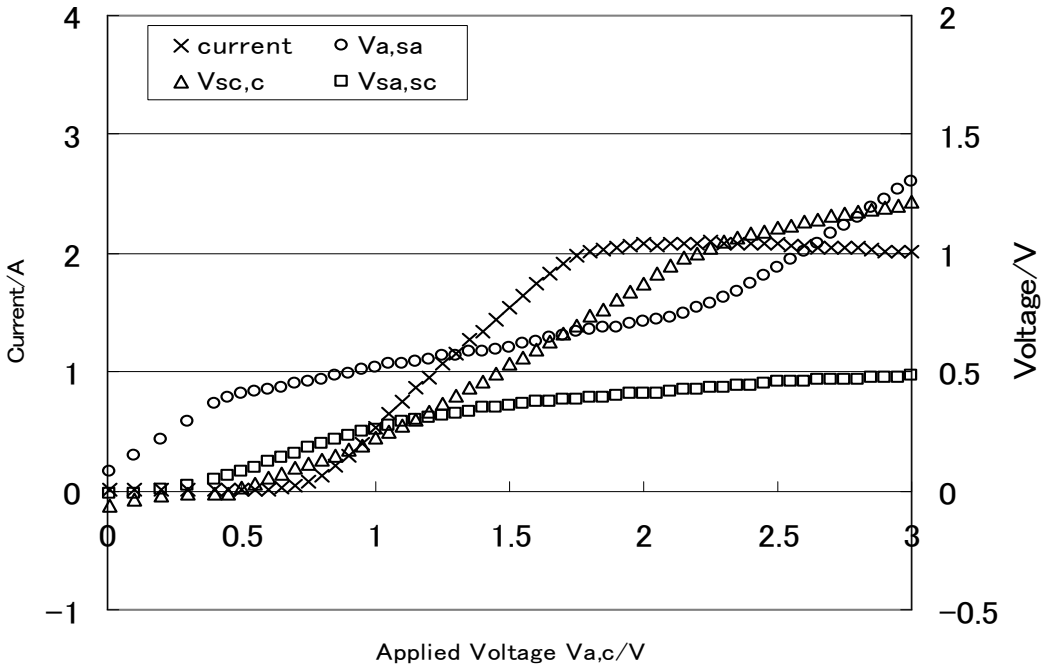

Fig.4.5 V-I measurements for the temperature and relative humidity (RH) of 293K and 60%

The voltage, denoted by $V_{sa,sc}$, is the difference in $V_{a,c}$ and ($V_{a,sa}$ + $V_{sc,c}$) and will be the voltage across the membrane itself. The voltage $V_{sa,sc}$ increases very slowly with increasing current.

These phenomena seem to be classified into the following three regions,

(1) The region in smaller applied voltage where no current flows and most of the applied voltage is shared with the anode-side boundary voltage $V_{a,sa}$.
(2) The middle region where the current increases with the applied voltage and the increasing rate of cathode-side boundary voltage is higher than that of the anode-side boundary voltage
(3) The region in the higher applied voltage where the current is saturated.

Figures 4.4 and 4.5 are the V-I measurements under the conditions of 303K and 60% and 293K and 60%, respectively. These figures show the V-I characteristics similar to that at 313K and 60% shown in Fig.4.3.

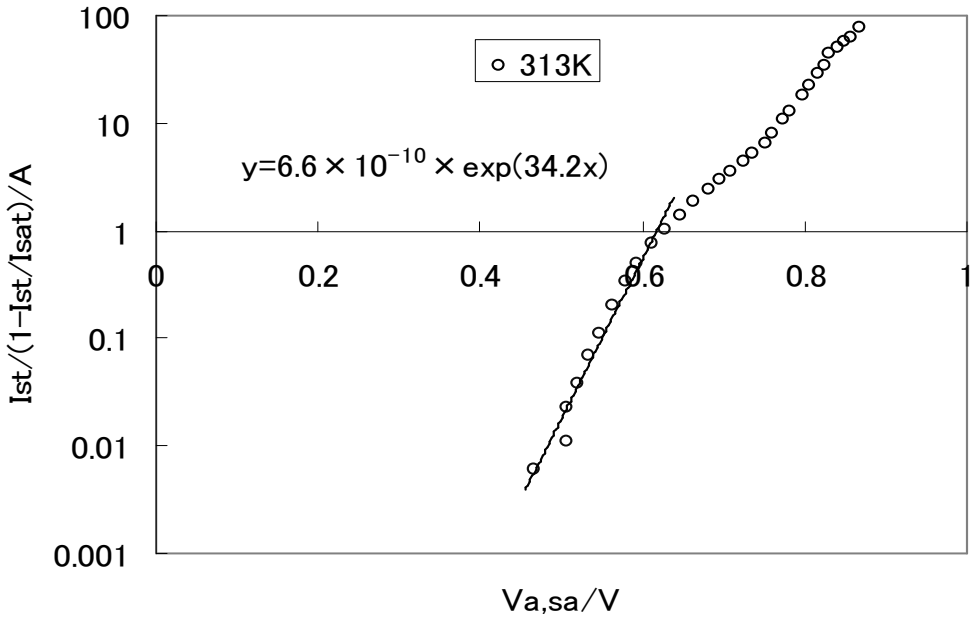

(a) Current vs. anode-side boundary voltage ($V_{a,sa}$) at 313K and 60% RH

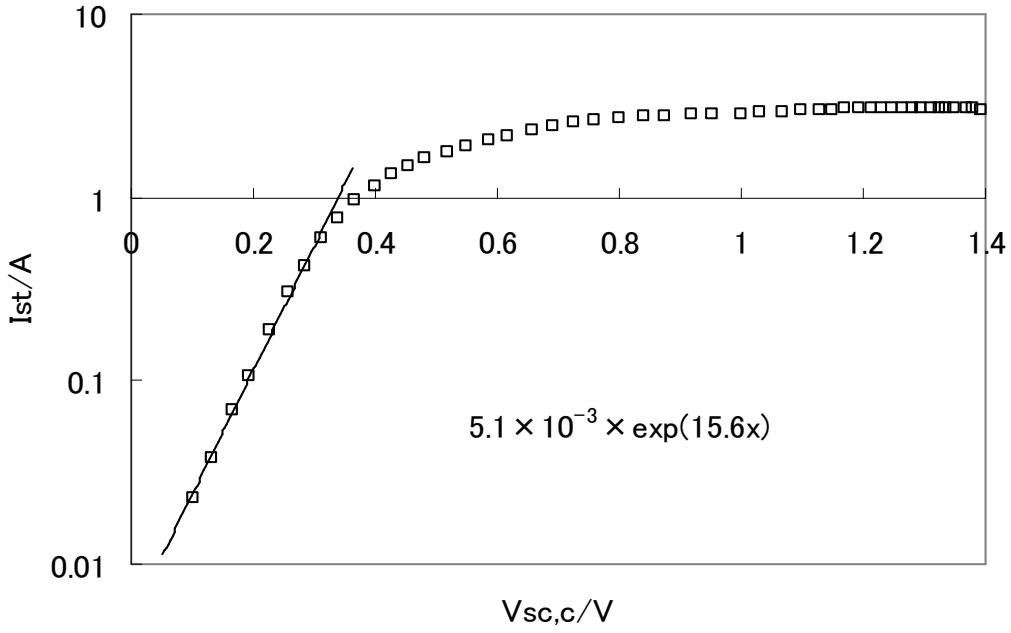

(b) Current vs. cathode-side boundary voltage ($V_{sc,c}$) at 313K and 60% RH

Fig.4.6 Characteristics of current for anode-side boundary voltage and cathode-side boundary voltage at 313K and 60% RH

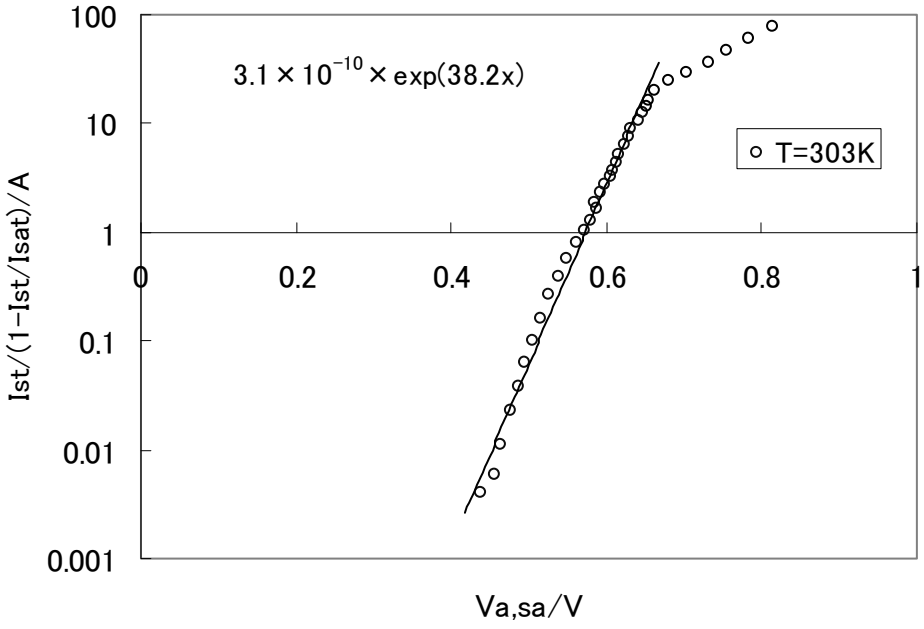

(a) Current vs. anode-side boundary voltage ($V_{a,sa}$) at 303K and 60% RH

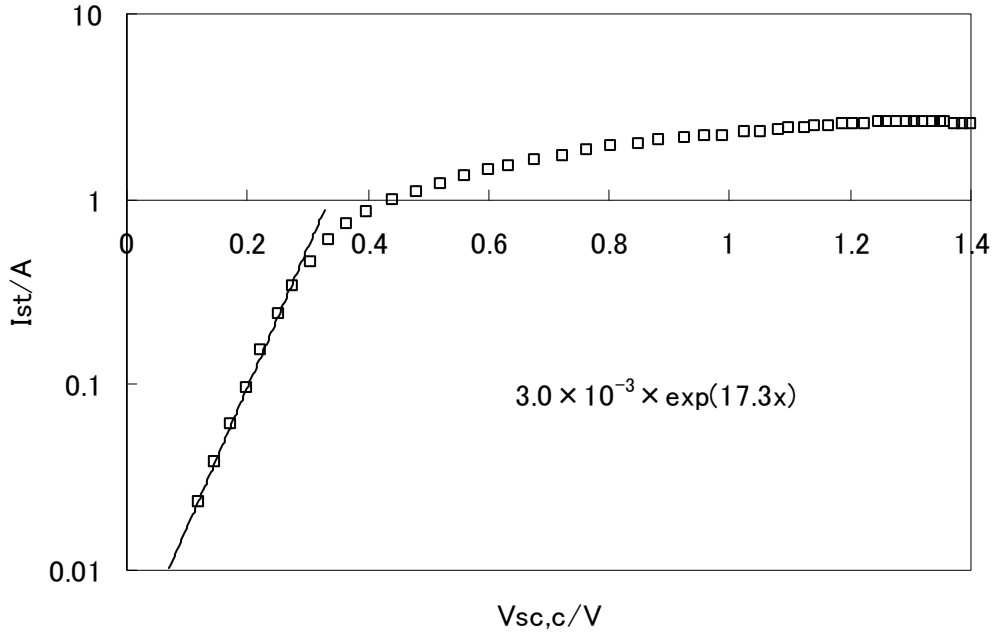

(b) Current vs. cathode-side boundary voltage ($V_{sc,c}$) at 303K and 60% RH

Fig.4.7 Characterictics of current for anode-side boundary voltage and cathode-side boundary voltage at 303k and 60% RH

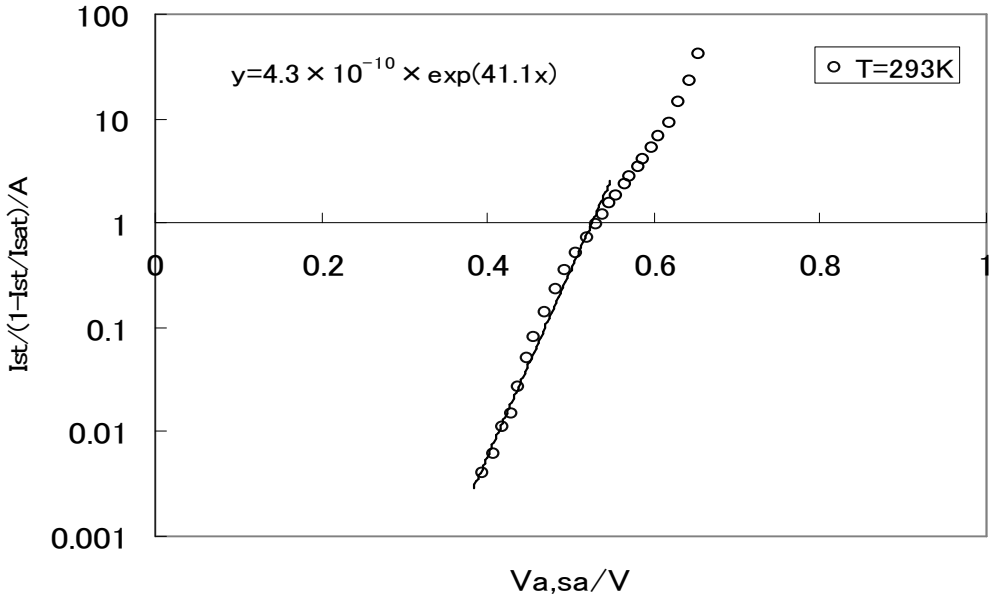

(a) current vs. anode-side boundary voltage (Va,sa) at 293K and 60% RH

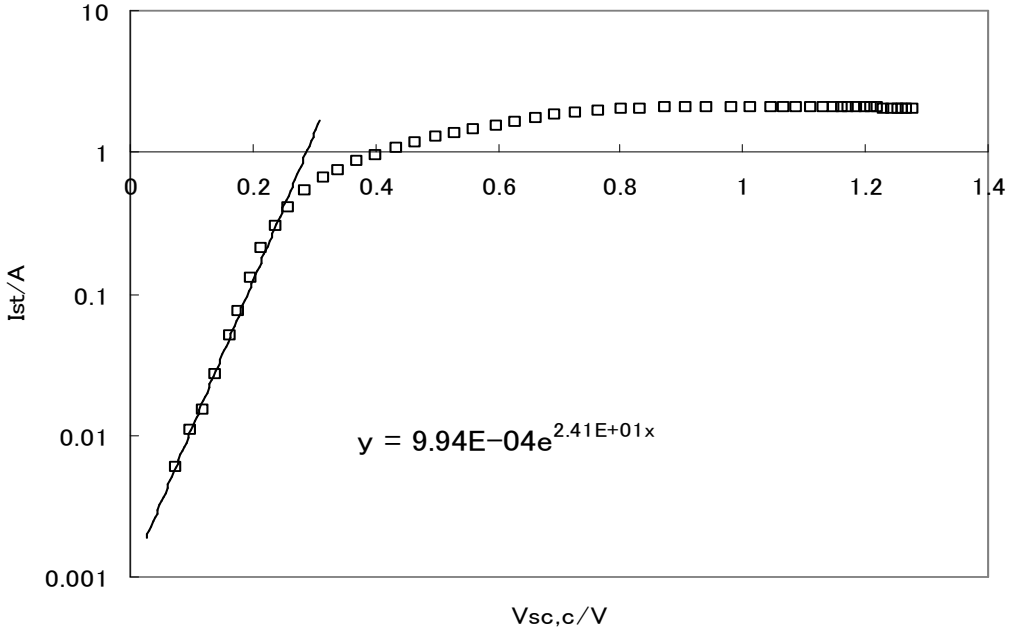

(b) current vs. cathode-side boundary voltage at 293K and 60% RH

Fig.4.8 Characteristics of current for anode-side boundary voltage and cathode-side boundary voltage at 293k and 60% RH

These V-I data shown in Fig. 4.3, 4.4 and 4.5 are processed to the form shown in Figs. 4.6, 4.7 and 4.8 to estimate $f(V_{a,sa})$ and $g(V_{sc,c})$ which are expressed by eq.(4-23) and (4-24), respectively.

Fig. 4.6(a) shows the current characteristics for the anode-side boundary voltage, $V_{a,sa}$ at 313K and 60%. The figure is represented in the form of $I_{st} / (1-I_{st} / I_{sat})$ against $V_{a,sa}$. It is found from the figure that the current begins to increase at 0.4 volt or more of $V_{a,sa}$, and the gradient of the current for the anode voltage in its lower region is about 34 V^{-1} as shown in Fig.4.6(a). The gradient slightly decreases in the larger anode voltage where the current I_{st} approaches I_{sat}. Fig.4.6(b) shows the current characteristics for the cathode-side boundary voltage, $V_{sc,c}$. As shown in Fig.4.6(b), the current increases at a rate of about $16V^{-1}$ at a voltage smaller than about 0.3V. The rate is nearly half compared to that shown in Fig.4.6(a). The current characteristics for the cathode voltage saturate in the higher applied voltage than 0.3V.

Figures 4.7 and 4.8 show the current characteristics at the temperature and humidity of 303K and 60% and 293K and 60%, respectively. As shown in Fig. 4.7(a) and Fig. 4.8(a), the gradients of the current for the anode-side boundary voltage are about $38V^{-1}$ and $41V^{-1}$ for the temperatures of 303K and 293k, respectively. The gradients of the current for the cathode voltage shown in Fig. 4.7(b) and Fig. 4.8(b), are about $17V^{-1}$ and $24V^{-1}$, respectively. The results obtained by this experiment are summarized in Table 4.1. As seen in Table 4.1, the gradient of the current for the anode-side boundary voltage is found to be about F/RT for each case.

Table 4.1 Electrical characteristic values of SPE dehumidifying element

tempera-ture, T	relative humidity, RH	water content, λ	F/RT	$(1-\beta_a)$ F/RT	β_c F/RT	resistance of membrane	conductivity of membrane
K	%	H_2O/SO_3H	V^{-1}	V^{-1}	V^{-1}	Rm/Ω	σ/Scm^{-1}
293	60	about 4	39.6	41.1	21.7	0.097	0.0021
303	60		38.3	38.2	19.2	0.065	0.0032
313	60		37.1	34.2	16.2	0.030	0.0069

These characteristics can be expressed in the following form.

$$I_{st} = C_a^*(T) A \rho_{s,a} \exp\left(\frac{F V_{a,sa}}{RT}\right) \tag{4-25}$$

At the cathode, the gradient of the current for cathode-side boundary voltage is about F/2RT in the region of voltage less than about 0.3V, and the characteristics can be expressed in the following form.

$$I_{st} = C_c^*(T) A_c \exp\left(\frac{F V_{sc,c}}{2RT}\right) \tag{4-26}$$

Figure 4.9 shows the relation of current and the voltage between the two reference electrodes calculated using the measured voltages of $V_{a,c}$, $V_{a,sa}$ and $V_{sc,c}$. As seen in Fig. 4.9, polarization within the level of 0.05V to 0.2V affects the voltage measurement at the reference electrodes in the region where no current flows. However, the voltage between the reference electrodes increases much more slowly where the current begins to flow, Therefore, polarization would not be developed in the region where current flows. Hence, the gradient of the voltage relative to the current reveals the electrical resistance of the SPE membrane.

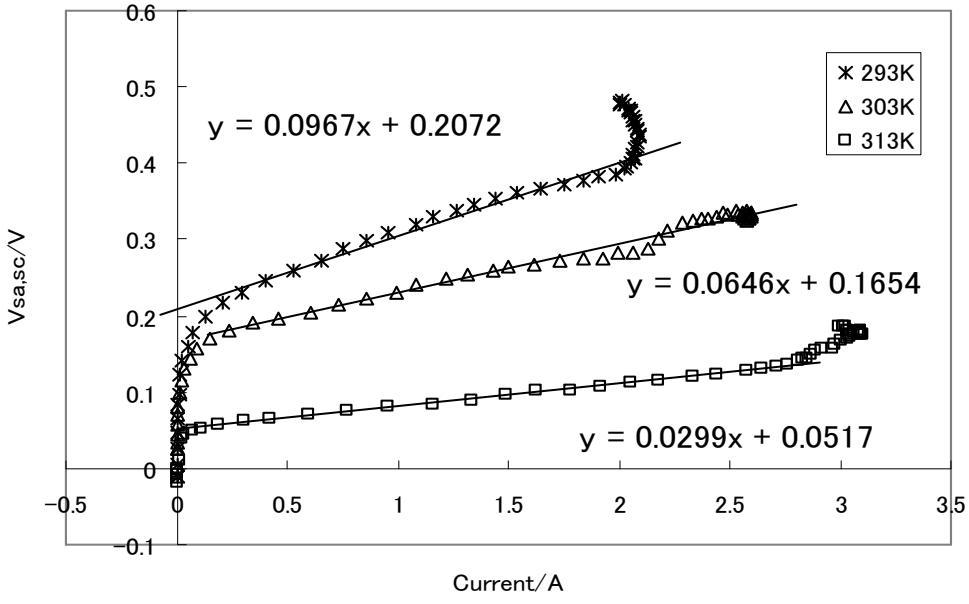

Fig.4.9 Voltage between the reference electrodes vs. current (voltage across the SPE membrane bulk vs. current)

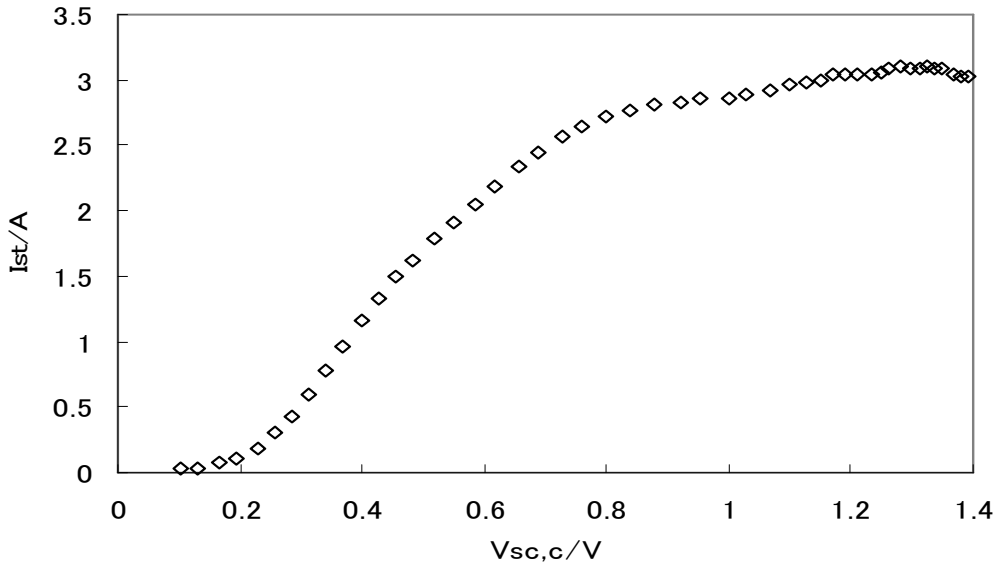

Fig.4.10 Typical data for current vs. cathode-side boundary voltage under the condition of 313K and 60% RH

The resistance of the SPE membrane obtained from the gradient is also shown in Table 4.1. The conductivity calculated assuming a membrane thickness is 0.01cm is also shown in Table 4.1. As the resistance was calculated using the data for the V-I measurements conducted under the condition where current flows, the water content distribution in the element would have a gradient. The average value of the water content expressed by the extent of hydration λ (=H_2O/SO_3H) is estimated to be about 4 based on a humidity of 60%.

4.4 Discussion

<Measurement of V-I characteristics>

V-I measurements of the dehumidifying element were done on a dehumidifying element with four electrodes so as to measure the voltage differences across the electrical double layers described in this chapter. From the result shown in Fig. 4.9, voltages across the membrane increases up to about 0.05V or up to 0.2V in the region where no current flows between the main current electrodes. Therefore, polarization at the reference electrodes seems to develop in the region. However, the polarization was not developed where the current flowed. Therefore, V-I measurements of the voltage of the reference electrodes seem to be roughly valid in the region where current

flows.

<V-I characteristics of the anode-side double layer>

Most of the applied voltage is shared with the anode-side double layer in the smaller voltage region. The voltage of the cathode-side double layer does not increase in this region. In the region where the current increases linearly, the applied voltage becomes shared with the anode-side double layer, the cathode-side double layers and the membrane. In the region where the current saturates, the voltage across the anode-side double layer increases more rapidly than in the region where the current increases linearly. The current can be roughly approximated by eq. (4-25) as a function of the water content in the vicinity of the anode and the anode-side boundary voltage. The Gibbs activation energy for the decomposition of water at the anode is strongly influenced by the anode-side boundary voltage.

<V-I characteristics of the cathode side double layer>

The applied voltage is not shared with the cathode-side double layer in the region where the applied voltage is small. The voltage across the cathode-side double layer increases linearly in the region where the current increases linearly. The increasing rate decreases in the region where the current saturates. In the middle region where the current and the voltage increase linearly, the exponent value expressed by eq.(4-26) is about FV/2RT. This means that β_c is 0.5 in eq. (4-12). The expression of Eq. (4-12) was introduced by eq. (4-5), which includes c_o , the molar concentration of the oxidant. The oxidant can be protons for the cathode reaction shown in eq.(4-2). Fig.4.10 shows a linear plot of I_{st} vs. $V_{sc,c}$. The current, or the supply rate of protons to the cathode, seems to increase linearly with the increase in the cathode-side boundary voltage in the voltage region higher than 0.3V up to 0.8V.

<Electrical resistance of SPE membrane: temperature dependence>

Zawodzinski et al. measured the transport properties of Nafion 117 and reported the protonic conductivity of Nafion 117 as a function of hydration level λ (=H_2O/SO_3H) and temperature[5]. The conductivity reported was about 0.02 S cm^{-1} for the temperature and hydration level of 303K and λ =4, and it decreases roughly linearly with a decrease in water content. Anantaraman et al. also reported that the conductivity of Nafion 117 is not linear with regard to water content and that it is about 0.002 S cm^{-1} for the

temperature and hydration level of 303K and λ =4 [6]. The author's results are similar to those of Anantaraman et al. who also measured the conductivity under the condition of a gradient water content and reported that the conductivity of Nafion 117 with a different RH of 45%/100% is 3.27 $\times 10^{-3}$ S cm^{-1}. This value is close to our results as shown in Table1. The conductivity measurements by us were conducted under a gradient distribution of water content by carrying the current under a uniform environmental humidity of 60%. The membrane condition of the authors' experiments is thought to be similar to that of Anantaraman et al.

4.5 Conclusions

The measurement of V-I characteristics of an SPE dehumidifier was performed using a modified SPE dehumidifier with four electrodes which include two electrodes to carry the main current and two other reference electrodes to measure the voltage change applied to the boundary between the electrodes and membrane.

The measuring method described in this chapter is thought to be effective in dividing the applied voltage into the anode-side boundary voltage, the cathode-side boundary voltage and the voltage across the membrane itself.

The relation of the steady-state current and the anode-side boundary voltage was shown to be expressed in the following form.

$$I_{st} = const. \times \rho_{s,a} \times \exp\left(\frac{FV_{a,sa}}{RT}\right)$$

The steady-state current for the cathode-side boundary voltage was shown to be expressed in the following form in the region where the boundary voltage is less than 0.3V.

$$I_{st} = const. \times \exp\left(\frac{FV_{sc,c}}{2RT}\right)$$

However the current saturates at more than 0.3V of the cathode-side boundary voltage.

The electric resistance of the SPE membrane (Nafion 117) itself is estimated from the differential voltage between the two reference electrodes. The estimated values are similar to those of Anantaraman et al. [6]. The dependence of the resistance on temperature was also presented.

This method would be useful for better understanding of the electrode phenomena of devices such as the SPE dehumidifier.

5 References

[1] Sakuma S, Yamauchi S, Takai O, “Water transfer simulation of an electrolytic dehumidifier”, J Appl. Electrochem., Vol. 39, pp.815-825, 2009.

[2[Sakuma S, Yamauchi S, Takai O, “Estimation of dehumidifying performance of solid polymer electrolytic dehumidifier for practical application”, J Appl. Electrochem., Vol. 40, pp.2153-2160, 2010.

[3] Atkins P, JD Paula (2006) Physical Chemistry, eighth edition, Tokyo Kagaku Doujin, 2009.

[4] Yamauchi S, Mitsuda K, Maeda H, Takai O, “Application of a hydrogen reference electrode to a solid state water removal device”, J Appl. Electrochem., Vol. 30, pp.1235-1241, 2000.

[5] Zawodzinski TA, Derouin C, Radzinski S, Sherman RJ, Smith VT, Springer TE, “Water Uptake by and Transport Through Nafion 117 Membranes”, J Electrochem. Society, Vol. 140, No.4, pp.1041-1047, 1993.

[6] Anantaraman AV, Gardner CL, “Studies on ion-exchange membranes. Part 1. Effect of humidity on the conductivity of Nafion”, J Electroanalytical Chem., Vo. 414, pp.115-120, 1996.

Chapter 5

Discussion

Abstract The measurements and the analysis developed in chaper 2, 3 and 4 are discussed in this chapter. (1) Measuring error of dehumidifying capability would be introduced by desorption of water from water absorbent material. The measurement of dehumidifying capability for the humidity in gas space is especially apt to produce the larger error because water mass in the space is rather small and so the desorption of water from the material may not be neglected. (2) Simplification employed by two-layer model introduces the calculation errors in current during the time to form gradient water distribution. (3) The diagram to give a set of variables (time constant of dehumidification, the attainable humidity) from a set of variables (dehumififying area, leakage area) is extended in more practical form. (4) Permeability of SPE dehumidifier is expressed by parameters employed in two-layer model. (5) V-I measurement by 4-electrode AC method is discussed in terms of activation energy.

5.1 Measurement of dehumidifying performance and possible errors

The dehumidifying capability of a SPE dehumidifier depends on the humidities inside and outside the chamber and the ambient temperature. The capability is usually determined from measurement of the time required for the humidity change in a chamber from 60% to 50%. Fig.5.1 shows the schematics for the measurement.

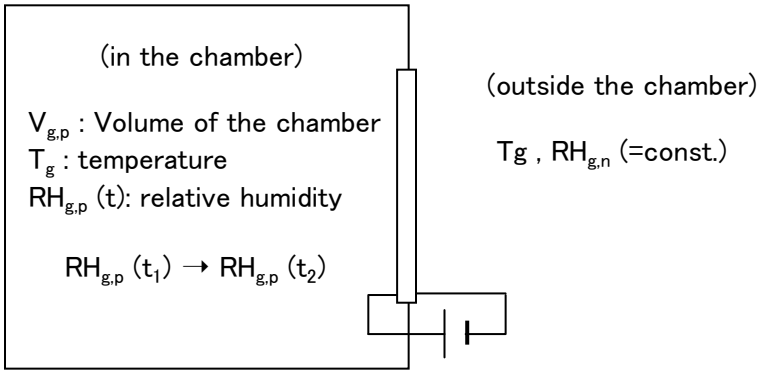

Fig. 5.1 Measurement of dehumidifying capability of a SPE dehumidifier

Using the measured data shown in Fig.5.1, the dehumidifying capability is calculated using the following formula:

$$\frac{\Delta m}{\Delta t} \equiv -\frac{V_{g,p}}{(t_2 - t_1)} \int_{t1}^{t2} \frac{d\rho_{g,p}}{dt} dt = -\rho_{g,sat} V_{g,p} \frac{RH_{g,p}(t_2) - RH_{g,p}(t_1)}{100(t_2 - t_1)} \qquad (5\text{-}1)$$

where $\rho_{g,sat}$ is the saturated water vapor density, which depends on the temperature. Therefore, the dehumidifying capability depends on the ambient temperature. In order to identify a dehumidifier, the nominal dehumidifying capability of the dehumidifier is defined by representing the capability under the condition of 303K and 60% RH. The dehumidifying capability of a dehumidifier may be specified by the nominal dehumidifying capability.

Water absorption on the inner-surface of the chamber or the materials in the chamber may cause the measuring errors. For example, assuming that $V_{g,p}$ is 50 dm^3, the amount of water including in the chamber under 303K and 60% RH is about 0.9 g. On the other hand, water absorbed in a post card for 295K and 22% RH is shown in Fig. 5.2. Figure 5.2 shows the weight change of a post card exposed in environmental condition of 295K and 22% RH after vacuum drying for 2h. The weight changes from 2.6 g to 2.7 g. The change in weight is about 0.1 g. This is due to water absorption from surrounding air. Hence, the post card can hold 0.1 g of water at 295K and 22% RH. The weight change is also shown in Fig.5.3 in which weight change in log scale is expressed as the subtraction of the weight at arbitrary time from the weight attainable at t=∞.

When the humidity is higher, the water absorbed is more,. This value of absorbed water is not so small to be neglected in the measurement. Some materials used for the measurement such as humidity sensors, jacket of electric wires, plastic, acrylic resin, paper etc. are apt to absorb considerable water. Such materials should be carefully removed from the chamber when measurement of dehumidifying capability is conducted.

The time constant of the humidification of a post card is found to be about 10 minutes from the gradient of the line in Fig. 5.3. Similar behavior was observed for the measurement of weight change of Nafion 117 shown in Fig. 2.4 in chapter 2 [1]. The time constant of Nafion 117 is also about 10 minutes. The time constant may depend on the thickness of the material because the desorption of water occurs on a surface though absorption of water spreads in the volume of the materials.

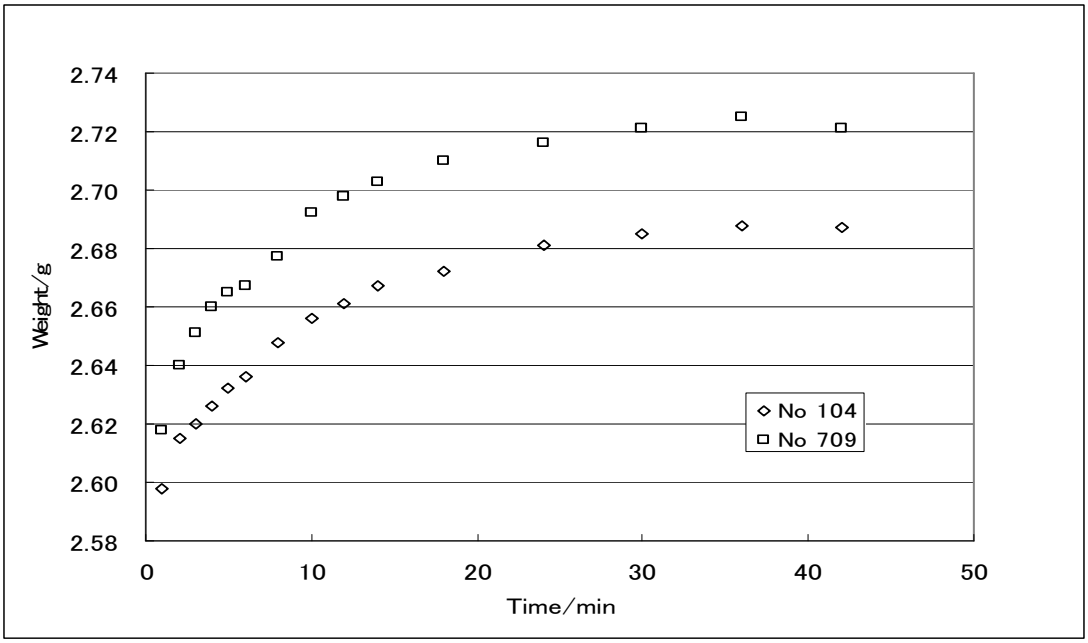

Fig. 5.2 Weight change of a post card exposed in the environmental condition of 295K and 22% RH after vacuum drying for 2h.

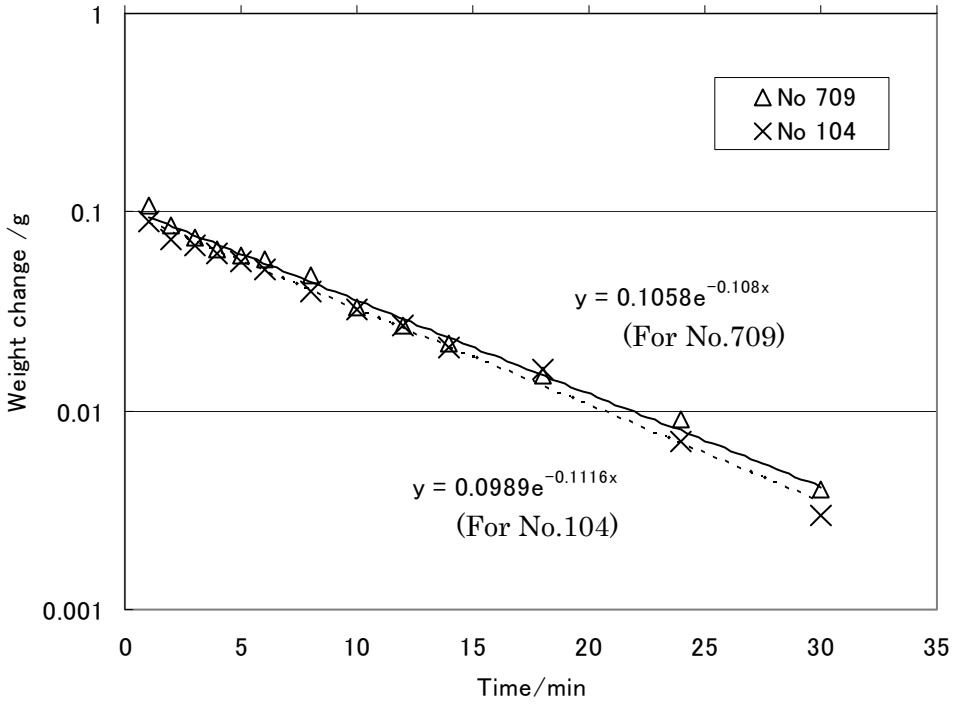

Fig. 5.3 Weight change (in log scale), of a post card exposed in environmental condition of 295K and 22% RH after vacuum drying for 2h. (The weight shown in the vertical axis is the subtraction of the weight at t=∞ from the weight at arbitrary time t.)

5.2 Discrepancy between the measurement and the calculation by two-layer model

Two-layer model for the dehumidifier can explain the excursion of current change from its initial change to its following change up to its steady-state, and the humidity change in a chamber. This seems to be the evidence to prove the validity of the model. However, a discrepancy in current change can be seen in the transient course from the initial change to its following change governed by the humidity change, which was shown in Fig. 2.10 in chapter 2. The time to correspond to the transient course seems to be the time to form the gradient shape of water content in the element. Therefore, this discrepancy is thought to be resulted from the simplification of the model for the dehumidifier.

5.3 The diagram to give the attainable humidity in a chamber and the time constant for the humidity change/ use of the diagram for practical applications [2]

Time variation of the humidity in a chamber to be dehumidified was approximately expressed by a differential equation which can give parameters such as an attainable humidity in the chamber and time constant on the humidity change. A diagram, shown in Fig. 3.7 in chapter 3, to convert the set of (S, Sℓ) into the set of ($RH_{g,p}$ /$RH_{g,n}$, $V_{g,p}$ /τ) was obtained. The dehumidifying capability of a dehumidifier is principally proportional to the dehumidifying area S, though it also depends on the environmental conditions. Therefore, the area S can correspond to the dehumidifying capability under a specific condition selected as a basis. By notating the nominal dehumidifying capability as P_n, the diagram can be expressed as the relation of the set of (P_n, $S\ell$) and the set of ($RH_{g,p}$ /$RH_{g,n}$, $V_{g,p}$ / τ). Such diagram is shown in Appendix I, in which P_n is the dehumidifying capability under the condition of temperature and humidity of 303 K and 60% RH. This diagram is very useful to select a dehumidifier of a capability adequate for the specific application conditions. The diagram is also useful to estimate the attainable humidity and the time constant when the dehumidifier capability is degraded, which is also indicated in Appendix I.

5.4 The relation between the current and the water content in the dehumidifier under steady-state condition at constant applied voltage of 3V.

Referring to Fig. 3.1 in chapter 3, the water transfer under steady-state conditions is expressed as following.

$$\frac{18I(1+2\alpha)}{2eN_AS}-\frac{D}{L}(\rho_{s,n}-\rho_{s,p})=\kappa_s\rho_{s,n}-\kappa_g\rho_{g,n}=\kappa_g\rho_{g,p}-\kappa_s\rho_{s,p}$$
$$=\frac{S\ell}{S}\kappa_g(\rho_{g,n}-\rho_{g,p}) \tag{5-2}$$

This is the equation of continuity under steady-state condition on the rate of water transfer. Each side of the equation is the water transfer rate for unit area through the virtual surface in the center of the element, cathode surface, anode surface and leakage area, respectively. This equation can be rewritten as follows.

$$\frac{18I}{2eN_AS}+\alpha\frac{18I}{eN_AS}=(\kappa_g\rho_{g,p}-\kappa_s\rho_{s,p})+\frac{D}{L}(\rho_{s,n}-\rho_{s,p}) \tag{5-3}$$

The left side of the equation is the rate of water removed from anode side to cathode, by decomposition of water molecules and by electro-osmotic drag. Terms of the right side of the equation are the rate of water supplied through anode surface and the rate of water supplied from cathode to anode by back diffusion, respectively. It is found from the equation that the steady-state current is proportional to the rate of water supply to the anode.

The water contents of the element in equilibrium conditions are introduced and the difference from the equilibrium is denoted as $\Delta\rho_s$.

$$\kappa_s\rho_{s,po}=\kappa_g\rho_{g,p}$$
$$\kappa_s\rho_{s,no}=\kappa_g\rho_{g,n} \tag{5-4}$$

$$\Delta\rho_s=\rho_{s,po}-\rho_{s,p}=\rho_{s,n}-\rho_{s,no} \tag{5-5}$$

Then the equation is transformed as the following form.

$$\frac{18I(1+2\alpha)}{2eN_AS}=(\kappa_s+\frac{2D}{L})\Delta\rho_s+\frac{D}{L}(\rho_{s,no}-\rho_{s,po})$$
$$=(\kappa_s+\frac{2D}{L})\Delta\rho_s+\frac{\kappa_g}{\kappa_s}\frac{D}{L}(\rho_{g,n}-\rho_{g,p}) \tag{5-6}$$

The relation among the quantities in eq.(5-6) is shown in the diagram of Fig. 5.4. The difference $\Delta\rho_s$ from the equilibrium condition can be estimated from the measurement of I and ambient humidities using eq.(5-6).

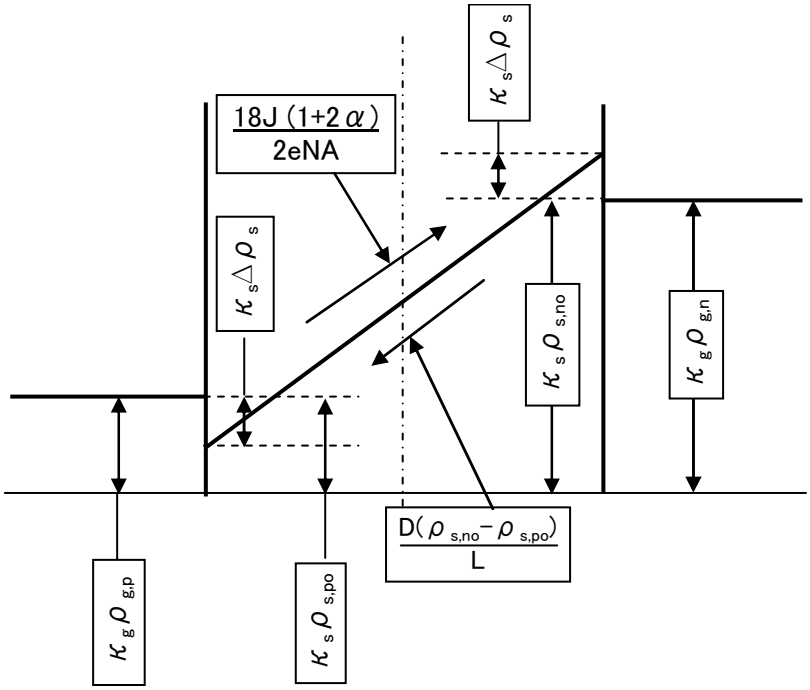

Fig.5.4 Water distribution and water transfer of the dehumidifier

If the current is measured for the element placed in open air, that is $\rho_{g,n} = \rho_{g,p}$, then the equation is:

$$\frac{18I(1+2\alpha)}{2eN_A S} = (\kappa_s + \frac{2D}{L})\Delta\rho_s \tag{5-7}$$

The current in the dehumidifier is proportional only to the difference $\Delta\rho_s$, when the dehumidifier is located in open air.

5.5 Water vapor transmission rate (WVTR) in dehumidifying element

The WVTR is defined as the following formula.

$$WVTR = \frac{Q}{St} \tag{5-8}$$

$$Q = \frac{D_{mg}(\rho_{g,n} - \rho_{g,p})St}{L} = \frac{P(p_{g,n} - p_{g,p})St}{L} \tag{5-9}$$

$$P \equiv D_{mg}\frac{\rho_{g,n} - \rho_{g,p}}{p_{g,n} - p_{g,p}} \tag{5-10}$$

Where Q : water mass transmitted through the membrane [kg]

D_{mg}: effective diffusion coefficient through membrane surface [$m^2\ s^{-1}$]

S: membrane area for water transmission [m^2]

$p_{g,n}$,$p_{g,p}$: water pressure in each space [Pa]

$\rho_{g,n}$,$\rho_{g,p}$: water density in each space [kg m^{-3}]

P: water vapor permeability coefficient (WVPC) [s]

WVTR can be expressed using the parameters employed in the two-layer model in the following form.

$$WVTR = \frac{D/L}{\kappa_s + 2D/L}\kappa_g(\rho_{g,p} - \rho_{g,n}) \tag{5-11}$$

By comparing eq.(5-9) and (5-11), water vapor diffusion coefficient D_{mg} can be expressed by the combination of the fundamental factors defined for two-layer model as follows.

$$D_{mg} = \frac{D\,\kappa_g}{\kappa_s + 2D/L} \tag{5-12}$$

$$P = \frac{D\kappa_g}{(\kappa_s + 2D/L)}\frac{(\rho_{g,n} - \rho_{g,p})}{(p_{g,n} - p_{g,p})} \tag{5-13}$$

The factor of $D\kappa_g/(\kappa_s + 2D/L)$ can also be obtained using eq.(3-10) experimentally. Fig. 5.5 is an example of measurement of the humidity change in a chamber with its volume of 51 dm^3 and equipping the dehumidifier with its area of 100 cm^3, while the dehumidifier is not operated. Humidity outside the chamber was kept at the condition of 38℃ and 60% RH during the measurement. The time constant of the humidity change can be graphically estimated as about 100 min. from the slope of the humidity curve in Fig. 5.5.

On the other hand, the time constant graphically obtained by such a way can be equal to the following factor which is obtained from eq.(3-10), by substituting the leakage area Sℓ=0 and current=0.

$$\tau = \frac{V_{g,p}}{S}\frac{(\kappa_s + 2D/L)}{\kappa_g D/L} = \frac{V_{g,p}}{S}\frac{L}{D_{mg}} \tag{5-14}$$

$$D_{mg} = \frac{V_{g,p}L}{S\tau} = \frac{51\times10^3\times0.017}{100\times6000} = 1.4\times10^{-3}[cm^2s^{-1}] \tag{5-15}$$

Where, τ is the time constant of the humidity change.

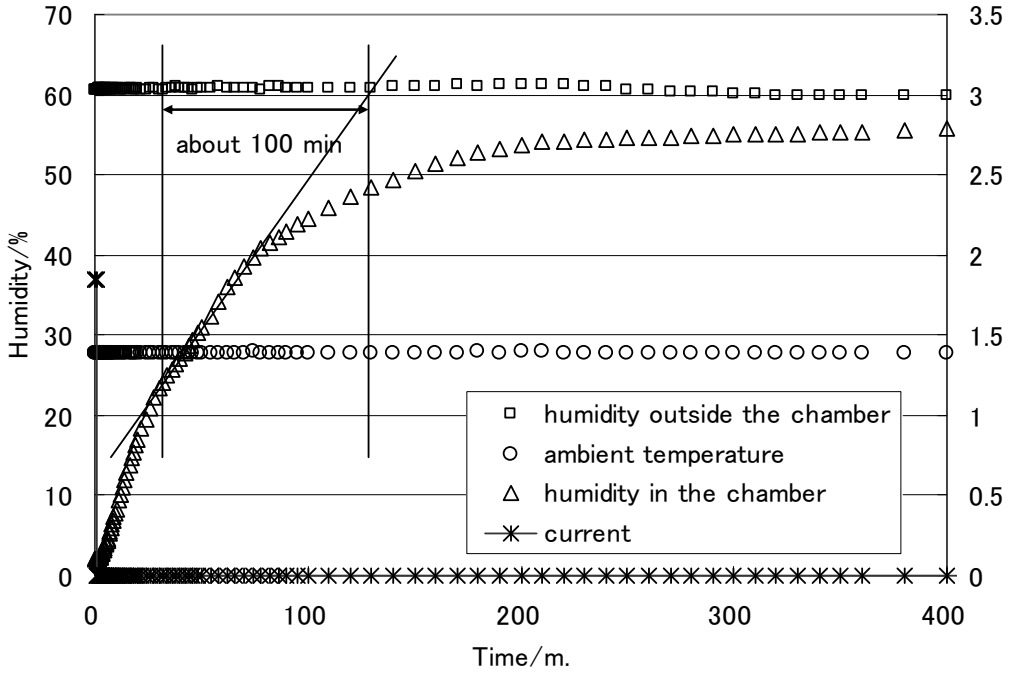

Fig. 5.5 Humidity change in a closed chamber with 51 dm^3 when dehumidifier is not operating. (The humidity goes out through SFE element with the area of 100 cm^2 to the space surrounding the chamber, which is kept under the condition of 28℃/60%.)

Such expressions as eqs.(5-12) and (5-13) can be useful to explain a physical quantity by more fundamental quantities.

5.6 Voltage distribution in the SPE dehumidifier

The voltage distribution measured by four-electrode method shown in chapter 4 can also be represented as a form of voltage profile along the dehumidifier axis. Fig. 5. 6 is an example of the voltage profile obtained using the data shown in chapter 4. In the figure, the distance from anode along the dehumidifier axis is given by the horizontal axis (not to scale). The positions numbered by 1,2, 9 and 10 are the anode, the anode-side reference electrode, the cathode-side reference electrode and the cathode, respectively. Voltages will be denoted by $V_{0,1}$, $V_{1,9}$ and $V_{9,10}$ and they are used as measured voltages between the anode and the anode-side reference electrode, between two reference electrodes and between cathode-side reference electrode and cathode, respectively.

The voltage $V_{0,1}$ is not exactly the anode-side double layer voltage because the measured voltage does not include the voltage difference of $E_{0,a}$, the equilibrium electrode voltage at current zero, which was defined in eq.(4-11) in chapter 4. The polarization voltage is defined as the difference of the electrode voltage E_a-E_{sa} at current I from the one at current 0. Therefore, the measured voltage $V_{0,1}$ is the electrode polarization voltage and expressed as follows.

$$V_{0,1} = (E_a - E_{sa}) - E_{0,a} \tag{5-14}$$

The change of the anode-side double layer voltage can also be expressed as follows:

$$\Delta(E_a - E_{sa}) = \Delta(V_{0,1} + E_{0,a}) \approx \Delta V_{0,1} \tag{5-15}$$

Therefore, eq.(4-23) is transformed as follows.

$$\begin{aligned} f(E_a - E_{s,a}) &= const_1 \times \exp\{F(E_a - E_{sa})/RT\} \\ &= const_2 \times \exp\{FV_{0,1}/RT\} \end{aligned} \tag{5-16}$$

Although figures of 4.6 to 4.8 in chapter 4 show directly the relations between I_{st} and $V_{0,1}$, they also show the relation between I_{st} and (E_a - $E_{s,a}$). The $const_2$ in eq. (5-16) is exchange current i_0 at current zero and can be estimated graphically using Fig. 4.6(a) to Fig. 4.8(a) as follows.

$$i_0 \approx 10^{-10} \sim 10^{-9}\, A \qquad \text{for the area } 49\text{cm}^2 \tag{5-17}$$

The most of the applied voltage is shared in the anode-side and the cathode-side boundaries. The voltage $V_{1,9}$ measured for the voltage between two reference electrodes is also include the electrode voltages produced on the boundaries of the reference electrodes and membarne. $V_{1,9}$ is assumed to be the sum of the voltage drop of RI^2 and the electrode voltage on the boundaries.

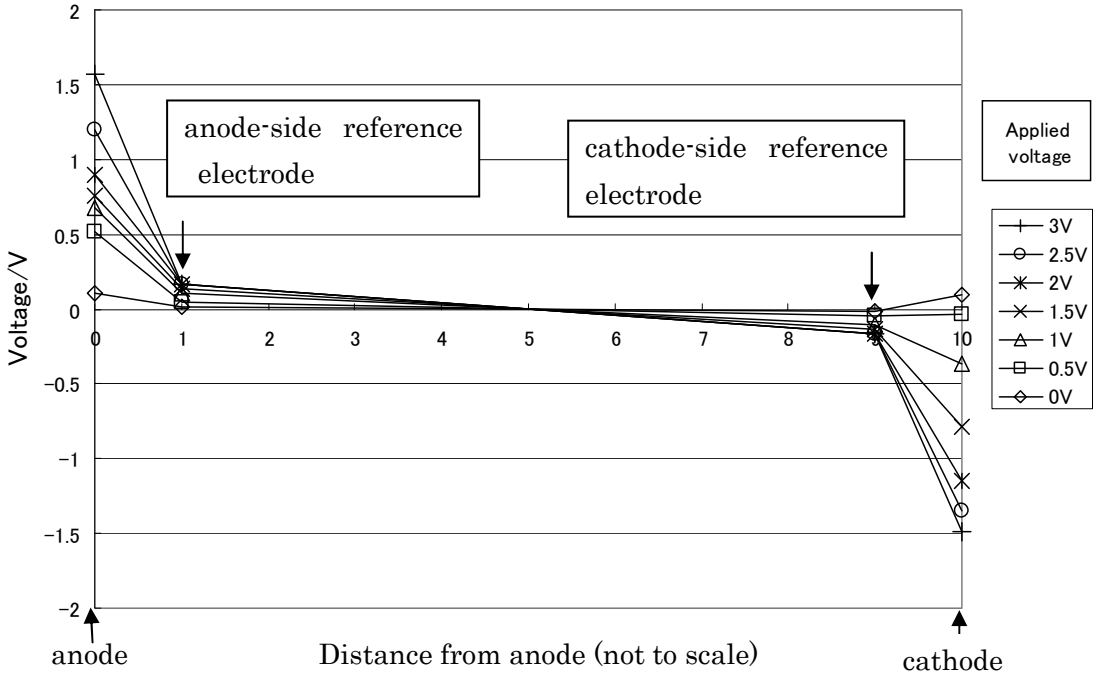

Fig. 5.6 Voltage profile along the dehumidifier axis (303K/60%), varying the applied voltage.

5.7 Activation energy of proton-conduction in the membrane (Nafion 117)

The electrical conductivity of the membrane (Nafion 117) was obtained from the measurement of voltage by four-electrode method and was shown in Table 4.1 in chapter

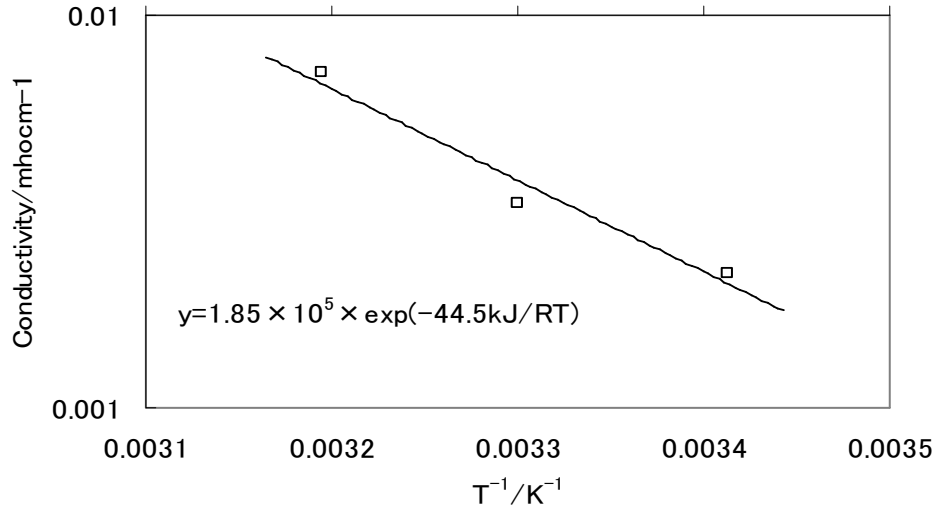

Fig. 5.7 Temperature dependence of electrical conductivity of Nafion 117

4. The conductivity shown in Table 4.1 can also be represented in the form of Arrhenius

plot as shown in Fig. 5.7. It is expected from Arrhenius plot that the activation energy of proton conduction in Nafion 117 is about 45kJ mol^{-1}. This is slightly larger than the vaporization energy of water.

5.8 Activation energy of electrode reactions

<Activation energy of anodic current>

As shown in eq.(4-25) in chapter 4, the anodic current that is the current produced by electrolysis of water was proportional to $\exp(FV_{a,sa}/RT)$. From this results, Gibbs activation energy for oxidation $\triangle^* G_a$ decreases with the increase of the anode voltage although the one for reductant $\triangle^* G_c$ is not changed. They are expressed as follows:

$$\Delta^* G_a = \Delta^* G_a(0) - F(E_a - E_{sa})/RT \tag{5-18}$$

$$\Delta^* G_c = \Delta^* G_c(0) \quad . \tag{5-19}$$

This result can be formally represented as the following diagram.

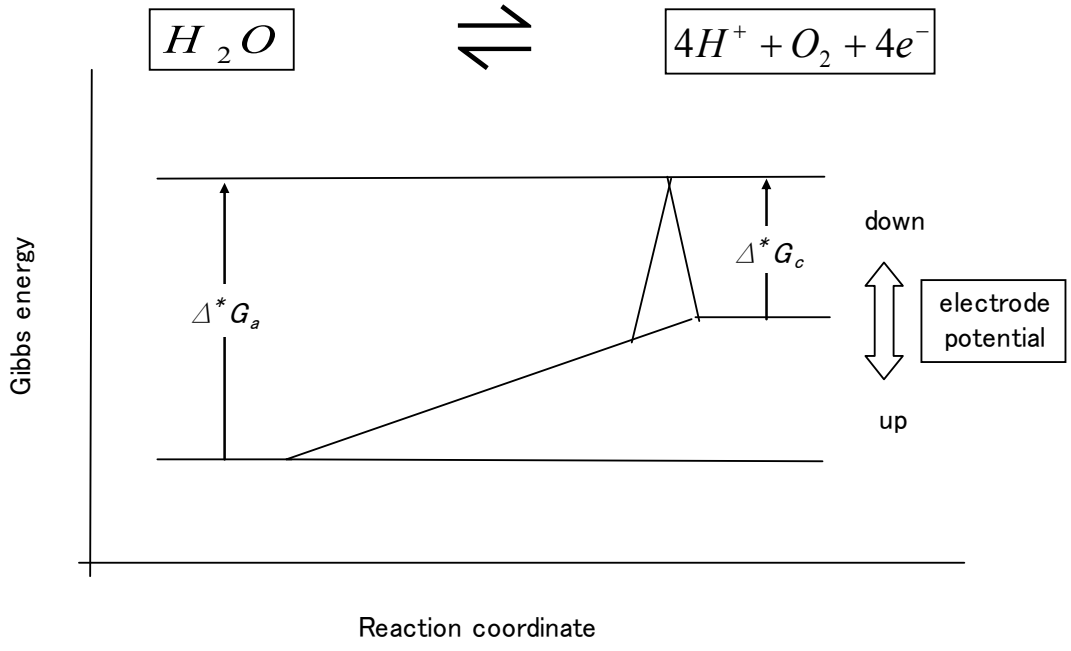

Fig. 5.8 Schematics of activation energy at anode

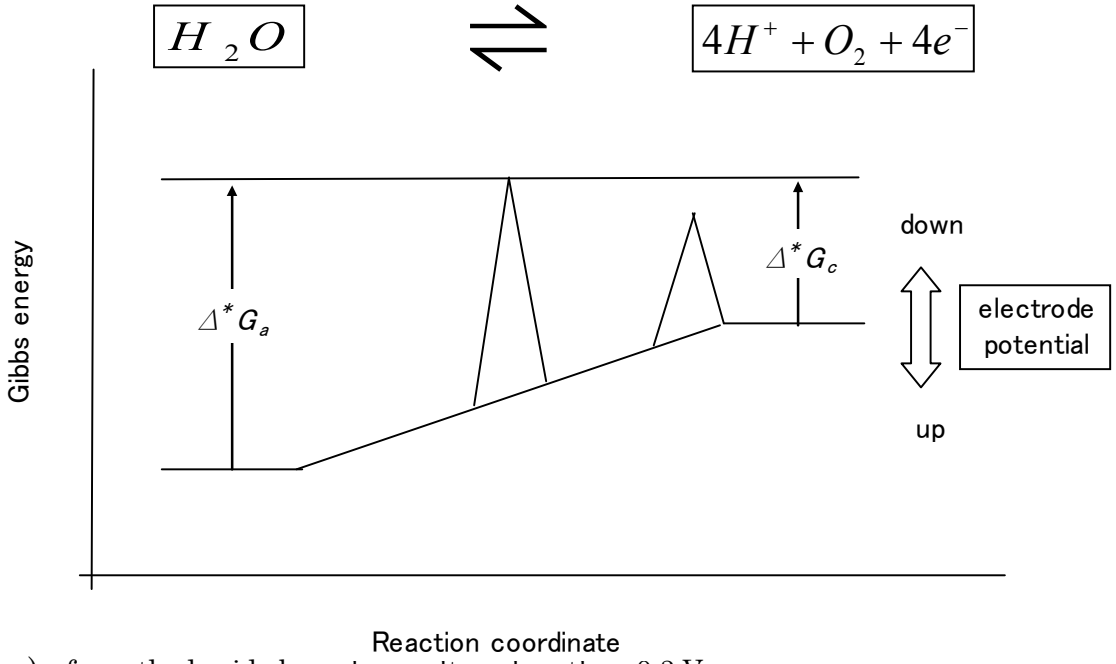

a) for cathode-side boundary voltage less than 0.3 V

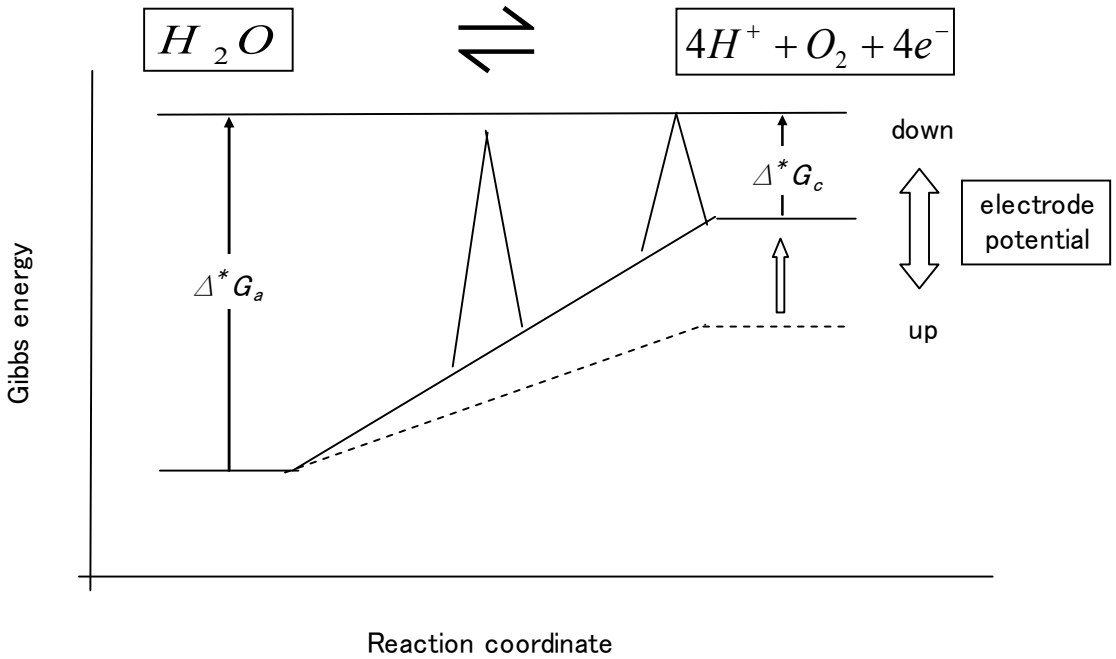

b) for cathode-side boundary voltage more than 0.8V

Fig. 5.9 Schematics of activation energy at cathode

<Activation energy of cathodic current>

The cathodic current produced by reductance of proton was expressed by eq. (4-26) for the cathode side boundary voltage less than about 0.3V and saturates for the voltage more than 0.8V.

From eq.(4-26), Gibbs activation energy at cathode is expressed as follows.

For the cathode-side boundary voltage less than 0.3V,

$$\Delta^* G_c = \Delta^* G_c(0) + F(E_c - E_{sc})/2RT \tag{5-20}$$

$$\Delta^* G_a = \Delta^* G_a(0) - F(E_c - E_{sc})/2RT \tag{5-21}$$

For the cathode-side boundary voltage more than 0.8V,

$$\Delta^* G_c = \Delta^* G_c(0) \tag{5-22}$$

$$\Delta^* G_a = \Delta^* G_a(0) - F(E_c - E_{sc})/RT \tag{5-23}$$

References

[1] Sakuma S, Yamauchi S, Takai O, "Water transfer simulation of an electrolytic dehumidifier", J Appl. Electrochem., Vol. 39, pp.815-825, 2009.

[2] Sakuma S, Yamauchi S, Takai O, "Estimation of dehumidifying performance of solid polymer electrolytic dehumidifier for practical application", J Appl. Electrochem., Vol. 40, pp.2153-2160, 2010.

Chapter 6

Conclusions

The characteristics of the SPE dehumidifier using solid polymer electrolytic membrane are studied. Dehumidifying characteristics were given in relation to current flowing in the device, water content in the membrane and humidity surrounding the device.

6.1 The water content in solid polymer electrolytic membrane (Nafion 117) in equilibrium conditions was given as a function of the temperature and the humidity of the space surrounding the membrane.

6.2 Two-layer model for a dehumidifying device using a solid polymer electrolytic (SPE) membrane was proposed. The validity of the model was verified by comparing the results calculated using the two-layer model with the experimental measurements.

6.3 The electrical resistance of the SPE dehumidifier was measured. It was found that the resistance changes linearly with the inverse of the water content in the dehumidifier and also depends on ambient temperature.

6.4 When current flows in the device, that means the electrolysis occurs at the anode, the electrical resistance is strongly influenced by the water content near the anode because the water content near the anode directly affects the amount of electrolysis. The simulation using the two-layer model supported the strong dependence of the resistance on the water content in the vicinity of the anode.

6.5 Parameters such as water vapor transmission rate, water vapor permeability coefficient of the dehumidifier can be derived as a function of fundamental physical quantities used in the two-layer model. This model is much useful to associate such parameters with the fundamental physical quantities.

Characteristics of the SPE dehumidifier under steady-state conditions were studied. The following results were obtained.

6.7 It was shown in chapter 3 that the current in the SPE dehumidifier under steady-state conditions is approximately proportional to the water content in the

vicinity of the anode.

6.8 The relations among current, water contents and humidities surrounding the dehumidifier under steady-state conditions was analyzed, assuming that the current is produced only by the decomposition of water molecules.

6.9 A simplified expression for the two-layer model was presented. The two-layer model for the SPE dehumidifier basically consists of 4 differential equations. As in most cases, the rate of water content changes in the dehumidifier is smaller than the rate of water transfer through it, the entire system including the dehumidifier can be approximately expressed by one differential equation with respect to time. Hence, the steady-state humidity in a vessel, which is attained after a long time dehumidification, and time constant to change the humidity can be obtained for specific application conditions. A diagram to estimate the attainable humidity and the time-constant was given for the practical application of the dehumidifier.

The V-I characteristics of an SPE dehumidifier were measured using a modified SPE dehumidifier with four electrodes which include two electrodes to carry the main current and two other reference electrodes to measure the voltage change applied across the boundary between the electrodes and membrane.

6.10 The measuring method seems to be effective in dividing the applied voltage into the anode-side boundary voltage, the cathode-side boundary voltage and the voltage across the membrane itself.

6.11 The current flowing in the dehumidifier under steady-state conditions is expressed as the function of water content in the vicinity of the anode and the voltage across the boundary between the anode and the membrane.

6.12 The relation of current and cathode-side boundary voltage under steady-state conditions was also obtained.

6.13 The electric resistance of the SPE membrane (Nafion 117) itself was estimated from the difference of the voltages across two reference electrodes. The temperature dependence of the membrane resistance was also suggested.

The studies on the water transfer characteristics and the electrical characteristics of solid polymer electrolytic (SPE) dehumidifier using Nafion 117 were useful to understand more precisely the phenomena around SPE dehumidifier and to have improved the performance of the SPE dehumidifier. I believe that these studies also contribute to the progresses of technology using proton-conductive electrolytic membrane by giving the better understanding on the mechanism of water transfer originated by water electrolysis in an electrolytic dehumidifier.

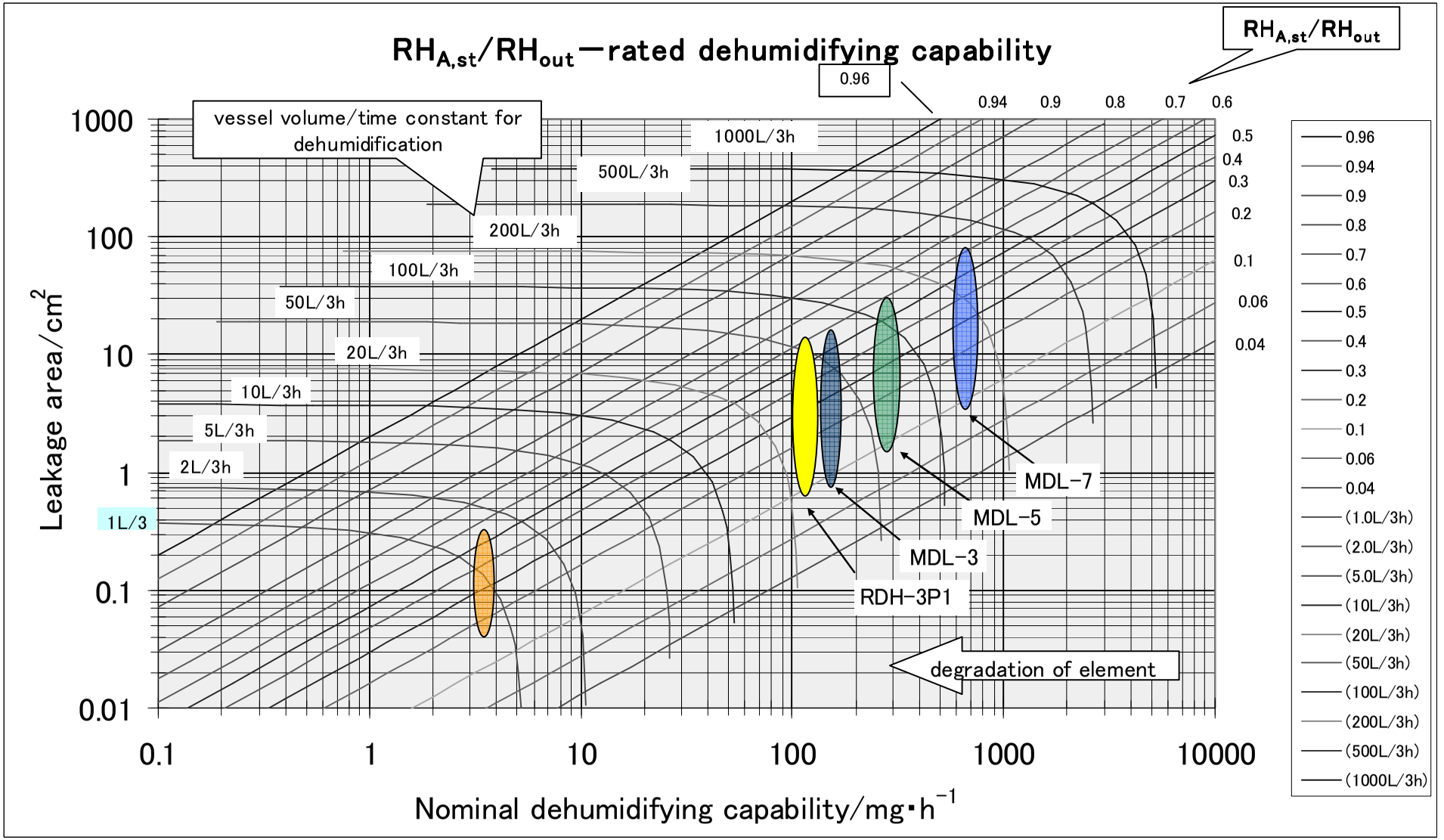

Appendix I　Diagram to estimate the dehumidifying time and the attainable humidity from nominal dehumidifying capability of a dehumidifier (the nominal dehumidifiying capability is the dehumidifying capability under the ambient condition of 30℃ and 60% RH)

Appendix Ⅱ (a)

Appendix II, Saturated vapor pressure and density of water
Table II (a) Saturated vapor pressure and density for solid water 2010/11/15

Temperature T/K	1/T	vapor pres. P/Pa	vapor density ρ_{cal}/g m^{-3}	vapor pressure/mmHg			vapor density ρ/g m^{-3}	vapor density ρ/g m^{-3}
		Rika nenpyo	cal. by eq. (2)	Smithsonian	I.C.T	Boernstein	(Smithsonian)	cal by eq. (4)
190	0.00526	0.032	3.650E-04	2.487E-04	0.00024		3.780E-06	3.704E-04
195	0.00513	0.074	8.223E-04	5.683E-04	0.00056		8.417E-06	8.234E-04
200	0.00500	0.163	1.766E-03	1.247E-03	0.00123		1.801E-05	1.759E-03
205	0.00488	0.344	3.636E-03	2.633E-03	0.00261		3.709E-05	3.621E-03
210	0.00476	0.702	7.244E-03	5.370E-03	0.00534	0.004	7.385E-05	7.201E-03
215	0.00465	1.387	1.398E-02	1.060E-02	0.0106	0.009	1.424E-04	1.387E-02
220	0.00455	2.656	2.616E-02	2.027E-02	0.0203	0.0203	2.661E-04	2.594E-02
225	0.00444	4.942	4.760E-02	3.770E-02	0.0378	0.0378	4.839E-04	4.716E-02
230	0.00435	8.953	8.435E-02	6.824E-02	0.0684	0.066	8.569E-04	8.356E-02
235	0.00426	15.81	1.458E-01	1.205E-01	0.1209	0.119	1.481E-03	1.445E-01
240	0.00417	27.28	2.463E-01	2.077E-01	0.2084	0.205	2.499E-03	2.442E-01
245	0.00408	46.03	4.071E-01	3.502E-01	0.351	0.345	4.128E-03	4.040E-01
250	0.00400	76.04	6.591E-01	5.782E-01	0.58	0.576	6.679E-03	6.551E-01
255	0.00392	123.2	1.047E+00	9.361E-01	0.939	0.935	1.060E-02	1.042E+00
260	0.00385	195.8	1.632E+00	1.488E+00	1.49	1.486	1.653E-02	1.629E+00
265	0.00377	306	2.502E+00	2.323E+00	2.326	2.321	2.532E-02	2.503E+00
270	0.00370	470.1	3.773E+00	3.568E+00	3.568	3.566	3.816E-02	3.785E+00
273.15	0.00366	611.15	4.848E+00	4.581E+00	4.579	4.579	4.843E-02	4.874E+00

Rika nenpyo: Chronological Scientific Tables (2001)
Smithsonian: R.J.List et al. "Smithsonian Meteological Tables, 6th Revised Edition.
I.C.T: E.W. Washbarn et al. International Critical Tables, III, 210 (1928)
Boernstein: Landolt Boernstein, Phy. Chem. Tabellen, II, 1314 (1931)
Cal. By eq. (3): calculated from date of Rika nenpyo assuming that vapor is ideal gas.

1 atm = 101325Pa = 760mmHg, eq. (1)

ρ (g/m3)=2.165P(Pa)/T(K), ideal gas (water) eq. (2)

Formula of saturated water density under the temperature above 273K.
ρ (g/m3)=3.09E8*exp(-4900/T), T≧273K eq. (3)

Formula of saturated water density under the temperature below 273K.
ρ (g/m3)=1.26E10exp(-5920/T), T≦273K eq. (4)

P(mmHg)=760/1.013E5*P(Pa), eq. (5)

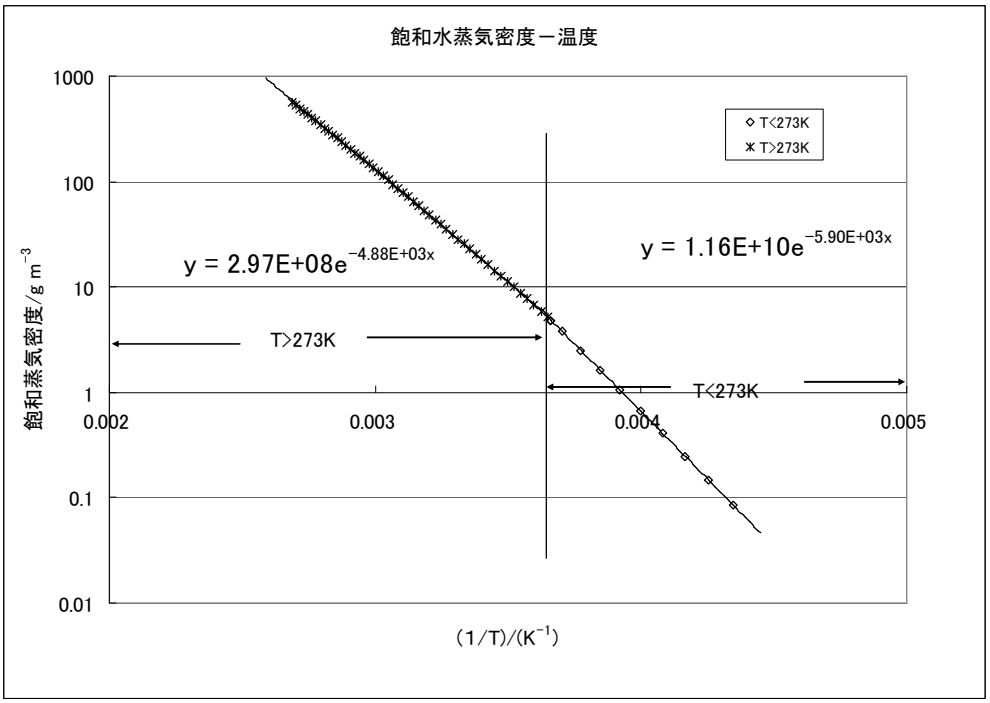

Appendix Ⅱ (b)

Appendix

Tablell (b) Saturated vapor pressure and density for liquid water

Temperature T/K	1/T	vapor pres. P/k Pa	vapor density ρ_{cal}/g m^{-3}	vapor pressure/mmHg		vapor density ρ_m/g m^{-3}	vapor density g m^{-3}
		Rika nenpyo	cal. by eq. (2)	Smithsonian	I.C.T	(Smithsonian)	cal. by eq. (3)
270	0.00370	0.4848	3.89				
272	0.00368	0.562	4.48				
274	0.00365	0.65	5.14	4.925	5.294	5.19	5.29
276	0.00362	0.7499	5.89	5.682		5.95	6.02
278	0.00360	0.8632	6.73	6.540	6.543	6.79	6.84
280	0.00357	0.9915	7.67	7.501	7.513	7.74	7.76
282	0.00355	1.1363	8.73	8.606	8.606	8.81	8.78
284	0.00352	1.2994	9.91	9.841	9.844	10.01	9.93
286	0.00350	1.4828	11.24	11.227	11.231	11.34	11.20
288	0.00347	1.6886	12.71	12.784	12.988	12.82	12.62
290	0.00345	1.9192	14.34	14.526	14.530	14.47	14.19
292	0.00342	2.1768	16.15	16.474	16.477	16.29	15.93
294	0.00340	2.4643	18.16	18.647	18.650	18.32	17.85
296	0.00338	2.7844	20.38	21.067	21.068	20.55	19.98
298	0.00336	3.1403	22.84	23.755	23.756	23.02	22.33
300	0.00333	3.5353	25.54	26.739	26.739	25.74	24.92
302	0.00331	3.9728	28.51	30.043	30.043	28.73	27.76
304	0.00329	4.4567	31.77	33.698	33.695	32.01	30.89
306	0.00327	4.991	35.34	37.731	37.729	35.61	34.32
308	0.00325	5.58	39.26	42.181	42.175	39.55	38.08
310	0.00323	6.2282	43.54	47.076	47.064	43.86	42.20
312	0.00321	6.9407	48.21	52.455	52.442	48.55	46.70
314	0.00318	7.7224	53.29	58.357	58.34	53.67	51.61
316	0.00316	8.579	58.83	64.830	64.80	59.25	56.97
318	0.00314	9.5162	64.85	71.897	71.88	65.30	62.81
320	0.00313	10.54	71.38	79.627		71.86	69.16
322	0.00311	11.658	78.46	88.058	88.02	78.98	76.06
324	0.00309	12.875	86.11	97.208	97.20	86.65	83.55
326	0.00307	14.2	94.39	107.244	107.20	95.01	91.67
328	0.00305	15.639	103.32	118.105	118.04	103.99	100.47
330	0.00303	17.202	112.96	129.896	129.82	113.68	109.99
332	0.00301	18.896	123.34	142.677	142.60	124.11	120.28
334	0.00299	20.73	134.50	156.51	156.43	135.33	131.39
336	0.00298	22.713	146.49	171.46	171.38	147.37	143.38
338	0.00296	24.856	159.36	187.67	187.54	160.35	156.31
340	0.00294	27.167	173.15	205.07	204.96	174.19	170.22
342	0.00292	29.659	187.93	223.86	223.73	189.04	185.19
344	0.00291	32.34	203.72	244.08	243.9	204.91	201.27
346	0.00289	35.224	220.61	265.82	265.7	221.88	218.55
348	0.00287	38.323	238.64	289.19	289.1	239.99	237.08
350	0.00286	41.647	257.85	314.23	314.1	259.28	256.94
352	0.00284	45.211	278.33	341.30	341.0	280.02	278.22
354	0.00282	49.028	300.12	369.91	369.7	301.78	300.98
356	0.00281	53.112	323.30	400.70	400.6	325.06	325.32
358	0.00279	57.477	347.91	433.61	433.6	349.79	351.32
360	0.00278	62.139	374.04	468.74	468.7	376.03	379.08
362	0.00276	67.112	401.75	506.24	506.1	403.87	408.68
364	0.00275	72.414	431.10	546.19	546.05	433.35	440.24
366	0.00273	78.059	462.17	588.74	588.60	464.56	473.84
368	0.00272	84.068	495.04	634.01	633.90	497.56	509.60
370	0.00270	90.453	529.76	682.15	682.02	532.45	547.63
372	0.00269	97.238	566.44	733.27	733.24	569.27	588.05

Formula of saturated water density under the temperature above 273K.

ρ (g/m3)=3.09E8*exp(-4900/T), T≧273K eq. (3)

Appendix Ⅱ (c)

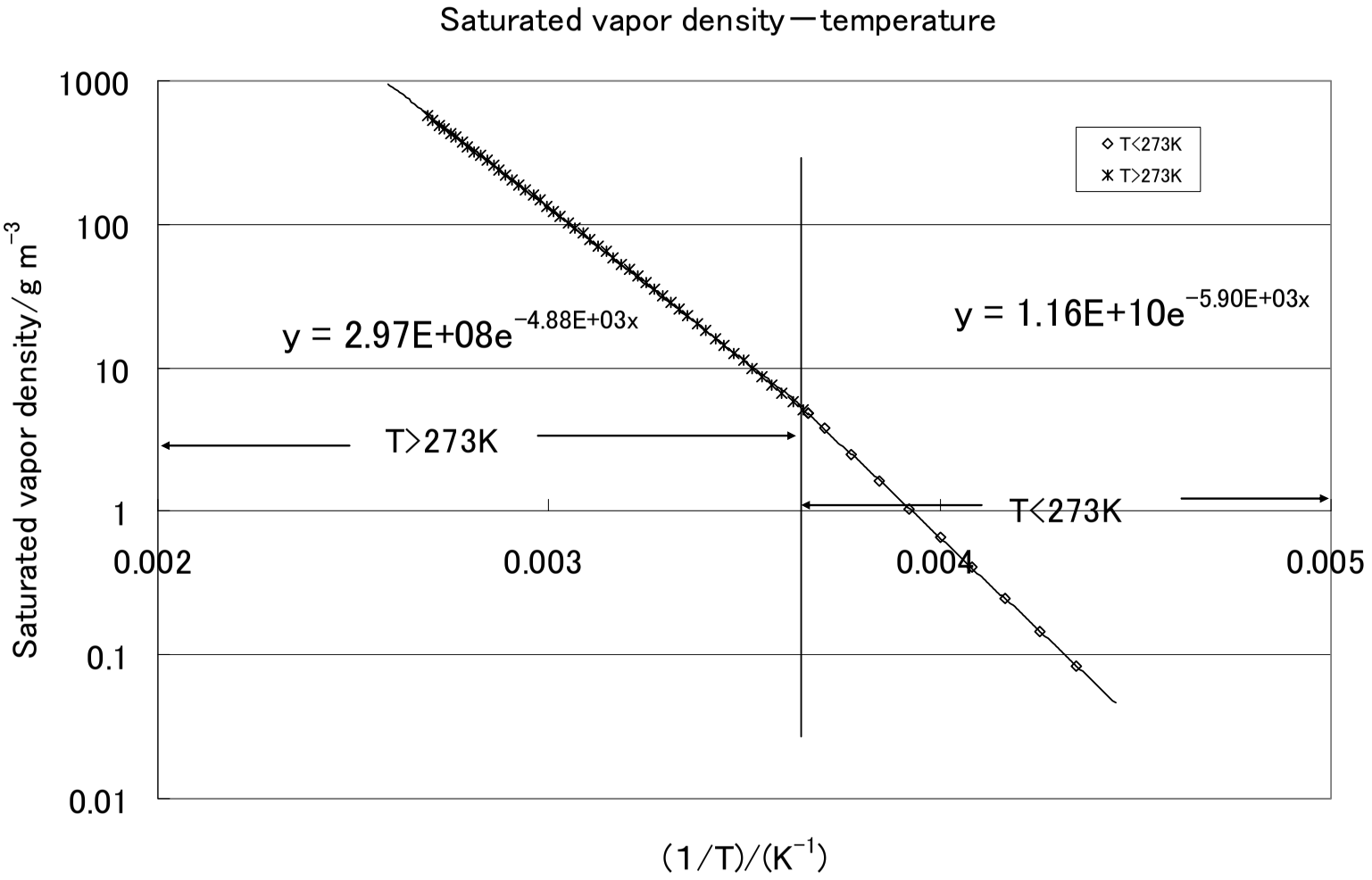
Saturated vapor density—temperature
1000
100
10
1
0.1
0.01
0.002
0.003
0.004
0.005
Saturated vapor density/g m-3
(1/T)/(K-1)
◇ T<273K
✳ T>273K
y = 2.97E+08e-4.88E+03x
y = 1.16E+10e-5.90E+03x
T>273K
T<273K

Appendix Ⅲ(a):program to simulate dehumidifying process

```
Public S, V1, V2, Tem, RRg1in, RRg2in, Mprint
Public Directry, Mstep
Sub main()
'    SPE model 13 2010/11/10(MR10→MR11)
'    back diffusion →  Dif*(Rs2-Rs1)/D
'    Dif=6.2E-7
'    modifications＊＊＊＊＊＊＊＊＊＊＊＊＊＊＊
'
     e = 1.602E-19                'electron charge (C)
     Na = 6.02E+23                'Avogadro number
     D = 0.017                    'thickness of membrane (Nafion 117) (ｃｍ)
'    multiplication factor for diffusion (cdif)          ********************
     cdif = 1                     'common multiplier
     Dif = 0.000000613 * cdif          'diffusion coefficient(cm2/sec.)
'    multiplication factor for dehumidifying performance (ablt) ************
     kgn = 0.245                       'coefficient factor from space to membrane
     ablt = 1#                         'new＝１、used＜１
     kg = 0.245 * ablt                 'rate of water transfer from space to element(cm/s)
     Kso = 108# * ablt                 'coefficient of water transfer from element to space(cm/s)
'    ****************************************
'     S = 100                          'dehumidifying area (cm2)
'     S = 0.28                         'dehumidifying area (cm2)
     Nh2o = 1.26                       'the number of water molecules accompanied by a proton (H2O/H+)
     A = 18 / (e * Na)                 '
'    ****************************************
'     Tem = 303                        'ambient temperature(K)
'         Form1.picture1.CurrentX = 500
'         Form1.picture1.CurrentY = 500
'         Form1.picture1.Print Tem

     Ks = Kso * Exp(-4510 / Tem)       'rate of water transfer from membrane to space (cm/s)
     Rgo = 309 * Exp(-4900 / Tem)      'saturated water density (g/cm3)
     Rg1in = RRg1in / 100 * Rgo        'water density of the space to be humidified (g/cm3)
     Rg2in = RRg2in / 100 * Rgo        'water density of the space to be humidified (g/cm3)
     Rsin = kg * (Rg1in + Rg2in) / (2 * Kso * Exp(-4510 / Tem))  'water content under equilibrium condition
     Rs1in = Rsin                      'initial water content of anode-side
     Rs2in = Rsin                      'initial water content of cathode-side
     Bgs = kg / (2 * Kso) * Exp(4510 / Tem)

'    **********  additional information  ******************************
'    the definition of leakage of the chamber(leakage area for water  : Sleak)    *
'     Sleak = S * 0.2 * 2
    Sleak = 0
'    **********  end of additional information  ************************
'
'    The value of full scale of current axis (JSfs)
     Zo = 0.1734 * 100                 'constant term of electrical resistance (Ohm*cm2)
     Ct = 0.067 * Exp(670 / Tem)       'exponential term of electrical resistance (Kelvin)
     Z1 = Ct / Rs1in + Zo              'electrical resistance (Ohm*cm2)
     Volt = 3                          '(V.)
     j = Volt / Z1                     'current density (A/cm2)
     Js = j * S                        'current (A)
     JSM = Js                          'initial current (A)
     JSfs = 2 * JSM                    'the value of full scale of current axis (A)
'     JSfs = 20                        'the value of full scale of current axis (A)
'    ************************************************
      Rg1fs = Rg1in * 2                'the value of full scale of water density (g/cm3)
      Rg2fs = Rg1fs                    'the value of full scale of water density (g/cm3)
      Rsfs = Rsin * 2                  'the value of full scale of water content (g/cm3)
      JSfs = JSfs                      'full scale of current axis
      Efffs = 2                        'efficiency od dehumidifying performande (molH2O/(2eNA))
'
'        *******  values of full scale  ******************
         GPHfs = 0.02 * S              'dehumidifying performance (g/h)    *
'         GPHfs = 2                    'dehumidifying performance (g/h)    *
'        *******  end  ******************************

'-- initial condition ---
     N1 = 5
'    *********  determination of observation time (min.)   ******************
'     Tfs = 3600 * 1                   'observation time (min.)              *
     Tfs = 60 * 10 / 2                  'observation time (min.)              *
'    *********  set the time to switch-off if necessary  ********************
'                                                  *
     toff = Tfs * 1.5                 'switch-off time  ********************
'    toff = Tfs * 0.45                 'switch-off time  ********************
'    *********  end    ******************************
     dt = 1                           'step time for calculation (sec)
'    dt = 0.1                         'step time for calculation (sec)
```

```
'    N = Tfs / dt / N1                '
    N = Tfs * 60 / dt / N1            'time step for output (seconds)
    T = 0                             'time
    Rg1 = Rg1in                       'water density in space 1
    Rg2 = Rg2in                       'water density in space 2
    Rs = Rsin                         'water content in the membrane
    Rs1 = Rs1in                       'water content in the anode-side half of the membrane
    Rs2 = Rs2in                       'water content in the cathode-side half of the membrane
'    Zo = 0.1734 * 100          '(Ohm*cm2)
'    Ct = 0.0337 * Exp(1080 / Tem) '(Kelvin)
'    Z1 = Ct / Rs1 + Zo             '(Ohm*cm2)
'    j = Volt / Z1                  '(A/cm2)
'    Js = j * S                  '(A)
'    JSM = Js
    Eff = 0
    Gph = 0
    Gphm = Gph
    GTint = 0
    Tm = 0
' グラフの軸の表示
        Form1.Picture1.Line (2000, 650)-(2000, 3050)
        Form1.Picture1.Line (1950, 2950)-(14000, 2950)
        Form1.Picture1.Line (14000, 650)-(14000, 3050)

        Form1.Picture1.CurrentX = 14400
        Form1.Picture1.CurrentY = 3100
        Form1.Picture1.Print "(min.)"
        Form1.Picture1.CurrentX = 1950
        Form1.Picture1.CurrentY = 3100
        Form1.Picture1.Print "0"
        Form1.Picture1.CurrentX = 900
        Form1.Picture1.CurrentY = 1000
        Form1.Picture1.Print "湿度(g/cm3)"

        Form1.Picture1.Line (14000, 650)-(14050, 650)
'        Form1.Picture1.CurrentX = 14100
'        Form1.Picture1.CurrentY = 600
'        Form1.Picture1.Print Format(GPHfs, "##")
        Form1.Picture1.CurrentX = 14200
        Form1.Picture1.CurrentY = 1000
        Form1.Picture1.Print "除湿能力"
        Form1.Picture1.CurrentX = 14200
        Form1.Picture1.CurrentY = 2000
        Form1.Picture1.Print "(g/h)"
        Form1.Picture1.Line (2000, 650)-(14000, 650), &HC0C0C0

        Form1.Picture1.Line (2000, 3450)-(2000, 5850)
        Form1.Picture1.Line (1950, 5750)-(14000, 5750)
        Form1.Picture1.Line (14000, 3450)-(14000, 5850)

        Form1.Picture1.CurrentX = 14400
        Form1.Picture1.CurrentY = 5900
        Form1.Picture1.Print "(min.)"
        Form1.Picture1.CurrentX = 1950
        Form1.Picture1.CurrentY = 5900
        Form1.Picture1.Print "0"
        Form1.Picture1.CurrentX = 1000
        Form1.Picture1.CurrentY = 3750
        Form1.Picture1.Print "膜の水分"
        Form1.Picture1.CurrentX = 1000
        Form1.Picture1.CurrentY = 4000
        Form1.Picture1.Print "(g/cm3)"

        Form1.Picture1.Line (14000, 3450)-(14050, 3450)
        Form1.Picture1.CurrentX = 14100
        Form1.Picture1.CurrentY = 3400
        Form1.Picture1.Print Format(Efffs, "##")
        Form1.Picture1.CurrentX = 14200
        Form1.Picture1.CurrentY = 3900
        Form1.Picture1.Print "効率"
        Form1.Picture1.CurrentX = 14200
        Form1.Picture1.CurrentY = 4800
'        Form1.picture1.Print "(%)"
        Form1.Picture1.Line (2000, 3450)-(14000, 3450), &HC0C0C0

        Form1.Picture1.Line (2000, 6250)-(2000, 8650)
        Form1.Picture1.Line (1950, 8550)-(14000, 8550)
        Form1.Picture1.CurrentX = 14400
        Form1.Picture1.CurrentY = 8700
```

```
        Form1.Picture1.Print "(min.)"
        Form1.Picture1.CurrentX = 1950
        Form1.Picture1.CurrentY = 8700
        Form1.Picture1.Print "0"
        Form1.Picture1.CurrentX = 1000
        Form1.Picture1.CurrentY = 6600
        Form1.Picture1.Print "電流(A)"
        Form1.Picture1.Line (2000, 6250)-(14000, 6250), &HC0C0C0
'
        Form1.Picture2.Line (2000, 650)-(2000, 3050)
        Form1.Picture2.Line (1950, 2950)-(14000, 2950)
        Form1.Picture2.Line (14000, 650)-(14000, 3050)

        Form1.Picture2.CurrentX = 14400
        Form1.Picture2.CurrentY = 3100
        Form1.Picture2.Print "(min.)"
        Form1.Picture2.CurrentX = 1950
        Form1.Picture2.CurrentY = 3100
        Form1.Picture2.Print "0"
        Form1.Picture2.CurrentX = 900
        Form1.Picture2.CurrentY = 1000
        Form1.Picture2.Print "湿度(g/cm3)"

        Form1.Picture2.Line (14000, 650)-(14050, 650)
'        Form1.Picture2.CurrentX = 14100
'        Form1.Picture2.CurrentY = 600
'        Form1.Picture2.Print Format(GPHfs, "##")
        Form1.Picture2.CurrentX = 14200
        Form1.Picture2.CurrentY = 1000
        Form1.Picture2.Print "除湿能力"
        Form1.Picture2.CurrentX = 14200
        Form1.Picture2.CurrentY = 2000
        Form1.Picture2.Print "(g/h)"
        Form1.Picture2.Line (2000, 650)-(14000, 650), &HC0C0C0

        Form1.Picture2.Line (2000, 3450)-(2000, 5850)
        Form1.Picture2.Line (1950, 5750)-(14000, 5750)
        Form1.Picture2.Line (14000, 3450)-(14000, 5850)

        Form1.Picture2.CurrentX = 14400
        Form1.Picture2.CurrentY = 5900
        Form1.Picture2.Print "(min.)"
        Form1.Picture2.CurrentX = 1950
        Form1.Picture2.CurrentY = 5900
        Form1.Picture2.Print "0"
        Form1.Picture2.CurrentX = 1000
        Form1.Picture2.CurrentY = 3750
        Form1.Picture2.Print "膜の水分"
        Form1.Picture2.CurrentX = 1000
        Form1.Picture2.CurrentY = 4000
        Form1.Picture2.Print "(g/cm3)"

        Form1.Picture2.Line (14000, 3450)-(14050, 3450)
        Form1.Picture2.CurrentX = 14100
        Form1.Picture2.CurrentY = 3400
        Form1.Picture2.Print Format(Efffs, "##")
        Form1.Picture2.CurrentX = 14200
        Form1.Picture2.CurrentY = 3900
        Form1.Picture2.Print "効率"
        Form1.Picture2.CurrentX = 14200
        Form1.Picture2.CurrentY = 4800
'        Form1.picture1.Print "(%)"
        Form1.Picture2.Line (2000, 3450)-(14000, 3450), &HC0C0C0

        Form1.Picture2.Line (2000, 6250)-(2000, 8650)
        Form1.Picture2.Line (1950, 8550)-(14000, 8550)
        Form1.Picture2.CurrentX = 14400
        Form1.Picture2.CurrentY = 8700
        Form1.Picture2.Print "(min.)"
        Form1.Picture2.CurrentX = 1950
        Form1.Picture2.CurrentY = 8700
        Form1.Picture2.Print "0"
        Form1.Picture2.CurrentX = 1000
        Form1.Picture2.CurrentY = 6600
        Form1.Picture2.Print "電流(A)"
        Form1.Picture2.Line (2000, 6250)-(14000, 6250), &HC0C0C0
'
```

```
    For Ln = 1 To 3
        Y1 = (Ln - 1) * 2800 + 650
        Y2 = Y1 + 1150
        Form1.Picture1.Line (1950, Y1)-(2000, Y1)
        Form1.Picture1.Line (1950, Y2)-(2000, Y2)
        Form1.Picture2.Line (1950, Y1)-(2000, Y1)
        Form1.Picture2.Line (1950, Y2)-(2000, Y2)
        Y1 = 150 + Ln * 2800
        Y2 = 250 + Ln * 2800
        TT = 0
    For Lm = 1 To 10
        X = 2000 + Lm * 1200
        Form1.Picture1.Line (X, Y1)-(X, Y2)
        Form1.Picture1.CurrentX = X - 200
        Form1.Picture1.CurrentY = Y2 + 50
        Form1.Picture2.Line (X, Y1)-(X, Y2)
        Form1.Picture2.CurrentX = X - 200
        Form1.Picture2.CurrentY = Y2 + 50
        TT = TT + Tfs / 10
        Form1.Picture1.Print TT
        Form1.Picture2.Print TT
    Next Lm
    Next Ln
'
        Call Sub1(Rg1fs, Nexp, Pexp)
        Form1.Picture1.CurrentX = 1200
        Form1.Picture1.CurrentY = 570
        Form1.Picture2.CurrentX = 1200
        Form1.Picture2.CurrentY = 570
            Pexp = Format(Pexp, "#.##")
        Form1.Picture1.Print Pexp; "e"; Nexp
        Form1.Picture2.Print Pexp; "e"; Nexp

        Call Sub1(GPHfs, Nexp, Pexp)
        Form1.Picture1.CurrentX = 14100
        Form1.Picture1.CurrentY = 600
        Form1.Picture2.CurrentX = 14100
        Form1.Picture2.CurrentY = 600
            Pexp = Format(Pexp, "#.##")
        Form1.Picture1.Print Pexp; "e"; Nexp
        Form1.Picture2.Print Pexp; "e"; Nexp

        Call Sub1(Rsfs, Nexp, Pexp)
        Form1.Picture1.CurrentX = 1200
        Form1.Picture1.CurrentY = 3370
        Form1.Picture2.CurrentX = 1200
        Form1.Picture2.CurrentY = 3370
            Pexp = Format(Pexp, "#.##")
        Form1.Picture1.Print Pexp; "e"; Nexp
        Form1.Picture2.Print Pexp; "e"; Nexp
'
        Call Sub1(JSfs, Nexp, Pexp)
        Form1.Picture1.CurrentX = 1200
        Form1.Picture1.CurrentY = 6170
        Form1.Picture2.CurrentX = 1200
        Form1.Picture2.CurrentY = 6170
            Pexp = Format(Pexp, "#.##")
        Form1.Picture1.Print Pexp; "e"; Nexp
        Form1.Picture2.Print Pexp; "e"; Nexp

'
' グラフの作成
'       Rg1fs = Rg1in
'       Rg2fs = Rg1fs
'       Rsfs = Rsin
'       JSfs = JSfs
'
        Y0 = 5750 - Eff * 2300 / Efffs
        Y1 = 2950 - Rg1 * 2300 / Rg1fs
        Y2 = 2950 - Rg2 * 2300 / Rg2fs
        Y3 = 5750 - Rs1 * 2300 / Rsfs
        Y4 = 5750 - Rs2 * 2300 / Rsfs
        Y5 = 8550 - Js * 2300 / JSfs
        Y6 = 2950 - Gph * 2300 / GPHfs
'
        X1 = 2000
        T = 0
        J0 = 0
        J1 = 0
```

```
    For I1 = 0 To N
    For I2 = 1 To N1
        T = T + dt
'        DRg1 = (S / V1) * (-Kg * Rg1 + Ks * Rs1) * dt
        DRg1 = (S / V1) * (-kg * Rg1 + Ks * Rs1) * dt - Sleak / V1 * kgn * (Rg1 - Rg2) * dt
'        DRg1 = 0
'        DRg2 = (S / V2) * (-Kg * Rg2 + Ks * Rs2) * dt
        DRg2 = (S / V2) * (-kg * Rg2 + Ks * Rs2) * dt + Sleak / V2 * kgn * (Rg1 - Rg2) * dt
'        DRg2 = 0
'  DOUBLE LAYER MODEL
        Fluxin = A * j * (0.5 + Nh2o) - Dif * (Rs2 - Rs1) / D
        DRs1 = (2 / D) * (kg * Rg1 - Ks * Rs1 - Fluxin) * dt
        DRs2 = (2 / D) * (kg * Rg2 - Ks * Rs2 + Fluxin) * dt
'  DOUBLE LAYER MODEL END
'  SINGLE LAYER MODEL
'        Fluxin = A * j * (0.5 + Nh2o)
'        DRs1 = (1 / D) * (Kg * (Rg1 + Rg2) - 2 * Ks * Rs1 - Fluxin) * dt
'        DRs2 = DRs1
'  SINGLE LAYER MODEL END
        Rg1 = Rg1 + DRg1
        Rg2 = Rg2 + DRg2
        Rs1 = Rs1 + DRs1
        Rs2 = Rs2 + DRs2
        Rs = (Rs1 + Rs2) / 2
        Z1 = Ct / Rs1 + Zo
        j = Volt / Z1
'       If T > toff Then j = 0
'        If T > toff * 60 Then j = 0
        If T > toff * 60 Then GoTo 1810
        Jsst = j * S
        Rg1st = Rg1
        GoTo 1820
1810    j = 0
1820    Js = j * S
        Gph = -DRg1 * V1 / dt * 3600
        If Gph > Ghmax Then Ghmax = Gph
        If Js = 0 Then
        Eff = 0
        Else: Eff = -DRg1 * V1 / (A / 2 * Js * dt)
        End If
'        Eff = -DRg1 * V1 / (A / 2 * JS * DT)
        If Rs1 > 0.2 * Rsin Then GoTo 2000
        Tm = Tm + dt
        GTint = GTint + Gph * dt
1900        If Rg1 < Rg1in * 5 / 6 Then GoTo 2000
        Gphm = GTint / Tm
2000    If Js > JSM Then JSM = Js

        If Directry <> "" Then
                J0 = J0 + 1
            If J1 = 0 Or J0 = Mstep Then
                Print #2, T, Rg1, Rg2, Rs1, Rs2, Js
                J0 = 0
                J1 = 1
            End If
        End If
    Next I2
        X11 = T * 12000 / (N * N1) + 2000
        Y11 = 2950 - Rg1 * 2300 / Rg1fs
        Y21 = 2950 - Rg2 * 2300 / Rg2fs
        Y31 = 5750 - Rs1 * 2300 / Rsfs
        Y41 = 5750 - Rs2 * 2300 / Rsfs
        Y51 = 8550 - Js * 2300 / JSfs
        Y01 = 5750 - Eff * 2300 / Efffs
        Y61 = 2950 - Gph * 2300 / GPHfs      '(g/h)
'
        Form1.Picture1.Line (X1, Y1)-(X11, Y11), QBColor(9)
        Form1.Picture1.Line (X1, Y2)-(X11, Y21), QBColor(13)
        Form1.Picture1.Line (X1, Y0)-(X11, Y01), QBColor(12)
        Form1.Picture1.Line (X1, Y3)-(X11, Y31), QBColor(9)
        Form1.Picture1.Line (X1, Y4)-(X11, Y41), QBColor(13)
        Form1.Picture1.Line (X1, Y5)-(X11, Y51), QBColor(9)
        Form1.Picture1.DrawWidth = 2
        Form1.Picture1.Line (X1, Y6)-(X11, Y61), QBColor(12)
        Form1.Picture1.DrawWidth = 1
'
        Form1.Picture2.Line (X1, Y1)-(X11, Y11), QBColor(9)
        Form1.Picture2.Line (X1, Y2)-(X11, Y21), QBColor(13)
        Form1.Picture2.Line (X1, Y0)-(X11, Y01), QBColor(12)
```

```
        Form1.Picture2.Line (X1, Y3)-(X11, Y31), QBColor(9)
        Form1.Picture2.Line (X1, Y4)-(X11, Y41), QBColor(13)
        Form1.Picture2.Line (X1, Y5)-(X11, Y51), QBColor(9)
        Form1.Picture2.DrawWidth = 2
        Form1.Picture2.Line (X1, Y6)-(X11, Y61), QBColor(12)
        Form1.Picture2.DrawWidth = 1
'
        X1 = X11
        Y0 = Y01
        Y1 = Y11
        Y2 = Y21
        Y3 = Y31
        Y4 = Y41
        Y5 = Y51
        Y6 = Y61
'        Form1.picture1.CurrentX = 500
'        Form1.picture1.CurrentY = 300
'        Form1.picture1.Print "JS"

    Next I1
        If Directry <> "" Then
                Print #2, T, Rg1, Js
        End If
'
          NL = Chr(13) + Chr(10)
'       Text = "Rg1fs =" & Str(Rg1fs) & NL
'        Text = Text & "Rso =" & Str(Rsin) & NL
'       Text = Text & " JSfs =" & Str(JSfs) & NL
'        Text = Text & " Rs =" & Str(Rs) & NL
'        Text = Text & " Rs1 =" & Str(Rs1) & NL
'        Text = Text & " Rs2 =" & Str(Rs2) & NL
'        Text = Text & "Rg1 =" & Str(Rg1) & NL
        Text = Text & " KG =" & Str(kg) & ",  kso=" & Str(Kso) & ", Nh2o=" & Str(Nh2o) & NL
'        Text = Text & "   KSo =" & Str(Kso) & NL
'       Text = Text & "    KJ =" & Str(kj) & NL
       Text = Text & " ρg1st =" & Str(Rg1st) & ",  ρg2=" & Str(Rg2) & NL
       Text = Text & " Cdif =" & Str(cdif) & ",  Sleak=" & Str(Sleak) & ", 除湿能力=" & Str(ablt) & NL
       Text = Text & " Jo =" & Str(JSM) & NL
       Text = Text & "Jst =" & Str(Jsst) & NL
       Text = Text & "Ghmax =" & Str(Ghmax) & NL
       Text = Text & "Gphm =" & Str(Gphm) & NL
'       Text = Text & "Rg2in =" & Str(Rg2in)

        Form1.Text7.Text = Text
End Sub


Sub Sub1(V, N, P)
       P = V
       N = 0
    If P > 0# Then
       K = 1
    Else
       K = -1
       P = Abs(P)
    End If

          M = 0
100 If P >= 1# Then
       If M = 2 Then GoTo 200
          M = 1
          N = N + 1
          P = P * 0.1
          GoTo 100
    Else
       If M = 1 Then GoTo 200
          M = 2
          N = N - 1
          P = P * 10
          GoTo 100
    End If
200       P = P * K
End Sub
```

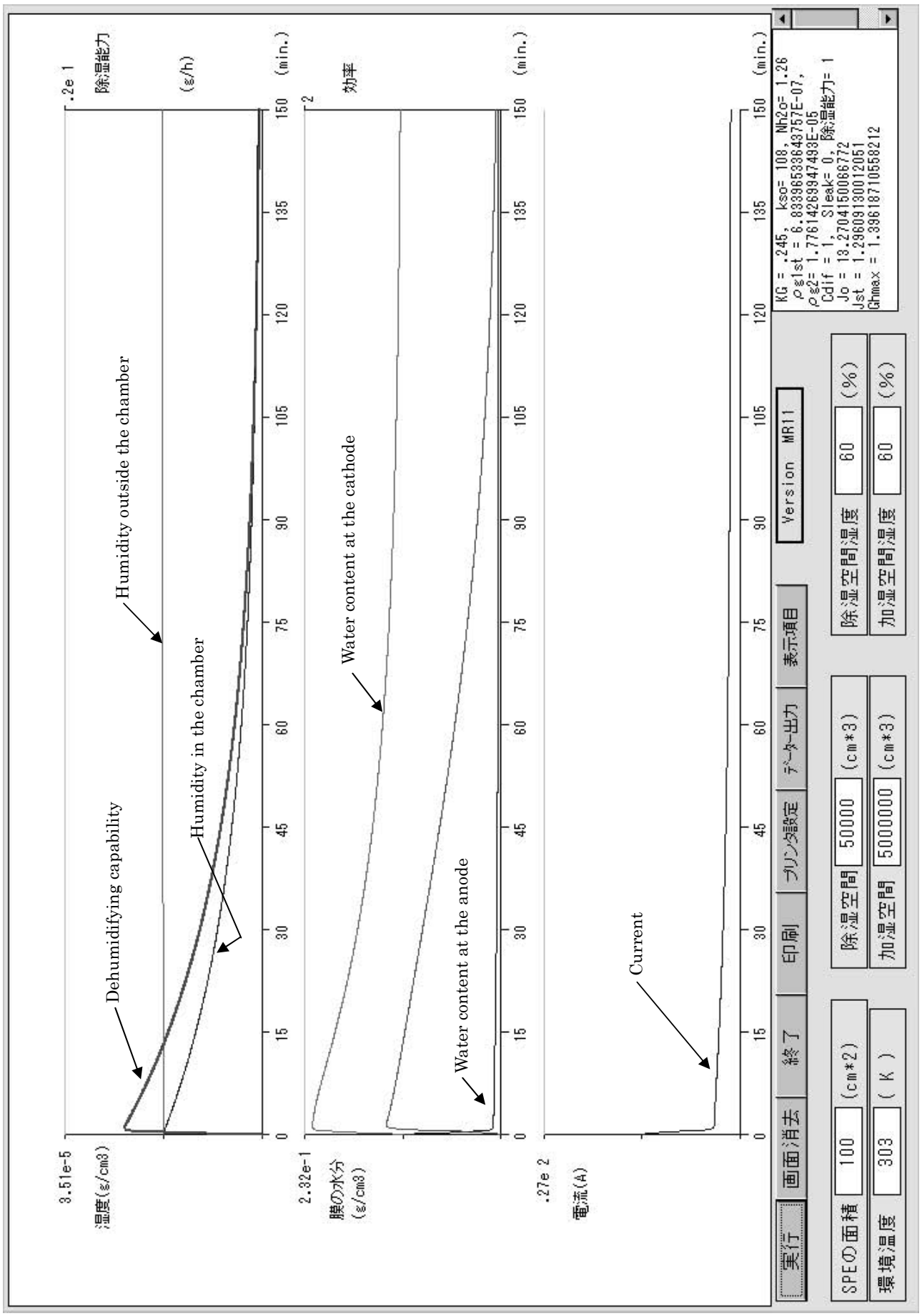
Dehumidifying capability
Humidity outside the chamber
Humidity in the chamber
Water content at the cathode
Water content at the anode
Current
除湿能力
(g/h)
効率
(min.)
温度(g/cm3)
膜の水分 (g/cm3)
電流(A)
実行
画面消去
終了
印刷
プリンタ設定
データ出力
表示項目
Version MR11
SPEの面積
環境温度
除湿空間
加湿空間
除湿空間湿度
加湿空間湿度
(cm*2)
(K)
(cm*3)
(%)

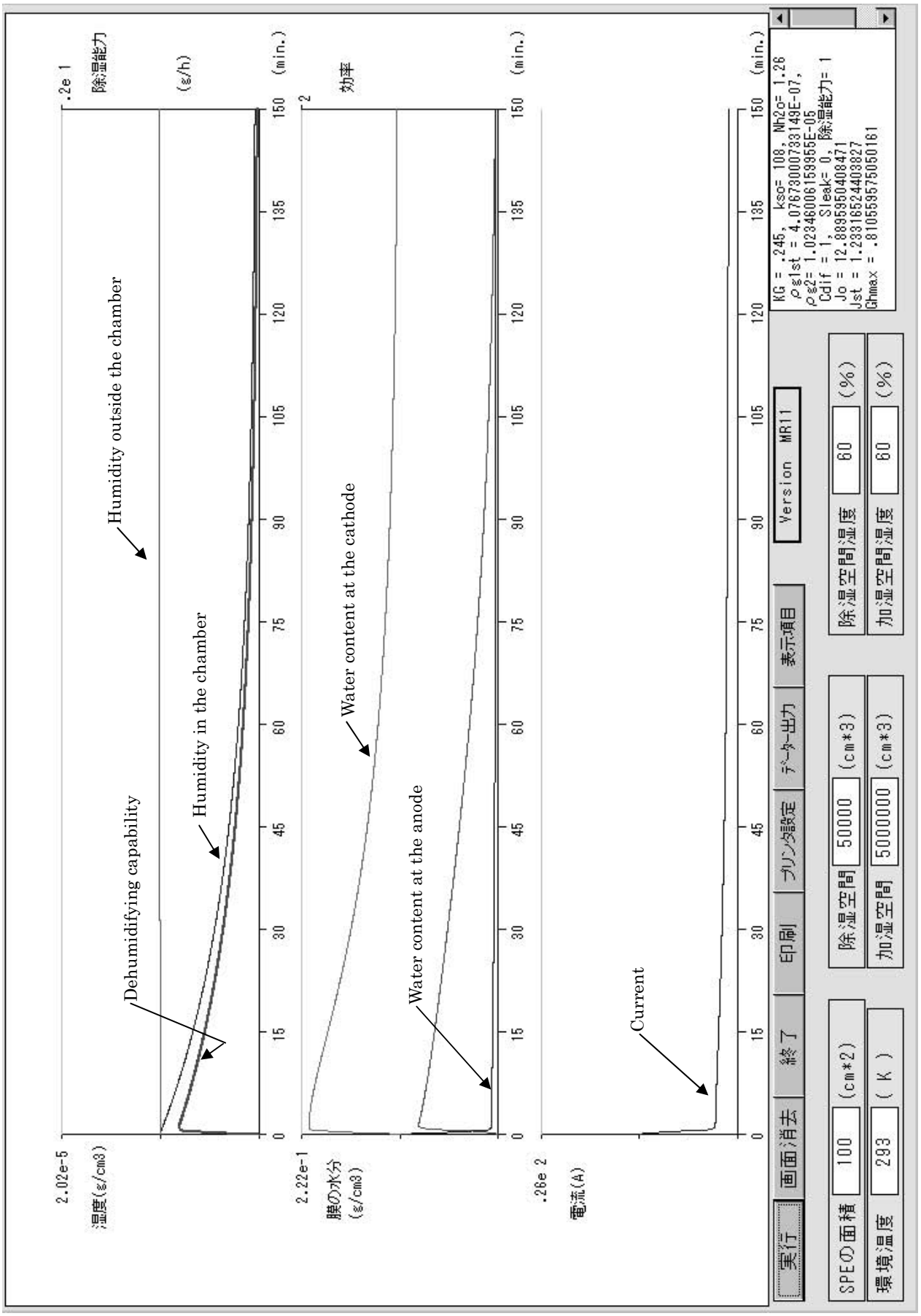
Humidity outside the chamber
Humidity in the chamber
Dehumidifying capability
Water content at the cathode
Water content at the anode
Current
除湿能力
(g/h)
効率
膜の水分 (g/cm3)
電流(A)
湿度(g/cm3)
(min.)
実行
画面消去
終了
印刷
プリンタ設定
データ出力
表示項目
Version MR11
SPEの面積
100
(cm*2)
環境温度
293
(K)
除湿空間
50000
(cm*3)
加湿空間
5000000
(cm*3)
除湿空間湿度
60
(%)
加湿空間湿度
60
(%)

Appendix IV, Van der Waals equation of state for water

The Van der Waals equation of state may be written：

$$\left(p+\frac{a}{V^2}\right)(V-b)=RT \tag{1}$$

Where V is molar volume, and a and b are substance-specific constants. They can be calculated from the critical properties p_c, T_c and V_c. The value of V_c is the molar volume at the critical point p_c and T_c. as

$$a=3p_cV_c^2 \tag{2}$$

$$b=\frac{V_c}{3} \tag{3}$$

Or

$$a=\frac{27(RT_c)^2}{64p_c} \tag{4}$$

$$b=\frac{Rt_c}{8p_c} \tag{5}$$

The constants for water are：

$$a=5.53\times10^{-1}\ [Pa\,m^3\,mol^{-2}] \tag{6}$$

$$b=33.0\times10^{-6}\ [m^3\,mol^{-1}] \tag{7}$$

For saturated vapor pressure of water at the temperature of 273K,

$$pV_m=RT\left(1+(b-\frac{a}{RT})\frac{1}{V_m}+\frac{b^2}{V_m^2}+\frac{b^3}{V_m^3}+\cdots\right)$$

$$=RT\left(1+(33.0\times10^{-6}-\frac{5.53\times10^{-1}}{8.31\times273})\frac{1}{3.7}+\frac{(33.0\times10^{-6})^2}{(3.7)^2}+\cdots\right) \tag{8}$$

$$=RT(1-5.7\times10^{-5}+8.0\times10^{-11}+\cdots)$$

Real water vapor at the temperature of 273K up to 373K can be approximated to be ideal gas.

Publication

<Paper related to chapters 1 and 5>

(1) S. Yamauchi, S. Sakuma, H. Nakatani, K. Mitsuda, "Mass transfer equations of electrolytic water removal device using solid polymer electrolytic membrane", Trans. IEE of Japan, Vol. 120-A, No. 5, pp. 607-613, 2000.

<Paper related to chapters 2 and 5 >

(2) S. Sakuma, S. Yamauchi, O. Takai, "Water transfer simulation of an electrolytic dehumidifier", J. Appl. Electrochem., Vol. 39, pp. 815-825, 2009.

<Papers related to chapters 3 and 5>

(3) S. Sakuma, S. Yamauchi, O. Takai, "Estimation of dehumidifying performance of sold polymer electrolytic dehumidifier for practical application", J. Appl. Electrochem., Vol.40, pp. 2153-2160, 2010.

<Paper related to chapters 4 and 5>

(4) S. Sakuma, S. Yamauchi, O. Takai, "V-I characteristics of solid polymer electrolytic (SPE) dehumidifier", submit to J. Appl. Electrochem., 2010.

<Other papers>

(5) K. Yoshanaga, S. Sakuma, H. Kuwahara, "Issue of high-frequency voltage divider used for circuit breaker interruption test", IEE Japan, ET-75-22, 1975.

(6) Y. Nakamura, S. Sakuma, T . Mori, "An investigation of the photo-electric current in low pressure gases", Trans. IEE of Japan, Vol. 96, No. 6, pp.267-273, 1976.

(7) K. Yoshinaga, S. Sakuma, H. Kuwahara, "Observation of SF6 gas-flow arc", IEE Japan, Technical Committee, SPD-77-4, 1977.

(8) S. Tominaga, H. Kuwahara, K. Yoshinaga, S. Sakuma, "Estimation and Performance investigation on SLF interrupting ability of puffer-type gas circuit breaker.", IEEE Trans. on Power Apparatus and Systems, Vol.Pas-98, No.1, pp.261-269, 1979.

(9) S. Tominaga, H. Kuwahara, K. Yoshinaga, S. Sakuma, "Investigation on gas flow of puffer-type gas circuit breaker based on observation of arc pressure measurement", IEEE Trans. PAS-99, No. 6, pp.2040-2049, 1980.

(10) S. Tominaga, H. Kuwahara, T. Tanabe, K. Yoshinaga, S. Sakuma, "Extremely short line fault tests of a puffer-type gas circuit breaker", IEEE Trans. PAS-100, No.2, 563-571, 1980.

(11) S. Tominaga, H. Kuwahara, K. Sato, K. Yoshinaga, S. Sakuma, "Severity of initial portion of transient recovery voltage (ITRV) for SG_6 gas circuit breaker", J.

of Electrical and Electronics Engineering, Australia, IE Aust. & IREE Aust. Vol. 2, No. 3, 1982.

(12) H. Kuwahara, K. Yoshinaga, S. Sakuma, T. Yamauchi, T. Miyamoto, "Fundamental investigation on internal arcs in SF6 gas-filled enclosure", IEEE Trans. Power Apparatua & Systems, Vol.PAS-101, N0. 10, pp.3977-3987, 1982.

(13) H. Kuwahara, T. Tanabe, K. Ibuki, M. Sakai, A. Sato, S. Sakuma, "New approach to analysis of arc interruption capability by simulation employed in the development of SF_6 GCB series with high capacity interrupter", IEEE Trans. On Power Apparatus & Systems, Vol.PAS-102, No. 7, pp.2262-2268, 1983.

(14) H. Kuwahara, T. Tanabe, K. Yoshinaga, S. Sakuma, K. Ibuki, K. Yamada, "Investigation of dielectric recovery characteristics of hot SF6 gas after current interruption for developing new 300 kV and 550 kV gas circuit breaker", IEEE Trans. PAS-103, No. 6, pp.1371-1376, 1984

(15) T. Tanabe, K. Ibuki, S. Sakuma, T. Yonezawa, "Simulation of the SF6 arc behavior by a cylindrical arc model", IEEE Trans. PAS-104, No. 7, pp.1903-1909, 1985..

(16) S. Sakuma, A. Ohnuma, T. Yonezawa, M. Hosomi, "Studies on temperature distribution of SF6 gas-flow arc", IEE Japan, Technical Committee, SPD-86-15, 1986.

(17) S. Sakuma (one of the CIGRE WG 13.01 members), "Practical application of arc physics in circuit breakers. Survey of calculation methods and application guide", ELECTRA No. 118, pp.65-79, 1988.

(18) K. Ibuki, T. Yoshizumi, T. Yonezawa, S. Sakuma, H. Kuwahara, "An arc model used in analysis of interruption test of GCB's", Proceeding of the 9th International Conference on Gas Discharge and Their Applications", 1988.

(19) S. Sakuma, S. Yamamoto, H. Nakamura, T. Yonezawa, M. Hosomi, "Studies on small inductive interruption of a gas circuit breaker", IEE Japan, Technical Committee, SPD-88-5, 1988.

(20) S. Yamamoto, S. Sakuma, "Studies on small inductive interruption of a gas circuit breaker (II)", IEE Japan, Technical Committee, SPD-88-17, 1988.

(21) S. Sakuma, S. Hirogane, S. Tada, "Diagnostics of electrical insulation of SF6 gas insulated switchgear", IEE Japan, Technical Committee HV-89-5, 1989.

(22) S. Sakuma, K. Kamei, S. Yamamoto, "Current oscillating phenomena in small inductive current interruption", IEE Japan, Technical Committee, SPD-89-21, 1989.

(23) S. Sakuma, S. Yamamoto, K.Kamei, H. Yamamoto, T. Mochizuki, "Development of bus-bar disconnector commutating high current", IEE Japan, Technical Committee, SPD-90-28, 1990.

(24) K. Kamei, S. Yamamoto, S. Sakuma, “Estimation of interruption performance of high-current interrupter arc”, IEE Japan, Technical Committee, SPD-91-18, 1991.

(25) K. Ibuki, S. Sakuma, H. Araki, “Dynamic characteristics of inductive current chopping by SF6 arc”, Proceeding of the Tenth International Conference on Gas Discharge and Their Applications, Vol. 1, pp.184-187, 1992.

(26) K. Kamei, S. Sakuma, T. Yoshizumi, T. Sugiyama, “Interruption test method of high-voltage and high-power interrupter with a closing resistance”, IEE Japan, Technical Committee SP-92-8, 1992.

(27) S. Okabe, E. Zaima, K. Inami, K. Sasamori, S. Sakuma, “Deterioration characteristics of model of insulating spacer for GIS under AC and impulse voltage”, T. IEE Japan, Vol. 115-B, No. 1, pp.30-35,1995.

(28) K.Kato, M. Kurimoto, H. Shumiya, H. Adachi, S. Sakuma, H. Okubo, “Application of functionally graded material for solid insulator in gaseous insulation system”, IEEE Trans. Dielectrics and Electrical Insulation, Vol.13, No. 1, pp.362-372, 2006.

Acknowledgments

The author would like to express his sincere gratitude to Professor Osamu Takai for the kind guidance and suggestions during the course of this dissertation. He would also like to express his appreciation to Professor Nagahiro Saito, Professor Masazumi Okido, Professor Ryoichi Ichino and Professor Toshinobu Yogo for their helpful comments. He also wishes to express thanks to Dr. Shiro Yamauchi and Mr. Mitsuhito Kamei for their help and encouragement in completing this work.

The studies reported here were carried out at Graduate School of Engineering, Nagoya University and Ryosai Technica Company. The author gratefully acknowledges for the economic assistance from Ryosai Technica Company.

The author also acknowledges Mr. Ken-ichi Yasuda, Tetsuya Abe and Tsuyoshi Yamaguchi for their help with the experiments and extends gratitude to all of other members in his laboratory. The author would like to thank Mr. Akiyoshi Ohnuma, the former president of Ryosai Technica Company for providing the opportunity to carry out this study. He is sincerely grateful to Dr. Hiroshi Kuwahara, Dr. Kiyoshi Yoshinaga, Dr. Tohei Nitta and Dr. Koji Ibuki for their useful advices and their continued support. He is also grateful to his parents and his family, his wife Keiko for her continuing encouragement and understanding.

Finally, the author hopes that this work will contribute to the development of today's Solid State Ionics.